Characterizing Sex-Related Differences in Brown Adipose Tissue from *Phb1* Knock-In Mouse Models

By

Niloofar Beheshti Dehkordi

A Thesis submitted to the Faculty of Graduate and Postdoctoral Studies of the University of Manitoba in partial fulfillment of the requirements of the degree of

MASTER OF SCIENCE

Department of Physiology and Pathophysiology

Rady Faculty of Health Sciences

University of Manitoba

Winnipeg

ABSTRACT

Brown adipose tissue (BAT) functions as a heat-producing organ that contributes to whole-body energy balance. The amount and activity of BAT differ between sexes: females typically display greater mitochondrial content and thermogenic responsiveness than males, largely influenced by estrogen signaling. Although sex steroids are known to affect BAT physiology, the intracellular mechanisms that connect hormonal input to metabolic outcomes remain incompletely understood. Prohibitin-1 (PHB1) is an evolutionarily conserved scaffold protein that supports mitochondrial organization and coordinates metabolic and hormonal signaling, including estrogen, androgen, and insulin pathways. Through various post-translational modifications (PTMs), PHB1 can relocate among subcellular compartments and influence multiple pathways, including those involved in lipid handling and insulin responses. Among its modification sites, two residues, Cys69 and Tyr114**,** appear particularly important for regulating PHB1 function, yet their physiological relevance in living systems has not been defined.

To explore this, two CRISPR-engineered knock-in mouse models were generated, *Phb1-Ki*C69A and *Phb1-Ki*Y114F, each lacking one of these critical sites. Analyses of glucose and insulin tolerance tests (GTT and ITT), along with histological evaluation of BAT morphology and mitochondrial density, revealed distinct and sex-dependent consequences for BAT architecture, mitochondrial quality, and metabolic regulation including glucose homeostasis and insulin sensitivity regulation. *Phb1-Ki*C69A females showed enlarged BAT depots and hypertrophic adipocytes, while males exhibited disrupted mitochondrial ultrastructure. In contrast, *Phb1-Ki*Y114F males displayed modest BAT expansion with relatively intact mitochondria, and females maintained small, densely structured adipocytes. Gonadectomy further indicated that endocrine

status modifies these traits: loss of testosterone enhanced insulin sensitivity in *Phb1-Ki*C69A males, whereas estrogen withdrawal slightly impaired glucose handling in *Phb1-Ki*Y114F females.

Together, the results indicate that mutating Cys69 and Tyr114 sites in PHB1 influence BAT structure and metabolic function in a sex-dependent manner, providing evidence that PHB1 could participate in the hormonal regulation of energy metabolism.

ACKNOWLEDGEMENTS

I would like to express my sincere appreciation to Dr. Suresh Mishra for his supervision, guidance, and continued support throughout my Master's studies. I also wish to thank Dr. Xie and Dr. Mizuno for their valuable input and constructive feedback as members of my advisory committee. Acknowledgment is also extended to the members of the Mishra Laboratory for their technical assistance and cooperation. The laboratory is supported by funding from the Canadian Institutes of Health Research (CIHR) and the Natural Sciences and Engineering Research Council of Canada (NSERC).

Finally, I would like to thank my family for their enduring encouragement and support throughout the course of my graduate studies.

TABLE OF CONTENTS

ACKNOWLEDGEMENTS ..... **iv**
TABLE OF CONTENTS ..... **v**
LIST OF TABLES ..... **vii**
List of figures ..... **viii**
Abbreviations ..... **ix**
CHAPTER I. INTRODUCTION **1**
1.1 Literature Review **1**
1.1.1 Overview of Adipose Tissue Biology **1**
1.1.1.1 Types of Adipose Tissue: WAT and BAT **1**
1.1.1.2 Role of BAT in Energy Expenditure and Thermogenesis **3**
1.1.1.3 Adipogenesis in brown adipose tissue **4**
1.1.1.4 Lipolysis and lipogenesis in BAT **6**
1.1.1.5 Fatty acid oxidation and mitochondrial biogenesis **8**
1.1.1.6 Sex Differences in BAT Physiology **10**
1.1.1.6.1 The effects of sex hormones on BAT **11**
1.1.1.6.1.1 Estrogens **11**
1.1.1.6.1.2 Androgens **12**
1.1.1.6.2 X-Linked Genes and Their Impact on Sex-Related Differences **12**
1.1.2 Prohibitin **13**
1.1.2.1 Mitochondrial and Cellular Functions of PHB1 ..... **15**
1.1.2.2 The Role of PHB1 in Adipose Tissue **16**
1.1.2.3 The Post-translational modifications of PHB1 ..... **20**
1.1.2.4 The Role of PHB1 in BAT Metabolism and Phenotype **23**
1.1.2.5 The Role of PHB1 in Glucose Homeostasis **26**
1.2 Research rationale **27**
CHAPTER II. HYPOTHESIS AND OBJECTIVES **31**
CHAPTER III. MATERIALS AND METHODS **33**
3.1. Materials **33**
3.2 Methods **34**
3.2.1 Development of *Phb1-Ki* mice **34**

3.2.2 Animal Housing and Tissue Collection 36
3.3 BAT weight measurements 36
3.4 Histology 36
3.5 Quantification of Cell Number in BAT Sections 37
3.6 Adipose Area Quantification in Histological Images 37
3.7 Gonadectomy 38
3.7.1 Animal Models and Surgical Procedures 38
3.7.2 Orchidectomy 38
3.7.3 Ovariectomy 39
3.8 Glucose Tolerance Test (GTT) and Insulin Tolerance Test (ITT) 39
3.9 Statistical Analysis 40
CHAPTER IV. RESULTS 42
4.1 *Phb1-Ki* Mice Display Altered Whole-Body Weight in a Sex-Dependent Manner 42
4.2 BAT Mass in Male and Female *Phb1-Ki* Mice 44
4.3 Quantification of BAT Cell Number and in *Phb1-Ki* Mice 46
4.4 Quantification of BAT and Adipocyte Area in *Phb1-Ki* Mice 48
4.5 *Phb1-Ki*C69A and *Phb1-Ki*Y114F Knock-in Mice Display Differences in BAT Morphology and Function 50
4.6 Transmission Electron Microscopy Reveals Mitochondrial Variations in BAT by Genotype and Sex 51
4.7 Effects of gonadectomy on body weight in *Phb1-Ki* mice 53
4.8 Effects of gonadectomy on BAT in *Phb1-Ki* mice 55
4.9 Effect of gonadectomy on glucose homeostasis in *Phb1-Ki* mice 57
4.9.1 Effect of gonadectomy on glucose homeostasis in *Phb1-Ki* female mice 57
4.9.2 Effect of gonadectomy on glucose homeostasis in *Phb1-Ki* male mice 61
4.10 Effect of gonadectomy on insulin sensitivity in *Phb1-Ki* mice 65
4.10.1 Effect of ovariectomy on insulin sensitivity in *Phb1-Ki* female mice 65
4.10.2 Effect of orchiectomy on insulin sensitivity in *Phb1-Ki* male mice 69
CHAPTER V. DISCUSSION 73
References 90

LIST OF TABLES

Table 3.1 Materials and reagents used in this thesis work.

Table 3.2 Experimental grouping of mice

Table 5.1 Summary of sex- and mutation-specific BAT and body phenotypes in *Phb1-Ki* mice

List of figures

Figure 3.1 Generation of *Phb1-Ki* mouse models by CRISPR-Cas9 technology.

Figure 4.1. *Phb1-Ki* mice show sex- and genotype-dependent differences in body weight.

Figure 4.2. BAT as a percentage of body weight in *Phb1-Ki* mice

Figure 4.3. Brown adipocyte cell number per field.

Figure 4.4. Adipocyte area (μm²) in brown adipose tissue was quantified from histological sections

Figure 4.5. Representative histological images of BAT from *Phb1-Ki* mice.

Figure 4.6. Representative electron microscopy images showing mitochondrial ultrastructure in BAT of *Phb1-Ki* mice by sex and genotype.

Figure 4.7. Body weight in male and female mice following sham surgery or gonadectomy.

Figure 4.8. BAT as a percentage of body weight in *Phb1-Ki* mice

Figure 4.9.1. Glucose Tolerance in Female Wild-Type and *Phb1-Ki* Mice.

Figure 4.9.2. Glucose Tolerance in Male Wild-Type and *Phb1-Ki* Mice.

Figure 4.10.1. Insulin Tolerance in Female Wild-Type and *Phb1-Ki* Mice.

Figure 4.10.2. Insulin Tolerance in Male Wild-Type and *Phb1-Ki* Mice.

Abbreviations

Abbreviation / Symbol	Full Form / Description
%	Percent
°C	Degrees Celsius
3′ UTR	3′ Untranslated Region
ABHD5	Abhydrolase Domain-Containing Protein 5 (also known as CGI-58)
ACACA	Acetyl-CoA Carboxylase Alpha
Acetyl-CoA	Acetyl Coenzyme A
Akt	Protein Kinase B
AMPK	Adenosine Monophosphate–Activated Protein Kinase
ANOVA	Analysis of Variance
ANXA2	Annexin A2
aP2	Adipocyte Protein 2 (also known as Fatty Acid–Binding Protein 4, Fabp4)
AUC	Area Under the Curve
ATP	Adenosine Triphosphate
ATGL	Adipose Triglyceride Lipase
BAP32	B-Cell Receptor-Associated Protein 32
BAT	Brown Adipose Tissue
BCR	B-Cell Receptor
β-AR	Beta-Adrenergic Receptor
BMP7	Bone Morphogenetic Protein 7
C/EBPβ	CCAAT/Enhancer-Binding Protein Beta
CACS	Central Animal Care Services
CAMP	Cyclic Adenosine Monophosphate
Cas9	CRISPR-Associated Protein 9
CD36	Cluster of Differentiation 36 (Fatty Acid Translocase)
CGI-58	Comparative Gene Identification-58 (Abhydrolase Domain-Containing Protein 5)
COX2p	Cytochrome c Oxidase Subunit 2 Protein
COX3p	Cytochrome c Oxidase Subunit 3 Protein
CPT1	Carnitine Palmitoyltransferase 1
CRISPR	Clustered Regularly Interspaced Short Palindromic Repeats
Cys69	Cysteine at Position 69 of PHB1
DAG	Diacylglycerol
DNL	De Novo Lipogenesis
EBF2	Early B Cell Factor 2
EC-KO	Endothelial Cell–Specific Knockout
ERα	Estrogen Receptor Alpha
ERK	Extracellular Signal-Regulated Kinase
FAO	Fatty Acid Oxidation
FABP	Fatty Acid-Binding Protein

Fabp4	Fatty Acid–Binding Protein 4
$FADH_2$	Flavin Adenine Dinucleotide (Reduced Form)
FASN	Fatty Acid Synthase
FFAs	Free Fatty Acids
G3P	Glycerol-3-Phosphate
GK	Glycerol Kinase
GSK-3β	Glycogen Synthase Kinase-3 Beta
GTT	Glucose Tolerance Test
H&E	Hematoxylin and Eosin
HFD	High-Fat Diet
HSL	Hormone-Sensitive Lipase
IMM	Inner Mitochondrial Membrane
ITT	Insulin Tolerance Test
Ki	Knock-In
LCFA	Long-Chain Fatty Acid
LPL	Lipoprotein Lipase
MAG	Monoacylglycerol
Malonyl-CoA	Malonyl Coenzyme A
MAPK	Mitogen-Activated Protein Kinase
m-Mito-Ob	Mutant Transgenic Obese Mouse Model (Adipocyte-Specific Expression of m-PHB1Y114F)
mRNA	Messenger Ribonucleic Acid
MGL	Monoacylglycerol Lipase
Mito-Ob	Transgenic Obese Mouse Model (Adipocyte-Specific PHB1 Overexpression)
MSC	Mesenchymal Stem Cell
mtDNA	Mitochondrial DNA
Myf5	Myogenic Factor 5
NADH	Nicotinamide Adenine Dinucleotide (Reduced Form)
NE	Norepinephrine
NEFA	Non-Esterified Fatty Acids
O-GlcNAcylation	O-Linked β-N-Acetylglucosaminylation
OPA1	Optic Atrophy 1 (Mitochondrial Dynamin-Like GTPase)
Palmitate	16-Carbon Saturated Fatty Acid Produced by Fatty Acid Synthase
PBS	Phosphate-Buffered Saline
PDH	Pyruvate Dehydrogenase
PET/CT	Positron Emission Tomography–Computed Tomography
PHB1	Prohibitin-1
PHB2	Prohibitin-2
Phb-1	Prohibitin-1 (*C. elegans* Ortholog of Mammalian PHB1)
Phb1EC-KO	Endothelial Cell–Specific PHB1 Knockout
PGC-1α	Peroxisome Proliferator-Activated Receptor Gamma Coactivator 1-Alpha
PI3K	Phosphoinositide 3-Kinase

PLIN1	Perilipin 1
PLIN5	Perilipin 5
PKA	Protein Kinase A
PM	Plasma Membrane
PPARα	Peroxisome Proliferator-Activated Receptor Alpha
PPARγ	Peroxisome Proliferator-Activated Receptor Gamma
PRDM16	PR Domain-Containing 16
PTM	Post-Translational Modification
qPCR	Quantitative Polymerase Chain Reaction
REA	Repressor of Estrogen Receptor Activity
SBP-1	Sterol Regulatory Element–Binding Protein 1 (*C. elegans* Homolog of Mammalian SREBP-1)
SDS-PAGE	Sodium Dodecyl Sulfate–Polyacrylamide Gel Electrophoresis
SH2	Src Homology 2 (Domain)
Shp1	SH2 Domain–Containing Phosphatase 1
SNS	Sympathetic Nervous System
SPFH	Stomatin/Prohibitin/Flotillin/HflK/C Superfamily
SREBP-1	Sterol Regulatory Element–Binding Protein 1
TAG	Triacylglycerol
TEM	Transmission Electron Microscopy
TFAM	Mitochondrial Transcription Factor A
TG–FA	Triglyceride–Fatty Acid Cycle
TCR	T-Cell Receptor
Thr-258	Threonine at Position 258 of PHB1
TRL	Triglyceride-Rich Lipoprotein
Tyr114	Tyrosine at Position 114 of PHB1
UCP1	Uncoupling Protein 1
VAT	Visceral Adipose Tissue
VLDL	Very Low-Density Lipoprotein
WAT	White Adipose Tissue
WNT	Wingless-Related Integration Site Signaling Pathway
WT	Wild Type
XCI	X-Chromosome Inactivation

CHAPTER I. INTRODUCTION

1.1 Literature Review

1.1.1 Overview of Adipose Tissue Biology

1.1.1.1 Types of Adipose Tissue: WAT and BAT

Over the past several decades, there has been a notable improvement in both public awareness and scientific understanding of obesity. Despite these advancements, the incidence of obesity and its related metabolic and chronic health conditions continues to escalate at a concerning pace (1), underscoring the critical need for further research into its underlying mechanisms. An adipocyte is a specialized cell that stores energy in the form of lipids. The fundamental basis of obesity lies in the excessive accumulation of lipids within adipocytes and their hypertrophy. This can lead to systemic metabolic dysregulation, contributing to the development of chronic diseases such as type 2 diabetes (2). This phenomenon highlights the importance of advancing our knowledge of adipose tissue function and structure and its relevance to the pathophysiology of obesity.

Mammals have two types of adipose tissue: white adipose tissue (WAT) and brown adipose tissue (BAT), which differ in structure, function, and distribution.(3).

The distinction between WAT and BAT begins with their fundamentally contrasting physiological roles. WAT primarily functions as a storage site for energy in the form of triglycerides (4), whereas BAT utilizes triglycerides to generate energy in the form of heat through thermogenesis (5). These functional differences are supported by their distinct cellular structures. White adipocytes are characterized by a single large lipid droplet and a relatively low mitochondrial density, reflecting

their role in energy storage. In contrast, brown adipocytes contain multiple small lipid droplets and are enriched with a high density of mitochondria, which facilitate their thermogenic activity (6).

In human, WAT is predominantly located in two main regions: subcutaneous fat, which lies beneath the skin and is distributed across various regions of the body, including the abdomen and thighs, and visceral fat, which surrounds internal organs within the abdominal cavity, such as the liver, intestines, and kidneys. In contrast, BAT is most abundant in infants, where it is primarily localized in areas such as the interscapular region (between the shoulder blades), supraclavicular region (above the collarbones), and suprarenal region (near the adrenal glands). Although its quantity diminishes with age, BAT persists in adults, albeit in reduced amounts (7), and is typically found in the supraclavicular region, paravertebral region (along the spine), mediastinal region (within the chest cavity), para-aortic region, and suprarenal region (above the kidneys) (8). Given the distinct structural, functional, and locational characteristics of WAT and BAT, it is reasonable to hypothesize that their roles in the development and progression of obesity may also differ significantly. These differences suggest that WAT and BAT may contribute uniquely to the pathophysiology of obesity and its associated metabolic complications.

In addition to WAT and BAT, there is a third type known as beige adipose tissue. Beige fat cells are typically found within white adipose depots, especially in subcutaneous regions, and can be recruited under specific conditions such as prolonged cold exposure or stimulation by certain hormones (9). Although they arise from a different cellular lineage than classical brown adipocytes, beige cells share several functional features with them, including the presence of multiple small lipid droplets, a high density of mitochondria, and the expression of uncoupling protein 1 (UCP1), which enables them to burn energy and generate heat through thermogenesis (10,11).

What makes beige fat distinct from brown fat is its inducible nature. While BAT is constitutively active and localized to well-defined regions like the interscapular area, beige fat becomes thermogenically active only in response to external stimuli and can revert to a white fat cell-like state once those stimuli are removed (12). Beige adipocytes can develop either from progenitor cells found near blood vessels within white fat or through trans differentiation of mature white adipocytes into thermogenic beige cells (13).

1.1.1.2 Role of BAT in Energy Expenditure and Thermogenesis

As mentioned earlier, BAT possesses a unique structural and functional profile that distinguishes it from WAT. Structurally, BAT is highly vascularized and contains a dense population of mitochondria, which imparts its characteristic brown color. Functionally, BAT specializes in non-shivering thermogenesis (the generation of heat) through the utilization of fatty acids. This thermogenic capacity is primarily mediated by uncoupling protein 1 (UCP1), a mitochondrial protein located in the inner mitochondrial membrane (14). Under specific stimuli, such as cold exposure or diet-induced thermogenesis, the activation of norepinephrine receptors triggers lipolysis, leading to an increase in free fatty acids (14). These free fatty acids then bind to UCP1, which uncouples the mitochondrial proton gradient from adenosine triphosphate (ATP) synthesis. Instead of driving ATP production, the protons dissipate across the mitochondrial membrane, releasing energy in the form of heat (5). This unique thermogenic feature positions BAT as a critical regulator of energy expenditure. By clearing glucose and fatty acids from the bloodstream and converting them into heat, BAT plays a significant role in metabolic homeostasis. Given its ability to enhance energy expenditure and improve metabolic health, BAT has emerged as a promising therapeutic target for combating obesity and related metabolic disorders (15).

Consequently, studying the physiology of BAT is important, as it could revolutionize strategies for managing obesity and metabolic diseases.

1.1.1.3 Adipogenesis in brown adipose tissue

Adipogenesis is the process by which mesenchymal stem cells (MSCs) differentiate into mature adipocytes. While both BAT and WAT adipocytes originate from MSCs, their developmental lineages, transcriptional regulation, and functional specializations differ significantly. BAT adipocytes arise from Myogenic factor 5 (Myf5)-positive progenitors, a lineage shared with skeletal muscle, and are programmed for thermogenesis via UCP1-dependent uncoupling. In contrast, WAT adipocytes derive from Myf5-negative MSCs and specialize in energy storage and endocrine signaling (12). Adipocyte lineage is triggered first by B cell factor-2 (EBF2), which plays an important role in initiating adipocyte commitment (16). Subsequent stimuli, such as bone morphogenetic protein7 (BMP7) (for brown adipogenesis) (17), WNT inhibition (18), or peroxisome proliferator-activated receptor gamma (PPARγ) activators, force the transition of preadipocytes (19). Other key transcription factors, including CCAAT/enhancer-binding proteinβ C/EBPβ (which acts upstream) (20) and PR Domain-Containing 16 (PRDM16), then reinforce adipocyte specification. It is worth noting that PR domain–containing 16 (PRDM16) plays a pivotal role in brown adipogenesis because it activates BAT-specific genes while suppressing those linked to WAT and muscle lineage. (21) The other important step is the coordination of PRDM16 with CCAAT/Enhancer-Binding Protein Beta (C/EBPβ) and proliferator-activated proliferator that result in activation of receptor gamma coactivator 1-alpha (PGC-1α) to promote brown fat metabolic programming, while PGC-1α drives mitochondrial biogenesis. The last step in differentiation is governed by PPARγ, it amplifies the effects of early factors like C/EBPβ to finalize metabolic programming. During the differentiation progresses, preadipocytes acquire

brown adipocyte traits, including UCP1 expression, increased mitochondrial content, and small lipid droplets, ultimately maturing into thermogenically active brown adipocytes (22).

Adipogenesis is regulated by the Sympathetic Nervous System (SNS) in response to stimuli such as cold exposure, which triggers the release of norepinephrine (NE). Then NE acts on beta-adrenergic receptors (β-ARs), particularly the β3-adrenergic receptor in BAT, triggering downstream signaling pathways that promote adipocyte differentiation and thermogenesis (23). It stimulates MSCs for proliferation and preadipocyte for differentiation into mature brown adipocytes (12). Therefore, BAT's thermogenic capacity will be enhanced. NE upregulates key adipogenic regulators like PGC-1α, which induces mitochondrial biogenesis, and PRDM16, which directs precursor cells toward the brown adipocyte lineage. Together, all these mechanisms upgrade BAT function and guarantee efficient energy expenditure and metabolic adaptation during highly demanding energy needs (12).

Similar to WAT, the number of brown adipocytes remains constant throughout adulthood under baseline conditions (24). However, BAT displays enhanced adaptive capacity in response to metabolic or environmental stimuli compared to WAT. This feature allows BAT to shrink or expand in response to various stimuli. For example, cold exposure acutely increases BAT activity, while chronic stimulation can recruit BAT subtypes, such as beige fat (5).

It is important to note that mature brown adipocytes do not proliferate. Instead, BAT homeostasis is regulated by two mechanisms. First, the precursor mesenchymal cells are located within the tissue, which increases their proliferation in response to demand. And second recruit BAT subtypes, such as beige fat (5). This proliferative capacity significantly declines with age (25,26).

1.1.1.4 Lipolysis and lipogenesis in BAT

BAT plays a critical role in adaptive thermogenesis; wherein stored lipids are catabolized to generate heat via mitochondrial uncoupling respiration rather than ATP synthesis.

Thermogenic capacity is primarily fueled by lipolysis (hydrolysis of triglycerides into free fatty acids), which provides substrates for mitochondrial UCP1. In BAT, a counterregulatory interplay between lipolysis and lipogenesis (re-esterification of fatty acids) creates a cycle that enhances energy dissipation and heat production.(5). BAT exhibits markedly elevated lipolytic activity compared to WAT, as the free fatty acids serve as the primary substrate for UCP1-mediated thermogenesis in brown adipocyte mitochondria. Although BAT is not specialized for long-term energy storage, lipogenesis persists at a basal level to maintain a pool of small, multilocular lipid droplets (27). These morphologically distinct droplets facilitate rapid lipid mobilization during sympathetic activation (e.g., cold exposure or β-adrenergic stimulation), ensuring immediate substrate availability for thermogenic demands (27). The lipolysis pathway in WAT and BAT demonstrates both shared regulatory mechanisms and distinct functional outcomes (28). Both tissues rely on β-adrenergic signaling as the primary lipolysis stimulus, which activates the cAMP-PKA pathway. Protein Kinase A (PKA) phosphorylates perilipins (PLIN1 in WAT, PLIN5 in BAT) (29), leading to the release of the coactivator CGI-58 (ABHD5) from PLINs. CGI-58 then binds and activates adipose triglyceride lipase (ATGL), the rate-limiting enzyme that initiates lipolysis by hydrolyzing triglycerides into diacylglycerols (DAGs). Subsequently, hormone-sensitive lipase (HSL) cleaves DAGs into monoacylglycerols (MAGs), and finally, monoacylglycerol lipase (MGL) completes the process, yielding free fatty acids (FFAs) and glycerol (30).

Despite this shared enzymatic cascade, the functional roles of lipolysis differ significantly between WAT and BAT. In WAT, lipolysis is primarily triggered by fasting, releasing FFAs and glycerol into circulation for systemic energy distribution to peripheral tissues (e.g., skeletal muscle, liver). In contrast, BAT lipolysis is activated by cold exposure, and the liberated FFAs are retained intracellularly to fuel UCP1-mediated thermogenesis (28). This fundamental divergence in FFA utilization in systemic energy mobilization (WAT) versus autocrine thermogenesis (BAT) highlights the specialized metabolic roles of these adipose depots (31). FFAs from lipolysis serve functions beyond energy production, as research indicates they also regulate critical signaling pathways involved in maintaining metabolic balance (31). When FFAs bind to fatty acid-binding proteins (FABPs), they can move into the nucleus and influence the activity of peroxisome proliferator-activated receptors (PPARs) (32). Inside the nucleus, these lipids either directly activate PPARs as ligands or indirectly contribute by generating other PPAR-activating molecules, leading to the expression of specific target genes. For example, studies highlight the importance of ATGL-dependent lipolysis in PPARα signaling within cardiac tissue (33). In mice, deleting the ATGL gene disrupts thermogenesis due to weakened PPARα activity, which is necessary for activating brown fat-specific genes like UCP1 (34,35).

While FFAs from lipolysis directly fuel UCP1, their role in PPAR signaling also sustains thermogenic capacity (32). However, maintaining a ready TAG pool for lipolysis requires constant replenishment, which BAT achieves through two primary sources. The first is the uptake of circulating triglyceride-rich lipoproteins (TRLs), such as chylomicrons and VLDL (36). Through the action of lipoprotein lipase (LPL), these particles are broken down into (MAG) and (FFAs), which BAT takes up via scavenger receptor fatty acid translocase (CD36). This process, stimulated by β-adrenergic receptor activation, allows BAT to clear plasma TRLs, contributing to systemic

energy homeostasis (37). Under most conditions, after the uptake of fatty acids, most are utilized for TAG synthesis through a well-defined metabolic pathway.

De novo lipogenesis (DNL) provides a secondary pathway for TAG synthesis in BAT, converting excess carbohydrates into fatty acids. Though most active in liver and WAT, BAT activates DNL under specific stimuli (38). Prolonged cold or carbohydrate surplus triggers DNL to utilize excess glucose (39). Glucose preferentially fuels thermogenesis but can be diverted to DNL when demands shift (40). This pathway primarily replenishes lipid droplets during high-demand states. The DNL pathway begins with glycolysis, converting glucose to pyruvate, which is then transformed into acetyl-CoA by pyruvate dehydrogenase (PDH). Acetyl-CoA carboxylase (ACACA) then catalyzes the formation of malonyl-CoA, which fatty acid synthase (FASN) converts into palmitate—the precursor for longer-chain fatty acids like stearate (41). Unlike in liver and WAT, where insulin primarily regulates DNL, BAT relies more on β-adrenergic signaling to activate this pathway, aligning with its thermogenic role (40).

1.1.1.5 Fatty acid oxidation and mitochondrial biogenesis

The high number of mitochondria in BAT allows this tissue to efficiently oxidize free fatty acids and glucose, a feature that makes it a major oxygen-consuming organ during processes like active non-shivering thermogenesis (5). BAT has three sources of fatty acids for oxidation when demand increases. While it prefers to use fatty acids from the lipolysis of its lipid droplets (42,43), it can also take up non-esterified fatty acids (NEFA) from the bloodstream. The third source is *de novo* lipogenesis. These two other sources are primarily used to replenish fatty acids already consumed from lipid droplets (44).

When activation is acute, the SNS triggers lipolysis. Since fatty acid oxidation takes place in the mitochondrial matrix, the fatty acids need to be transported across mitochondrial membranes. To facilitate this process, the SNS also activates carnitine palmitoyl transferase 1 (CPT1) (42,44), the enzyme that helps shuttle fatty acids into the mitochondria. If activation is chronic, the SNS enhances BAT's overall capacity by increasing PGC1α, a key regulator of mitochondrial biogenesis (45).

Interestingly, BAT has several reasons to prefer the oxidation of fatty acids over glucose for thermogenesis (44): First, FAO produces more acetyl-CoA (8 per palmitate vs. 2 per glucose); second, it's more efficient at generating NADH and $FADH_2$ (5,40); and third (and most importantly), free fatty acids directly activate UCP1(14). During fatty acid oxidation, triglycerides are hydrolyzed into two FFAs and one glycerol molecule. While we have already discussed the role of FFAs in BAT, glycerol also plays an important role in this tissue. Unlike FFAs, most of the glycerol released in BAT is not directly oxidized. Instead, it is primarily released into the bloodstream and transported to the liver, where it serves as a substrate for gluconeogenesis. However, a portion of the glycerol can be recycled within brown adipocytes. In this pathway, glycerol is phosphorylated by glycerol kinase to form glycerol-3-phosphate (G3P), which is then used to re-esterify fatty acids back into triglycerides. This forms a continuous cycle of lipolysis and re-esterification known as the triglyceride–fatty acid (TG–FA) cycle.

The TG–FA cycle is crucial for several reasons. First, it helps maintain intracellular lipid stores, which provide a steady supply of FFAs necessary for sustained fatty acid oxidation and thermogenesis. Second, it prevents the harmful accumulation of excess FFAs, which can be cytotoxic if not properly regulated. Third, it supports metabolic flexibility by enabling BAT to

rapidly replenish its triglyceride stores and maintain thermogenic activity over time. Finally, this cycle contributes to overall energetic efficiency. Although fatty acid re-esterification requires energy, the resulting increase in energy expenditure enhances the thermogenic capacity of BAT, an advantageous adaptation for maximizing heat production. Surprisingly, BAT still takes up a lot of glucose from circulation when it is active. However, studies have shown that less than 15% of this glucose fuels thermogenesis directly (46,47). The rest goes into *de novo* lipogenesis, producing new fatty acids to refill droplets after they've been used up (46,48).

1.1.1.6 Sex Differences in BAT Physiology

Obesity influences susceptibility to chronic diseases such as metabolic syndrome and type 2 diabetes differently in males and females (49). Disruptions in energy homeostasis are a major contributor to these metabolic disorders, and since energy regulation varies by sex, understanding these differences is critical. Additionally, BAT activity plays a key role in energy homeostasis. Therefore, it is essential to investigate the mechanisms driving these sex-based differences (50). Research indicates that female rodents have a higher prevalence of BAT, greater BAT activity, and larger BAT mass compared to males (51,52). Additionally, females display greater metabolic plasticity, as evidenced by studies in which rats fed a high-fat or high-fat, high-sugar diet showed more pronounced increases in thermogenic proteins, mitochondrial biogenesis, and fatty acid oxidation enzymes than their male counterparts (53,54). These findings align with human studies, where retrospective PET/CT scans reveal that women tend to have higher BAT activity than men (55,56). While some research suggests that BAT mass is also greater in women (53,57), other studies reported inconsistent results (58,59). The underlying mechanisms for these sex differences in BAT biology remain an area of active investigation, which will be explored further in this section.

1.1.1.6.1 The effects of sex hormones on BAT

One of the key aspects of BAT activity is its dynamic regulation across the lifespan, which is profoundly influenced by sex hormones (60). This hormonal dependence highlights their critical role in modulating BAT function. For instance, one study showed that during puberty, girls exhibit higher basal BAT activity and greater cold-induced thermogenic responses compared to boys, suggesting that female sex hormones (e.g., estrogen) may enhance BAT activation (61).

In adulthood, women maintain significantly greater BAT activity than men (50), further supporting estrogen's role in promoting metabolic health through BAT (50,60). Another notable shift occurs during menopause: as estrogen levels decline, BAT activity is similarly affected, diminishing alongside the reduction in circulating sex hormones (62).

1.1.1.6.1.1 Estrogens

Estrogen exerts its effects on cells via two receptors, ERα and ERβ, with its influence on BAT primarily mediated through ERα (63). Female mice typically express higher levels of these receptors (64), and cold exposure further upregulates their expression in females. This elevated receptor expression promotes mitochondrial biogenesis and increases both UCP1 mRNA and protein levels (64,65).

Evidence shows that ovariectomy in mice, which depletes estrogen, reduces UCP1 expression, whereas systemic estrogen administration restores it (66,67). Moreover, mice lacking the ERα receptor in BAT show markedly lower UCP1 levels and a diminished response to cold exposure (68).

Key metabolic processes involved in thermogenesis, such as fatty acid oxidation, depend on the activation of Adenosine Monophosphate-activated Protein Kinase (AMPK) pathways as an initial step. Estrogen further enhances BAT activity by stimulating these pathways, thereby amplifying metabolic responses. Beyond its direct receptor-mediated effects, estrogen indirectly activates BAT through the Sympathetic Nervous System (SNS), a critical regulator of BAT function (66).

1.1.1.6.1.2 Androgens

In contrast to estrogens, androgens, particularly testosterone and its metabolite dihydrotestosterone (DHT), inhibit BAT function (50). The literature suggests that testosterone suppresses BAT activity in males by decreasing mitochondrial biogenesis, reducing BAT differentiation, and ultimately impairing BAT mass and thermogenic capacity (86-88).

Additionally, while norepinephrine, as mentioned earlier, induces lipolysis in BAT, testosterone has been shown to attenuate this lipolytic response (69). Further evidence from *in vitro* studies reveals that testosterone dose-dependently inhibits UCP1 expression and mitochondrial respiration in immortalized BAT cells (70).

Crucially, orchiectomy studies (surgical removal of testes, which depletes testosterone) provided *in vivo* evidence for testosterone's inhibitory role: castrated male mice show elevated UCP1 mRNA levels and increased protein expression, confirming that testosterone negatively regulates BAT activation (71,72).

1.1.1.6.2 X-Linked Genes and Their Impact on Sex-Related Differences

A key difference between males and females lies in their sex chromosomes: males typically have XY chromosomes, while females have XX. During development, one of the two X chromosomes

in females undergoes X-chromosome inactivation (XCI) to balance gene expression between the sexes (73). However, approximately 15–20% of genes on the inactivated X chromosome escape this silencing mechanism, leading to higher expression of certain genes and proteins in females (74).

Notably, some genes encoding mitochondrial proteins are located on the X chromosome, and a subset of these can escape XCI (75). As a result, females may have an increased dosage of these genes, which can influence mitochondrial morphology, quantity, and function. This differential gene expression may contribute to sex-specific metabolic differences. One example is thermogenesis, a mitochondria-dependent process critical for energy expenditure and heat production, which may vary between males and females due to these underlying genetic and mitochondrial distinctions (74).

1.1.2 Prohibitin

Prohibitin 1 (PHB1) is an evolutionarily conserved protein that belongs to the SPFH superfamily, which includes stomatin, flotillin, and HflK/C proteins (76). This protein family is found in a broad range of living organisms, from basic prokaryotes to more advanced eukaryotes (76). A defining trait of PHB1 is its conserved SPFH (also known as Band-7 or PHB) domain, which is a signature feature shared among members of this protein family (77). The protein's structure includes several key elements: an N-terminal transmembrane region that mediates attachment to both mitochondrial and plasma membranes, a C-terminal coiled-coil motif (spanning amino acids 175-252) essential for forming heterodimers with PHB2, and the C-terminal region includes a sequence that enables the protein to be transported out of the nucleus (77). The functional relationship between PHB1

and PHB2 is highly mutual, they form a heterodimeric complex where the absence of either subunit can compromise mitochondrial structure and function (78).

The name "prohibitin" reflects its initial characterization as a potential cell cycle inhibitor. Researchers first isolated PHB1 through comparative RNA analysis between normal and regenerating liver tissue, noting its significantly reduced levels in actively dividing cells (79). Later studies demonstrated that this apparent growth-suppressive effect was mediated by regulatory sequences in its mRNA's 3' untranslated region (3' UTR) rather than the PHB1 protein itself (80). Moreover, PHB1 has been found to be associated with the B-cell receptor and is sometimes called B-cell receptor-associated protein 32 (BAP32) (81). This name comes from its role in helping B cells send signals, which is important for the immune response (81).

Similarly, PHB2 is known as BAP37 and repressor of estrogen receptor activity (REA). As REA, PHB2 directly binds ERα's ligand-binding domain to repress estrogen-responsive transcription by blocking coactivator recruitment and altering helix-12 conformation. PHB1 also acts as an ERα corepressor, overexpression inhibits target gene expression, and forms stabilizing heteromers with PHB2 that fine-tune repression through cross-squelching.(82,83). These names point to its role in B-cell receptor and estrogen-related signaling pathways, respectively.

Overall, these different names for PHB1 and PHB2 reflect both the historical context in which they were first discovered and the diverse functions they perform in cell communication. Moreover, mouse and human PHB1 are almost identical at the protein level and assemble into the same mitochondrial prohibitin complex, so mechanistic data from mouse (and other rodent) models are generally applicable to human PHB1 biology, with the usual caveats regarding species- and tissue-specific physiology (84).PHB1 and PHB2 are two distinct proteins with differences in

their genetic location, size, and molecular weight. The *PHB1* gene is found on human chromosome 17q21.33 and encodes a protein of 272 amino acids with a molecular weight of about 30 kDa, whereas *PHB2* is located on chromosome 12p13.31 and encodes a 299–amino acid protein of approximately 33 kDa (85). What makes prohibitin particularly important to study is its versatility and involvement in numerous essential cellular processes (86–88).

1.1.2.1 Mitochondrial and Cellular Functions of PHB1

Studies have expanded our understanding of PHB1, revealing its compartment-specific functions that extend beyond the mitochondria and influence a broad range of cellular processes. PHB1 is essential for preserving mitochondrial integrity by forming a large scaffolding complex with PHB2 in the inner mitochondrial membrane (IMM) (89). This complex helps stabilize important proteins like cytochrome c oxidase subunits (COX2p, COX3p) and the mitochondrial fusion protein OPA1 mitochondrial dynamin like GTPase (OPA1) (89,90), which are crucial for maintaining the proper shape of mitochondrial cristae. PHB1 also binds to mitochondrial transcription factor A (TFAM), linking it to mitochondrial nucleoids and supporting mtDNA transcription (91). Loss of either PHB1 or PHB2 leads to mitochondrial dysfunction and structural abnormalities, emphasizing their cooperative role in mitochondrial maintenance (78).

Outside the mitochondria, PHB1 can move to the plasma membrane (PM) through a post-translational modification called palmitoylation at PHB1-Cys69 (92). At the membrane, it helps regulate signaling pathways that control cell growth, such as PI3K-Akt and MAPK-ERK, particularly in insulin response (92). PHB1 also plays a role in immune regulation by participating in B-cell and T-cell receptor signaling (93–95). Interestingly, PHB1 on the cell surface can act as

a receptor for certain viruses, including dengue and Chikungunya, allowing them to enter the cell (96,97).

PHB1 is also present in other parts of the cell, including the nucleus, where it may affect gene expression, and in various organelles, where it contributes to lipid metabolism and cellular stress responses (98). Altogether, PHB1 plays a wide range of roles that are vital for maintaining cellular balance.

1.1.2.2 The Role of PHB1 in Adipose Tissue

Research into the role of PHB1 in lipid regulation first gained traction in studies using *Caenorhabditis elegans*, where PHB1 depletion was shown to significantly reduce lipid accumulation in the intestine, the organism's main fat storage tissue (99). These early observations suggested a conserved role for PHB1 in energy storage. Further analysis in *C. elegans* demonstrated that PHB1 influences lipid metabolism through its regulation of SBP-1, the worm homolog of mammalian SREBP-1, a key transcription factor in lipogenesis (100). Mechanistically, PHB1 supports mitochondrial function, including cristae integrity and oxidative capacity (90), which provides substrates such as acetyl-CoA necessary for lipogenesis. Simultaneously, PHB1 stabilizes nuclear-encoded mitochondrial proteins that influence *Sbp-1* transcription. For example, knockdown of *Phb-1* results in ~40% reduction in *Sbp-1* expression .These dual roles place PHB1 at a pivotal point in lipid homeostasis, as it influences both the metabolic machinery and the transcriptional regulation required for lipid synthesis (100,101).

Building on these findings, studies in murine models revealed PHB1's essential role in mammalian adipose tissue homeostasis. Adipocyte-specific deletion of *Phb1* in mice leads to a dramatic reduction in fat mass, defective adipogenesis, and resistance to high-fat diet–induced obesity,

resembling a lipodystrophic phenotype (102). Conversely, mice with adipocyte-targeted overexpression of PHB1 display increased fat accumulation, enlarged adipocytes, and expanded WAT mass (104). These opposing outcomes highlight the importance of PHB1 not only in adipocyte differentiation but also in lipid storage capacity, suggesting that PHB1's effects depend on context, potentially influenced by metabolic state or hormonal signals.

Beyond its mitochondrial roles, PHB1 also localizes to the plasma membrane of adipocytes and endothelial cells, where it participates in fatty acid uptake. Specifically, it interacts with CD36, a fatty acid translocase, and annexin A2, a scaffolding protein within lipid rafts. PHB1 binds annexin A2 to form a lipid raft domain that anchors CD36 on the cell surface, enhancing its ability to capture and transport non-esterified fatty acids (NEFAs) (105). Loss of PHB1 disrupts this membrane complex, resulting in reduced surface localization of CD36 and a corresponding decrease in fatty acid uptake (106). Conversely, PHB1 overexpression enhances CD36 surface retention and promotes greater lipid influx. This membrane-associated role of PHB1 is crucial not only in adipocytes, where it supports triglyceride storage, but also in endothelial cells, where it facilitates lipid trafficking between tissues (105,107).

Collectively, these findings underscore the evolutionary conservation of PHB1 as a key player in lipid metabolism. In mammalian adipose tissue, PHB1 functions as a multifaceted regulator, coordinating mitochondrial performance, adipocyte differentiation, and lipid transport across cellular compartments.

While previous studies have revealed PHB1's cellular roles in fatty acid transport and adipocyte function, its systemic metabolic effects remain poorly understood. To bridge this gap, our lab developed a transgenic mouse model (Mito-Ob) with adipose-specific PHB1 overexpression,

achieved by introducing a transgene encoding PHB1 under the control of the adipocyte protein 2 (*aP2,* also known as *Fabp4*) promoter in CD1 background mice. Since aP2 is expressed in both macrophages and adipocytes, this model allows us to investigate how elevated PHB1 levels in adipose tissue and macrophages influence whole-body metabolism, including potential effects on energy balance, lipid distribution, and insulin sensitivity (104).

The primary observation from the Mito-Ob model is the pronounced sexual dimorphism in response to PHB1 overexpression. Both male and female mice accumulate excess adipose tissue; however, only males develop significant metabolic complications, including insulin resistance, hepatic lipid accumulation, hyperglycemia, and tumor development. In contrast, females remain metabolically healthy despite equivalent fat mass. This suggests that adipose expansion alone does not determine metabolic risk, and that hormonal context, particularly sex steroids, modulates PHB1's effects on metabolism (104).

One potential explanation for these differences lies in PHB1's role in maintaining mitochondrial health. While obesity is typically associated with reduced mitochondrial content and impaired function in WAT, PHB1 overexpression in Mito-Ob mice appears to preserve mitochondrial biogenesis and activity. This is supported by evidence of elevated mitochondrial DNA copy number, enhanced expression of genes involved in oxidative phosphorylation, and increased mitochondrial density (104). PHB1 thus contributes to both adipocyte differentiation and mitochondrial maintenance, potentially mitigating the mitochondrial dysfunction commonly observed in obesity (108).

Interestingly, while mitochondrial biogenesis is enhanced in both sexes, only female Mito-Ob mice display increased adiponectin levels, an adipokine linked to insulin sensitivity and anti-

inflammatory signaling. In males, this coupling between mitochondrial health and adiponectin production is disrupted (104). This sex-specific decoupling suggests that downstream signaling mechanisms governing adipokine secretion may differ between males and females, contributing to the divergent metabolic phenotypes (109).

The sexually dimorphic effects of PHB1 in Mito-Ob mice appear to be shaped by the interaction between PHB1 and sex steroid hormones. PHB1 is both regulated by and a regulator of hormone receptor activity: it functions as a transcriptional corepressor of estrogen receptor alpha (ERα) and androgen receptor (AR), while its own expression is enhanced by estrogen and suppressed by testosterone. Given that adipose tissue itself has steroidogenic capacity, these mutual interactions likely contribute to depot-specific and sex-dependent regulation of PHB1 activity (104).

Experimental evidence from gonadectomy studies supports this idea. In males, orchiectomy not only reduces body fat but also lowers PHB1 and OPA1 expression in adipose tissue, suggesting that androgens are required to maintain the full adipogenic and mitochondrial effects of PHB1 overexpression (110). In females, ovariectomy removes their natural protection, resulting in tumor formation and insulin resistance similar to that seen in males. These outcomes underscore the importance of estrogen in enabling PHB1's beneficial effects, particularly in sustaining mitochondrial homeostasis and suppressing inflammatory responses (104,111).

Moreover, hormonal regulation of mitochondrial proteins appears to occur independently of PHB1. In both wild-type and Mito-Ob mice, sex hormone deprivation leads to reduced expression of OPA1, a mitochondrial fusion protein critical for maintaining cristae structure and oxidative capacity. This suggests that sex steroids directly support mitochondrial integrity in WAT, and that this support operates in parallel with, but is not contingent upon, PHB1 overexpression (104).

In summary, PHB1 serves as a central regulatory node linking mitochondrial function, lipid metabolism, and sex hormone signaling in adipose tissue. Its overexpression in the Mito-Ob model highlights how fat accumulation can lead to markedly different outcomes depending on hormonal context. In females, the synergistic effect of estrogen and PHB1 promotes metabolically adaptive adipose expansion, characterized by preserved mitochondrial integrity and increased adiponectin production. In males, lack of estrogenic signaling and the suppressive effects of testosterone on PHB1 impair these protective mechanisms, leading to metabolic dysfunction and disease.

These findings reinforce the need to consider biological sex as a fundamental variable in metabolic research. They also point to PHB1 as a potential therapeutic target, where modulation of its expression or function, possibly in a sex-specific manner, could offer novel strategies to prevent or treat obesity-associated metabolic disorders.

1.1.2.3 The Post-translational modifications of PHB1

Post-translational modifications (PTMs) are essential biochemical mechanisms that expand protein function beyond the genetic code (112). These covalent modifications, including phosphorylation, glycosylation, acetylation, ubiquitination, and palmitoylation, are catalyzed by specific enzymes and regulate nearly every aspect of protein behavior, including activity, stability, localization, and interaction networks (112,113). By modulating protein function in response to environmental cues, PTMs provide dynamic and reversible control over complex biological processes. For instance, phosphorylation can activate or inhibit enzymes, ubiquitination often directs proteins toward degradation, and lipidation, such as palmitoylation, enables membrane association. The physiological significance of PTMs is broad, encompassing gene expression, metabolic regulation, immune signaling, and cellular stress adaptation. Dysregulation of PTMs

contributes to pathologies ranging from cancer and neurodegeneration to metabolic syndromes, underscoring their central role in maintaining cellular and systemic homeostasis (112,114,115).

Given their regulatory potential, PTMs represent an important layer of control for PHB1, a multifunctional protein that governs mitochondrial integrity, adipocyte differentiation, and systemic metabolic balance. Although overexpression of PHB1 in adipocytes in Mito-Ob mice profoundly alters adipose tissue biology and whole-body metabolism, changes in gene or protein abundance alone cannot fully account for PHB1's tissue-specific, sexually dimorphic, and hormone-dependent effects (116). Complementary *in vitro* study demonstrated that insulin stimulation induces phosphorylation of PHB1 at tyrosine 114 (Tyr-114), enabling recruitment of SH2 domain-containing phosphatase 1 (Shp1). Shp1 negatively regulates insulin signaling by dephosphorylating intermediates such as Akt and GSK-3β, thereby attenuating insulin responsiveness (117). Mutation of PHB1-Tyr114 to phenylalanine (mutant-PHB1-Tg mice), which prevents phosphorylation, blocks Shp1 recruitment and enhances Akt phosphorylation, sustaining insulin signaling. This regulation is site-specific: other residues, such as Thr-258, have been implicated in opposite roles, potentially promoting insulin sensitivity (116,118). Furthermore, crosstalk between phosphorylation and other PTMs, such as O-GlcNAcylation, highlights the existence of a multilayered regulatory network fine-tuning PHB1's metabolic actions (119).

To evaluate the physiological importance of PHB1-Tyr114 phosphorylation *in vivo*, the m-Mito-Ob mouse model was developed in our laboratory, in which the PHB1Y114F mutant form was overexpressed in adipocytes under the *aP2* gene promoter. Comparative analysis of m-Mito-Ob and Mito-Ob mice revealed that, despite comparable adiposity, m-Mito-Ob mice displayed improved insulin sensitivity and distinct immune phenotypes. These findings indicate that PHB1-

Tyr114 phosphorylation functions as a molecular switch, selectively modulating insulin responsiveness and immune regulation without disrupting PHB1's adipogenic role (120).

To further investigate how hormonal cues shape PHB1 function and its PTM landscape, gonadectomy experiments were performed in both male and female Mito-Ob and m-Mito-Ob mice. Removal of gonadal androgens and estrogens allowed assessment of the contribution of sex hormones to PHB1-mediated regulation. In gonadectomized m-Mito-Ob mice, reduced adiposity, enhanced insulin sensitivity, and attenuated mitochondrial biogenesis in WAT were observed, demonstrating that PHB1's metabolic effects are partially hormone-dependent (110). Nonetheless, depot- and sex-specific differences in PHB1 localization and signaling persisted in the absence of sex hormones, suggesting the involvement of additional, uncharacterized PTMs in PHB1 regulation (110).

This hypothesis led to the investigation of modifications beyond phosphorylation. Sequence analysis of vertebrate PHB1 identified a conserved cysteine at position 69 (Cys69), structurally positioned for lipid-based modification (92). Experimental studies confirmed that PHB1-Cys69 undergoes palmitoylation, a lipid modification essential for PHB1 localization to the plasma membrane in adipocytes and immune cells (92). Loss of this modification, through substitution of cysteine with alanine (PHB1C69A), disrupted PHB1 membrane localization and signaling, establishing palmitoylation at PHB1-Cys69 as a critical determinant of PHB1 function (92).

To dissect the physiological relevance of these PTMs *in vivo*, two knock-in mouse models were generated in our laboratory using CRISPR-Cas9 technology: one carrying the *Phb1-Ki*Y114F mutation, which prevents phosphorylation at PHB1-Tyr114, and another carrying the *Phb1-Ki*C69A mutation, which blocks palmitoylation. Both models express PHB1 at normal levels but

solely in the mutant form. These precise genetic modifications provide powerful tools to define how individual PTMs direct PHB1's metabolic, signaling, and tissue-specific functions.

Together, findings from these models underscore the importance of PTMs in shaping PHB1's context-dependent actions. Rather than acting through a fixed mechanism, PHB1 integrates signals *via* a combinatorial PTM code that modulates its role across tissues and physiological states. Crosstalk between modifications, such as the mutual exclusivity of phosphorylation and O-GlcNAcylation, further refines its actions (119). Palmitoylation at PHB1-Cys69 is indispensable for plasma membrane anchoring and scaffolding functions, whereas PHB1-Tyr114 phosphorylation governs insulin sensitivity and immune cell regulation (121). Additional modifications, including redox-sensitive S-nitrosylation, may expand PHB1's repertoire in stress responses and mitochondrial control (122).

As PHB1 emerges as a protein with striking tissue specificity (78), investigating the consequences of its PTMs in physiologically relevant models is critical. In this thesis, particular attention is devoted to characterizing BAT in the *Phb1-Ki*Y114F *and* C69A *knock-in* models. Comprehensive analysis of BAT morphology, mitochondrial abundance, protein expression, and thermogenic capacity will clarify how distinct PTMs shape PHB1's function in this metabolically unique tissue. This work advances our mechanistic understanding of PHB1 regulation and provides insights with broad implications for metabolic disease, tissue-specific signaling, and therapeutic intervention.

1.1.2.4 The Role of PHB1 in BAT Metabolism and Phenotype

Emerging studies highlight a pivotal role for prohibitin proteins, particularly PHB1, in shaping mitochondrial function within BAT. Prohibitins are well recognized as scaffolding proteins that maintain cristae architecture and stabilize respiratory chain super complexes, , in diverse cellular

models (90,123,124),While this role is well established in non-adipose systems and white adipocytes, evidence specific to BAT is more limited. Nonetheless, given BAT's dense mitochondrial network and reliance on oxidative metabolism during thermogenesis, PHB1's influence on mitochondrial stability is highly relevant (125).

The first direct exploration of PHB1 in BAT was performed by Gao et al. 2021, who demonstrated that adipocyte-specific deletion of PHB1 disrupted BAT development. This loss impaired lipid accumulation, reduced mitochondrial content, and downregulated thermogenic markers such as UCP1 and PGC-1α. Functionally, PHB1-deficient mice displayed reduced energy expenditure and poor cold tolerance, underscoring PHB1's dual role in sustaining mitochondrial structure and enabling metabolic activation. Importantly, reintroducing PHB1 rescued these defects, confirming its essential role in maintaining brown adipocyte identity and thermogenic competence (102).

Complementing this, Wang et al. (2022)(126) examined PHB1 deletion in adipocytes under high-fat diet conditions, highlighting its metabolic significance in BAT. In their study, loss of PHB1 caused a reduction in BAT mass, altered droplet morphology, and impaired lipid storage capacity. These defects reduced BAT's ability to buffer circulating lipids, which in turn aggravated hepatic steatosis in diet-challenged mice. Interestingly, while BAT structural and metabolic functions were compromised, the absence of PHB1 did not exacerbate hepatic inflammation or fibrosis, suggesting that its role in protecting systemic metabolism lies primarily in sustaining BAT integrity and lipid handling (126).

Another work by Gao et al. (2022) (127) introduced another perspective by identifying a non-mitochondrial role for PHB1 in BAT, specifically within endothelial cells. Using an endothelial cell-specific *Phb1* knockout (EC-KO) mouse model, they demonstrated that PHB1 is essential for

efficient transport of long-chain fatty acids (LCFAs) across the vascular endothelium into brown adipocytes. In *Phb1*EC-KO mice, fatty acid uptake into BAT was significantly impaired, not due to intrinsic defects in adipocytes, but because of disrupted endothelial transport. Although basal BAT vascularization and thermogenic gene expression remained intact, these mice exhibited impaired triglyceride clearance and diminished lipolytic fatty acid release upon stimulation. As a result, there was a compensatory metabolic shift toward increased glucose utilization, leading to enhanced insulin sensitivity under high-fat diet conditions (127). Mechanistically, PHB1 was proposed to facilitate LCFA trafficking through interactions with CD36 and annexin A2. Thus, beyond its canonical mitochondrial functions, PHB1 also acts as a vascular gatekeeper, ensuring that brown adipocytes receive sufficient lipid substrates for thermogenic activation and systemic lipid regulation. This feature has also seen in WAT (127).

Evidence from the Mito-Ob mouse model further supports PHB1's role in BAT. In this model, adipocyte-specific overexpression of PHB1 led to sex-dependent alterations in BAT morphology. Male Mito-Ob mice exhibit an increase in lipid droplet size, deviating from the typical small, multilocular structure of healthy brown adipocytes, suggesting a shift toward lipid accumulation and potential dysfunction. In contrast, female Mito-Ob mice maintain normal multilocular droplet morphology, indicating preserved brown adipocyte identity. These findings highlight the tissue-specific and sexually dimorphic effects of PHB1 (104). At the mitochondrial level, no increase in mitochondrial number was observed in either sex; however, mitochondrial size was found to be reduced in males. Despite these structural changes, thermogenic protein levels such as UCP1 remain unaltered, suggesting that PHB1 overexpression does not activate thermogenic programming in BAT (104).

Mechanistically, previous studies have shown that PHB1 promotes cross-talk between mitochondrial and nuclear genomes, supporting transcriptional programs essential for oxidative metabolism (98), processes that are also critical in BAT (128).

Collectively, these findings establish PHB1 as a central regulator of mitochondrial content, lipid handling, and metabolic homeostasis in BAT, with its effects modulated by tissue type, sex, and hormonal environment. However, several aspects of PHB1's role in BAT remain underexplored. While existing studies have elucidated its involvement in adipocyte differentiation, mitochondrial respiration, lipid metabolism, and redox balance, questions remain regarding the regulation of PHB1 by sex hormones, its potential interaction with immune cells within BAT, and how its function changes with age. Future research should aim to clarify these molecular mechanisms and explore sex-specific interventions to leverage PHB1's metabolic benefits

1.1.2.5 The Role of PHB1 in Glucose Homeostasis

The role of PHB1 in glucose homeostasis is closely tied to its involvement in various cellular processes and its context-dependent function. That is, PHB1's effects can differ depending on the tissue type and the organism's metabolic state. According to current literature, several tissues and signaling pathways have been identified in which PHB1 contributes to glucose regulation. In the pancreas, PHB1 helps protect β-cells against oxidative stress by maintaining mitochondrial function and also plays a role in insulin secretion (129). In granulosa cells, overexpression of PHB1 leads to a shift toward glycolysis, especially under conditions of mitochondrial dysfunction (130). The role of PHB1 in adipose tissue appears to be more complex. While adipocyte-specific overexpression of PHB1 promotes obesity, only male mice develop glucose intolerance and fatty liver, suggesting a sex-specific metabolic effect (131). Additionally, PHB1 regulates glucose and

fatty acid metabolism partly through modulation of key enzymes such as pyruvate carboxylase (132). In the liver, the consequences of PHB1 deficiency differ between sexes: in males, it is associated with insulin resistance and increased adiposity, while in females, it improves glucose tolerance, possibly by reducing gluconeogenic activity (131). These findings reflect systemic roles of PHB1 in energy balance. At the signaling level, PHB1 has also been linked to the insulin pathway. It interacts with phosphatidylinositol (3,4,5)-trisphosphate (PIP3) and undergoes important post-translational modifications such as phosphorylation at PHB1-Tyr114 and O-GlcNAcylation, which may influence downstream protein kinase B (Akt) signaling and cellular glucose uptake (116,119,133). Altogether, PHB1 emerges as a versatile regulator of glucose metabolism, with effects that vary depending on the cellular and physiological context.

1.2 Research rationale

Adipose tissue in mammals comprises several distinct types, white, brown, and beige each playing specialized roles in systemic energy metabolism (4). WAT acts as the body's principal energy store, with unilocular adipocytes accumulating large lipid droplets found in subcutaneous layers (beneath the skin) and around internal organs (visceral fat) (4). In contrast, BAT consists of multilocular adipocytes harboring numerous mitochondria rich in uncoupling protein 1 (UCP1), localized predominantly in the interscapular, cervical, and supraclavicular regions in infants, and persisting as smaller depots in adults (125). BAT is uniquely equipped for non-shivering thermogenesis, producing heat by dissipating energy (134), while beige adipocytes represent inducible, thermogenic cells that transiently develop within WAT in response to stimuli such as cold exposure, acquiring BAT-like properties but reverting to a white phenotype once the stimulus

diminishes (135). These depots differ not only in anatomical location and cellular morphology but also in metabolic function, with WAT storing and BAT expending energy (4).

Like the well-known sex differences in WAT (136), BAT also exhibits marked sex differences (137). In both rodents and humans, females tend to possess higher BAT mass and more active thermogenic capacity than males (137). These sex-dimorphic traits are observed in depot size, UCP1 expression, mitochondrial content, and responsiveness to metabolic challenges. For example, female rodents display greater upregulation of BAT thermogenic genes and more substantial mitochondrial adaptations compared to males, and human imaging studies frequently report more active BAT in women (137,138). However, the magnitude and consistency of these differences can vary between different anatomical depots and populations.

Sex steroids play a decisive role in shaping this BAT dimorphism. Estrogen, via ERα signaling, enhances BAT development, stimulates mitochondrial biogenesis, boosts UCP1 expression, and promotes thermogenic responsiveness, particularly in females (139). Loss of estrogen, whether due to menopause or experimental ovariectomy, leads to decreased BAT activity, while estrogen replacement restores thermogenic competence (140). Conversely, androgens such as testosterone exert inhibitory effects on BAT, reducing mitochondrial abundance and functional capacity (66). Experimental studies, including orchiectomy in males, reinforce that removing testosterone partially rescues BAT thermogenesis. These findings highlight that sex hormone signaling is central to the regulation of BAT mass and function (141).

This raises a key mechanistic question: How do sex hormones mediate their regulatory effects on BAT? While classical nuclear hormone receptor pathways are well-studied, the molecular targets

and intracellular mediators that translate hormonal cues into adipose-specific metabolic adaptation remain incompletely defined.

Prohibitin 1 (PHB1) emerges as a potential candidate in this context. PHB1 is a highly conserved scaffold protein, best known for its roles in organizing mitochondrial structure, maintaining their cristae integrity, and ensuring efficient oxidative metabolism (78). Yet PHB1's influence extends far beyond mitochondria; it can localize to the plasma membrane, nucleus, and other cellular compartments depending on its post-translational modifications and cellular context (78). Importantly, PHB1 is increasingly recognized as an integrator of metabolic and hormonal signals, participating in insulin signaling, immune responses, and cellular stress pathways. This multifaceted relationship with sex hormones, including regulation of its expression and function by both estrogens and androgens (111), positions PHB1 as a plausible mediator of sex-specific metabolic regulation in adipose tissue, particularly in BAT. Thus, PHB1 is a potential candidate gene for sex-related metabolic differences.

Focusing on BAT is especially justified for several reasons. First, BAT plays a critical role in energy expenditure and thermoregulation and is central to observed sex differences in systemic metabolism (142). Second, prior studies using the Mito-Ob mouse model (characterized by adipocyte-specific PHB1 overexpression) revealed profound sex-specific phenotypes: both WAT and BAT developed metabolic alterations, but males and females differed in susceptibility to insulin resistance, lipid accumulation (104). More recent work and additional literature confirm the essential function of PHB1 in BAT mitochondrial maintenance and thermogenesis, yet the intracellular mechanisms remain unsettled (102,127).

Although it is established that PHB1 is required for BAT health and metabolic function, how PHB1 mediates these effects within BAT, especially in response to hormonal cues, remains unknown. *In vitro* and *in vivo* studies have revealed that phosphorylation of PHB1 at tyrosine 114 (Tyr-114) responds to insulin, recruiting negative regulators such as SHP1 and modulating metabolic signaling (117). However, observations from the m-Mito-Ob mouse model (overexpressing a non-phosphorylatable mutant) suggest there must be additional, more complex regulatory layers, since metabolic phenotypes extend beyond the effects explained solely by PHB1-Tyr114 phosphorylation (120).

Cysteine 69 (Cys69) appears as a likely candidate for such regulation, as it is the unique site for palmitoylation, a lipid modification that governs PHB1's trafficking to the plasma membrane and its interaction with signaling partners (92).

Given the sex-dimorphic role of BAT in energy balance and the centrality of PHB1 in mitochondrial and metabolic regulation, it would be interesting to know how specific PTMs (at PHB1-Tyr114 and PB1-Cys69) direct PHB1 activity within BAT. The development of targeted knock-in mouse models creates a unique opportunity to unravel, at a systemic and depot-specific level, the combinatorial mechanisms through which hormonal signals and post-translational modifications converge to control BAT function and, by extension, sex-specific metabolic health.

CHAPTER II. HYPOTHESIS AND OBJECTIVES

Sex differences play an important role in various aspects of metabolism, including energy balance, fat distribution, and how adipose tissue functions (136). BAT in particular shows distinct sex-specific features. For example, females typically have more active BAT and higher thermogenic capacity compared to males. These differences are largely driven by sex steroid hormones, which influence not only BAT activity but also the molecular pathways that control its development and function (142).

In this context, PHB1 has gained attention as a key regulatory protein in adipose tissue (126). PHB1 is a highly conserved multi-functional protein that undergoes PTMs, including palmitoylation at Cys69 site and phosphorylation at Tyr114 site. These modifications determine intracellular trafficking of PHB1, and different location influences its function (104,116,143). However, the importance of these conserved PTM sites (i.e., Cys69 and Tyr114) in biological sex-related differences in BAT biology is unexplored.

Given PHB1's dual role in metabolic and hormonal pathways, I hypothesize that the PTM at Cys69 and Tyr114 sites plays a role in PHB1's cell compartment-specific functions and contribute to the sex-specific regulation of BAT. To test this, I am using *Phb1* knock-in mouse models to examine how mutating Cys69 and Tyr114 PTM sites affect PHB1 function in males and females, with the goal of understanding how these molecular mechanisms shape sex differences in BAT.

Objective 1. ***To define changes in the BAT phenotype in male and female Phb1-Ki mice as compared to respective wild-type mice***.

The goal of this objective is to characterize how BAT phenotype is altered in male and female *Phb1*-mutant mice carrying either the *Phb1-Ki*C69A or *Phb1-Ki*Y114F mutation, compared to

their wild-type counterparts. This analysis will focus on identifying both genotype and sex-dependent differences in BAT phenotype, which includes morphology, metabolic activity, and biochemical features, all of which may result from disruptions in PHB1 post-translational modifications.

Objective 2. ***Investigate the effects of gonadectomy on BAT phenotype in male and female Phb1-Ki mice.***

This objective is focused on understanding how sex hormones influence the phenotype and metabolic function of BAT in *Phb1*-mutant mice carrying the *Phb1-Ki*C69A or *Phb1-Ki*Y114F mutations, in comparison to wild-type controls. To begin, I will establish the baseline metabolic profile of BAT in wild-type mice under normal hormonal conditions to capture natural sex differences. I will then assess how removing gonadal sex hormones through surgical gonadectomy could impact BAT phenotype across different genotypes. Finally, I will investigate how the specific post-translational modifications of PHB1, disrupted in the *Phb1-Ki*C69A and *Phb1-Ki*Y114F mutants, interact with the presence or absence of gonadal sex hormones to influence BAT function. This approach will help clarify how PHB1 modifications and hormonal signaling work together to regulate BAT biology in a sex-dependent manner.

CHAPTER III. MATERIALS AND METHODS

3.1. Materials

Materials and reagents used in this thesis are listed in Table 3.1.

Reagent	**Source**
4x Laemmli Sample Buffer	Bio-Rad
Acrylamide	Fisher Scientific
Ammonium persulfate	Fisher Scientific
2-mercaptoethanol	Sigma-Aldrich
80% Ethanol (Molecular Biology Grade)	Thermo Scientific
Bis-acrylamide	Fisher Scientific
Bromophenol blue	Bio-Rad
Formalin	Fisher Scientific
Isopropanol	Fisher Scientific
KCl	Sigma-Aldrich
Glycine	Fisher Scientific
HCl	Fisher Scientific
Insulin	Sigma-Aldrich
NaCl	Fisher Scientific
NaOH	Fisher Scientific
PhosSTOP (phosphatase inhibitors)	Roche
Tris base	Fisher Scientific
Triton X-100	Fisher Scientific

Tween-20	Amresco
D-(+)-glucose	Sigma-Aldrich
Ponceau S Solution	Sigma-Aldrich (Mississauga, ON, Canada)

3.2 Methods

3.2.1 Development of *Phb1-Ki* mice

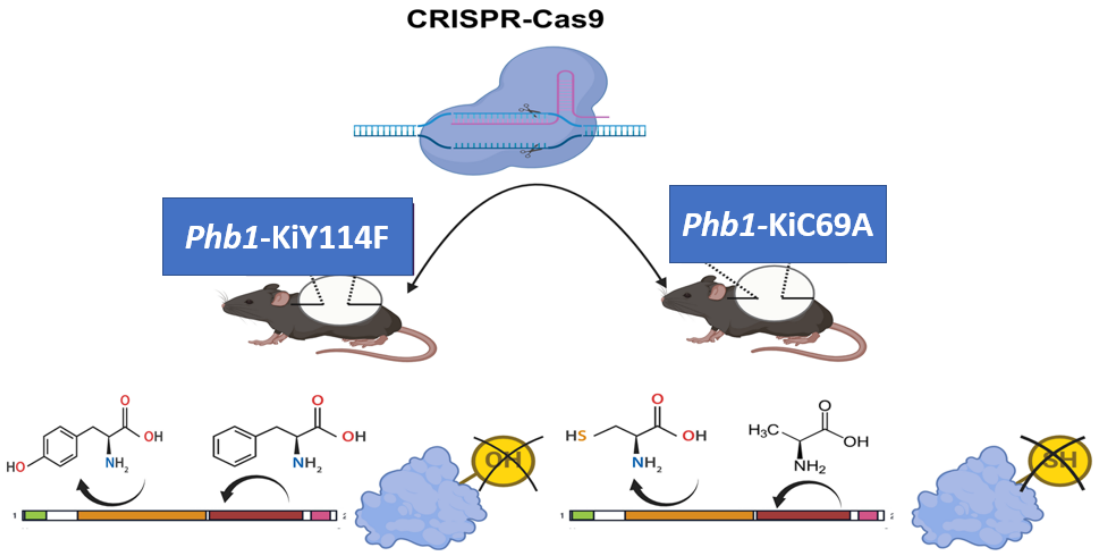

Figure 3.1 Generation of *Phb1-Ki* mouse models by CRISPR-Cas9.CRISPR-Cas9 mediated genome editing was used to create two *Phb1 knock-in* lines: *Phb1-Ki* Y114F, in which the tyrosine at position 114 was mutated to phenylalanine to prevent phosphorylation, and *Phb1-Ki* C69A, in which the cysteine at position 69 was mutated to alanine to prevent palmitoylation or other cysteine-based modifications, as illustrated by the loss of the corresponding post-translational modification icons on the PHB1 schematic

The *Phb1 knock-in* mouse lines were generated at the University of Manitoba's Transgenic Core Facility through CRISPR-Cas9-mediated genome editing (143). In the C69A variant, the codon for cysteine at position 69 was substituted with one encoding alanine. Additionally, a Hae III restriction site was introduced to facilitate genotyping, and the protospacer adjacent motif (PAM) sequence was altered in the donor DNA to avoid repeated cleavage by Cas9. Genomic DNA was isolated from ear punch biopsies, and homozygosity was determined by PCR amplification of the targeted region, enzymatic digestion using Hae III, and subsequent analysis by agarose gel electrophoresis.

Similarly, for the Y114F model, the codon for tyrosine at position 114 was substituted with one encoding phenylalanine at this position in the *Phb1* gene. Genotyping of offspring was performed using PCR amplification, and successful incorporation of the mutation was confirmed via DNA sequencing. As with the C69A model, homozygous mice were selected based on PCR amplification followed by gel electrophoresis of the amplicons. Homozygous Phb1 knock-in mutants were selected to achieve complete disruption of the targeted post-translational modifications (Cys69 palmitoylation or Tyr114 phosphorylation), ensuring maximal phenotypic penetrance in BAT without partial compensation from wild-type alleles, which is critical for detecting subtle mitochondrial and metabolic effects. Heterozygous Phb1 mutants generally lack spontaneous phenotypes but show increased susceptibility to stressors like hepatotoxicity in liver-specific models, suggesting subthreshold effects that may not manifest under baseline conditions. The C57BL/6 background strain was used, as it is the standard at the University of Manitoba's Transgenic Core Facility, providing well-characterized BAT activity, genetic stability, and extensive wild-type metabolic reference data for robust comparisons (144).

3.2.2 Animal Housing and Tissue Collection

All animal procedures were conducted in accordance with protocol number 24-023 (AC11900), approved by the University of Manitoba's animal ethics committee. Mice were housed under standard conditions with unrestricted access to a regular chow diet and maintained on a 12-hour light/dark cycle. Tissues were harvested promptly and either processed immediately or snap-frozen in liquid nitrogen and stored at –80°C for future experiments.

3.3 BAT weight measurements

In this study, BAT was consistently collected from the interscapular region in all animals. Immediately after sacrifice, the tissue was snap-frozen and placed on ice.

3.4 Histology

BAT from the interscapular region was collected from 3- to 4-month-old mice immediately after euthanasia and fixed in 10% buffered formalin. Tissues were then dehydrated, embedded in paraffin, and sectioned at a thickness of 5 μm. The sections were stained with hematoxylin and eosin (H&E) for morphological evaluation. Imaging was performed using the EVOS XL Core Imaging System at 40× magnification. And the pictures are utilized for two purposes cell counting and measuring adipose area. One image was acquired per animal (n = 3), each representing a carefully selected region of BAT. Due to the close embedding of BAT with surrounding beige and white fat, additional fields of view were not included, as they risked capturing non-BAT regions and introducing bias because beige adipose tissue can represent compromised BAT. Only clearly distinguishable BAT regions were analyzed to ensure tissue specificity.

3.5 Quantification of Cell Number in BAT Sections

To quantify cell number in BAT, hematoxylin and eosin (H&E)–stained sections were imaged at 40× magnification using the EVOS XL Core Imaging System. Images were analyzed using ImageJ software (NIH, USA). Each image was first converted to 8-bit grayscale, followed by color deconvolution to isolate the hematoxylin (blue) channel for enhanced nuclear contrast. Thresholding was applied to highlight nuclei while minimizing background and debris, and the image was converted to binary format. The "Analyze Particles" function was used to count individual nuclei. To exclude non-cellular elements and artifacts, a size filter was applied, and only particles with areas between 250 and 2000 pixels² were included in the analysis. This range corresponds approximately to nuclei sizes between 20 and 150 μm² based on the imaging scale. Only nuclei fully within the field of view were counted.

3.6 Adipose Area Quantification in Histological Images

BAT sections stained with hematoxylin and eosin (H&E) were imaged at 40× magnification. To measure the lipid-rich (white) regions, images were analyzed using a threshold-based segmentation method. Each image was first converted to grayscale to improve contrast between adipose areas and surrounding tissue. A brightness threshold was then applied to detect and isolate the white spaces corresponding to lipid droplets. Sensitivity settings were fine-tuned through visual inspection to account for variability in staining intensity and droplet size. The identified adipose regions were quantified in square micrometers (μm²) using the pixel-to-micron scale associated with 40× magnification. For images with low contrast or incomplete detection, threshold sensitivity was increased to improve accuracy. These measurements were used to compare lipid content between experimental groups.

3.7 Gonadectomy

3.7.1 Animal Models and Surgical Procedures

12 weeks old male and female C57BL/6 mice were used as wild-type controls, alongside two *Phb1 knock-in* models including C69A or Y114F. The number of animals per group, categorized by sex, genotype, and surgical treatment (sham or gonadectomy), is summarized in Table 3.2.

Animals were anesthetized using 2–4% isoflurane delivered in oxygen, and anesthesia depth was verified by the absence of a response to toe pinch. Subcutaneous injection of Metacam (2 mg/kg) was administered subcutaneously for postoperative analgesia. Mice were monitored during recovery and for three days post-surgery for changes in body weight and signs of discomfort or distress. Additional analgesic doses were provided if it was required.

Sham-operated animals underwent identical anesthetic, surgical, and postoperative procedures as those in the gonadectomy groups, with the exception that gonads were left intact. In these cases, the reproductive organs were exposed, visually examined, and then the surgical incisions were closed using the same method as the gonadectomy group.

3.7.2 Orchidectomy (male gonadectomy)

For male gonadectomy, mice were placed in a supine position, and a midline incision (~1 cm) was made in the scrotum to expose the underlying tunica. Each testis was carefully extracted, and the spermatic cord was ligated at the junction with the epididymis and blood vessels. The testes were then excised. In sham-operated males, testes were exposed but not removed or manipulated. Skin incisions were closed with wound clips, and all animals received equivalent postoperative care.

3.7.3 **Ovariectomy** (female gonadectomy)

For female gonadectomy, mice were positioned prone, and a dorsal midline skin incision (1–2 cm) was made between the ribcage and the tail base. Using blunt dissection, the muscle wall was exposed and pierced ~1 cm lateral to the spine on both sides. The ovary and oviduct were externalized, and the uterine vasculature was clamped. Each ovary and part of the oviduct were removed with a single cut. Sham females underwent the same procedure without excision of the ovaries. Incisions were closed with surgical clips, and postoperative care was identical to that of the gonadectomy group.

Table 3.2 Experimental grouping of mice by sex, treatment, and genotype (WT, C69A, Y114F). Sham = control surgery; Ox = gonadectomy (orchidectomy or ovariectomy).

Sex	Treatment	Wild-type	C69A *Phb1* knock-in mice	Y114F *Phb1* knock-in mice
Male	Sham	2	2	2
	Ox	4	4	4
Female	Sham	2	2	2
	Ox	4	4	4

***** One of the female shams C69A *Phb1* knock-in mice died after surgery. The analysis will report with one.

3.8 Glucose Tolerance Test (GTT) and Insulin Tolerance Test (ITT)

At six months of age, corresponding to twelve weeks post-surgery, glucose and insulin tolerance tests were performed. For the glucose tolerance test (GTT), food was withdrawn for 12 hours overnight (10:00 p.m. to 10:00 a.m.). To prevent ingestion of bedding or waste during fasting, mice were transferred to fresh cages and housed individually with free access to water. The following morning, mice were gently restrained using a tube, and a baseline blood glucose measurement was obtained from the tail vein (time 0). Mice then received an intraperitoneal injection of sterile-filtered glucose (1 g/kg body weight, dissolved in saline). Blood glucose levels

were subsequently measured from tail blood samples collected at 15, 30, 60, and 120 minutes post-injection using a handheld glucometer and test strips according to the manufacturer's instructions.

For the insulin tolerance test (ITT), a similar procedure was followed, with the exceptions that mice were fasted for 4 hours (6:00 a.m. to 10:00 a.m.) and injected intraperitoneally with insulin (0.75 U/kg body weight). Blood glucose concentrations were measured at 0, 15, 30, 60, and 120 minutes following insulin administration using the same glucometer-based method.

For both GTT and ITT, glucose measurements over time were summarized by calculating the area under the curve (AUC) using the trapezoidal method, in which the area between consecutive time points was calculated as the average of the two glucose values multiplied by the corresponding time interval. Total AUC values were used for statistical comparisons between experimental groups.

3.9 Statistical Analysis

All statistical evaluations were conducted using GraphPad Prism (version 10). Based on the nature of each dataset, we applied one-way ANOVA, two-way ANOVA, or repeated measures ANOVA as required. For group comparisons, Tukey's test was used following ANOVA. When comparing treatment groups directly to controls, either Dunnett's post hoc test or an unpaired Student's t-test was employed. Results are reported as the mean with corresponding standard deviation (mean ± SD), and a threshold of $P < 0.05$ was used to determine statistical significance.

In experiments involving BAT tissue, wild-type C57BL/6 mice were used as the reference group to evaluate phenotypic differences in *Phb1-Ki* lines carrying C69A or Y114P mutations. For metabolic assessments such as GTT and ITT, statistical comparisons focused on the effects of

gonadectomy by analyzing differences between sham-operated and hormone-depleted mice across genotypes and sexes.

To improve clarity and ease of interpretation, GTT data for the C69A and Y114F groups are presented separately. When all six experimental groups were included in a single plot, substantial overlap of glucose curves resulted in crowded figures that obscured group-specific trends. Importantly, all GTT data were analyzed using the same statistical methods across groups, and separation was performed solely for visualization purposes.

CHAPTER IV. RESULTS

4.1 *Phb1-Ki* Mice Display Altered Whole-Body Weight in a Sex-Dependent Manner

Prohibitin-1 (PHB1) is known to influence adipocyte differentiation in a sex-dependent manner(145). Since adipocyte differentiation plays a critical role in regulating whole-body weight (146), understanding PHB1's mechanisms in adipose tissue development and metabolic regulation is important. Previous studies on PHB1-Tg (Mito-Ob) mice have demonstrated that overexpression of PHB1 in WAT leads to increased body weight (104). However, the potential role of the key post-translational modifications (PTMs) of PHB1 on body weight regulation at a systemic level remains unexplored. In this study, female *Phb1-Ki*C69A mice exhibited significantly higher body weight compared to age-matched wild-type females ($P = 0.0015$) (Fig. 4.1A). Although *Phb1-Ki*Y114F females also showed elevated body weight relative to wild-type, this difference did not reach statistical significance (Fig. 4.1A). In male mice, body weights of both *Phb1-Ki*C69A and *Phb1-Ki*Y114F were not significantly different from their wild-type counterparts (Fig. 4.1A). When comparing sexes within each genotype, *Phb1-Ki*Y114F males weighed significantly more than *Phb1-Ki*Y114F females ($P = 0.0024$; Fig. 4.1B). A similar pattern was observed in wild-type mice, with males displaying significantly higher body weights than females ($P = 0.0007$) (Fig. 4.1B). In contrast to the typical pattern observed in wild-type and *Phb1-Ki*Y114F mice, male *Phb1-Ki*C69A mice did not weigh more than the females; instead, female *Phb1-Ki*C69A mice tended to have greater body weight than their male counterparts, but this difference did not reach statistical significance (Fig. 4.1B).

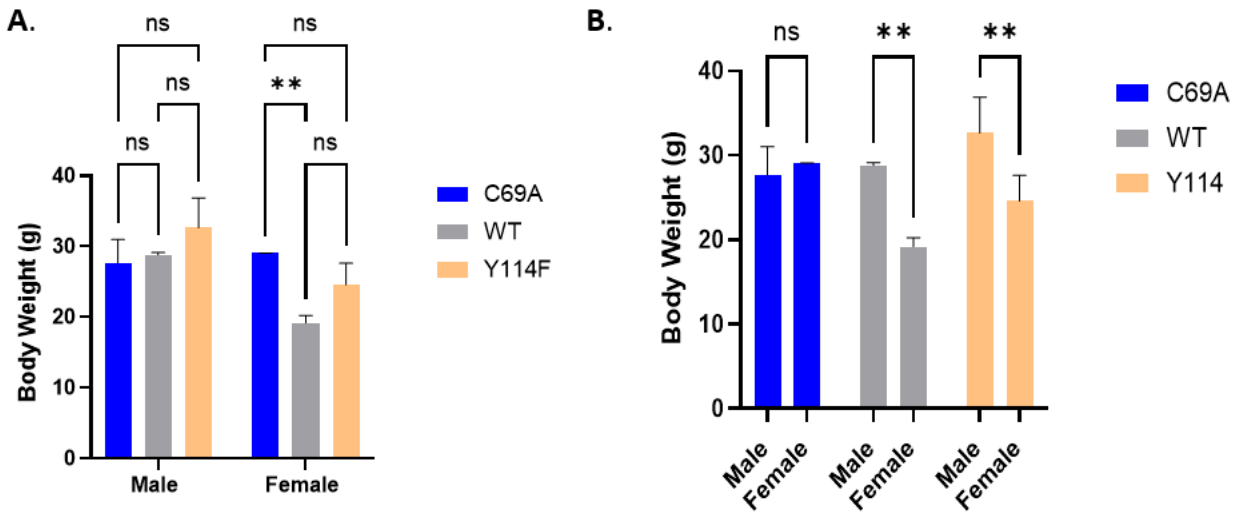

Figure 4.1. *Phb1-Ki* mice show sex- and genotype-dependent differences in body weight. (A) Body Weight (g) by genotype within sex (C69A, WT, Y114F). (B) Body Weight (g) by sex within genotype. Bars represent mean ± SD (n = 3 mice). Statistics: two-way ANOVA (genotype × sex) followed by Tukey's multiple-comparisons test; $P < 0.05$ considered significant. **$P \leq 0.01$.

4.2 BAT Mass in Male and Female *Phb1-Ki* Mice

Previous work from our laboratory demonstrated that overexpression of PHB1 in adipose tissue alters BAT characteristics (104). The interscapular BAT depot was collected and weighed, and its ratio to total body weight was calculated. Preliminary observations from a single biological sample revealed BAT as a percentage of body weight of approximately 0.2% in wild-type males, 0.4% in *Phb1-Ki*C69A males, and 0.4% in *Phb1-Ki*Y114F males. In females, ratios were approximately 0.2% in wild-type, 0.4% in *Phb1-Ki*C69A, and 0.2% in *Phb1-Ki*Y114F mice (Fig. 4.2). It is important to note the limitations that these data represent initial observations from single animals per group (n=1) and therefore cannot support statistical conclusions about genotype effects or sex differences. The apparent differences in BAT: body weight ratios require validation in adequately powered studies with larger, prospectively calculated sample sizes. In comparable rodent metabolic studies, formal power analyses frequently indicate a need for group sizes in the range of 6–8 animals per group before meaningful conclusions can be drawn(147).

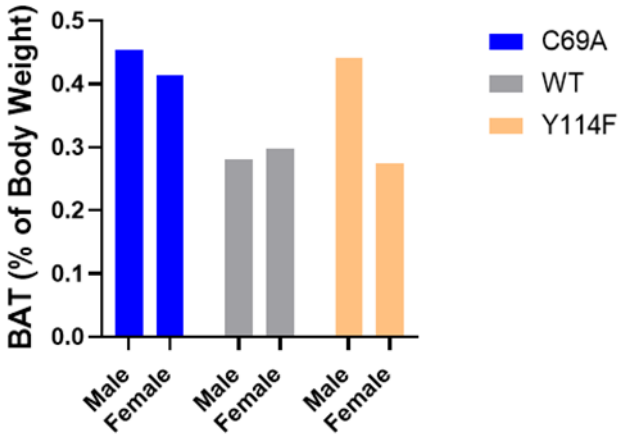

Figure 4.2. BAT as a percentage of body weight in *Phb1-Ki* mice, including *Phb1-Ki*C69A, *Phb1-Ki*Y114F, and wild-type controls. Data are shown for both males and females for each genotype; n = 1 mice. No statistical analysis was performed due to the limited sample size.

4.3 Quantification of BAT Cell Number and in *Phb1-Ki* Mice

Studying adipocyte number and adipose area in the BAT of *Phb1-Ki* mice is essential because PHB1 plays a key role in maintaining mitochondrial structure (99) and regulating BAT cell development (102). Mutations in PHB1 that prevent specific post-translational modifications may interfere with these functions, potentially altering BAT composition and organization. A decrease in cell number could suggest defects in adipocyte formation or recruitment of precursor cells. At the same time, shifts in fat area may signal abnormalities in lipid accumulation, mitochondrial performance, or thermogenic function. Although previous studies have shown that loss of PHB1 reduces BAT mass and impairs mitochondrial function (102), the specific role of PHB1 C69 and Y114 sites on cellular features of BAT, such as adipocyte proliferation and lipid droplet structure, has not yet been investigated. Quantitative analysis of BAT cell numbers from hematoxylin and eosin (H&E) stained BAT sections demonstrated no significant differences between wild-type, *Phb1-Ki*C69A, and *Phb1-Ki*Y114F mice within either sex (Fig. 4.3A). However, notable sex-specific differences in cell number were observed within genotypes. In *Phb1-Ki*Y114F mice, females exhibited significantly greater BAT cell numbers per field compared to their male counterparts ($P = 0.0001$), and a similar pattern was observed in *Phb1-KiC69A* mice ($P = 0.0009$) (Fig. 4.3B). In contrast, wild-type mice showed no significant sex difference in BAT cell number. These results indicate that PHB1 mutations, particularly at C69A and Y114F, are associated with an increased number of BAT in females relative to males, whereas this sex difference is absent in wild-type controls.

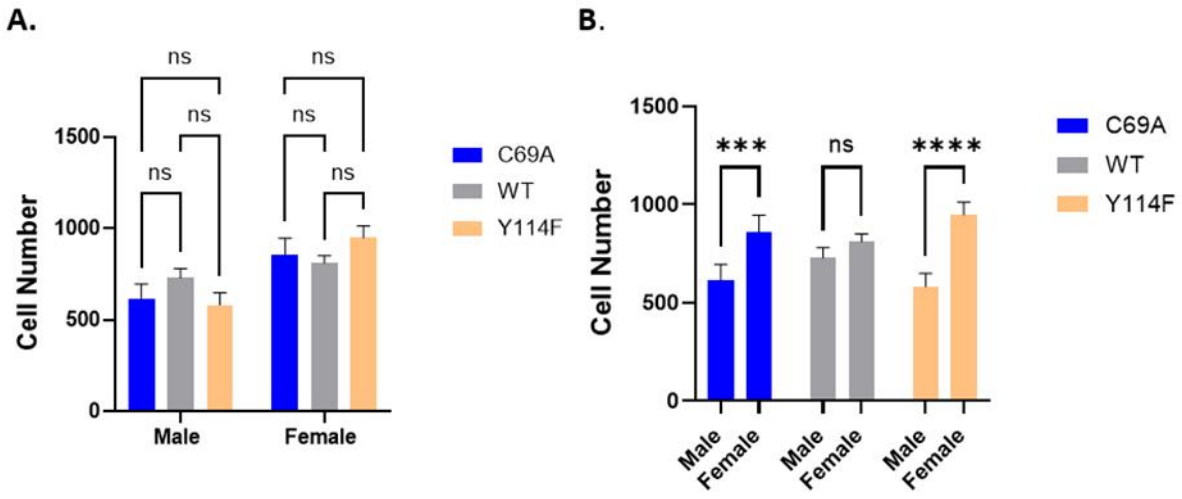

Figure 4.3. BAT cell number per field was quantified in hematoxylin and eosin (H&E) stained BAT sections from *Phb1-Ki* (C69A, Y114F) and WT mice. (A) Data are grouped by genotype within sex (C69A, WT, Y114F). (B) Data are grouped by sex within genotype. Bars represent mean ± SD (n = 3 mice). Statistics: two-way ANOVA (genotype × sex) followed by Tukey's multiple-comparisons test; $P < 0.05$ considered significant. ***: $P \leq 0.001$; ****: $P \leq 0.0001$; ns: not significant.

4.4 Quantification of BAT and Adipocyte Area in *Phb1-Ki* Mice

Quantitative analysis of BAT adipocyte area revealed that male *Phb1-Ki*C69A mice exhibited significantly greater average adipocyte area compared to wild-type males ($P < 0.0001$), while the difference between male *Phb1-Ki*Y114F and male wild-type mice was not statistically significant (Fig. 4.4A). Additionally, adipocyte area in male *Phb1-Ki*C69A mice was significantly larger than that in male *Phb1-Ki*Y114F mice ($P < 0.0001$) (Fig. 4.4A). In female mice, *Phb1-Ki*C69A animals exhibited significantly greater BAT area compared to wild-type females ($P = 0.0313$), whereas the difference between *Phb1-Ki*Y114F and wild-type females did not reach statistical significance (Fig. 4.4A). Furthermore, female *Phb1-Ki*C69A mice showed a significantly larger adipocyte area than female *Phb1-Ki*Y114F mice ($P = 0.007$).

Comparison between sexes within each genotype showed that, for all genotypes analyzed (*Phb1-Ki*C69A, wild-type, and *Phb1-Ki*Y114F), male mice consistently displayed higher adipocyte area than their female counterparts, with the difference reaching statistical significance ($P < 0.0001$ for *Phb1-Ki*C69A and *Phb1-Ki*Y114F, $P < 0.001$ for wild-type) (Fig. 4.4B). These results indicate that the *Phb1-Ki*C69A mutation leads to pronounced adipocyte hypertrophy in male mice, and highlight a robust sex effect whereby males of all genotypes possess greater adipose area than females.

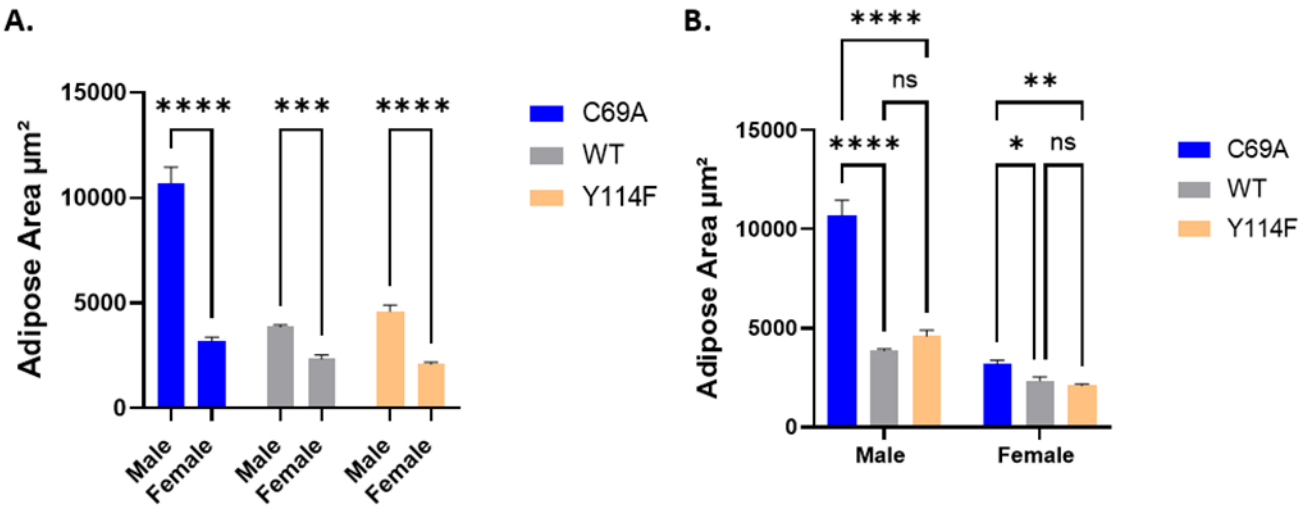

Figure 4.4. Adipocyte area (µm²) in BAT was quantified from histological sections by genotype and sex (*Phb1-KiC69A, Phb1-KiY114F, and WT*). (A) Data are grouped by genotype within sex; (B) data are grouped by sex within genotype. Bars represent mean ± SD (n = 3 mice). Statistical analysis was performed using two-way ANOVA (genotype × sex) followed by Tukey's multiple-comparisons test; $P < 0.05$ was considered significant. * = $P \leq 0.05$, ** = $P \leq 0.01$ ***: $P \leq 0.001$; ****: $P \leq 0.0001$; ns: not significant.

4.5 *Phb1-Ki*C69A and *Phb1-Ki*Y114F Knock-in Mice Display Differences in BAT Morphology and Function

The combined analysis of BAT morphology and cellularity highlights distinct effects of the *Phb1* mutations. The *Phb1-Ki*C69A mutation appears to promote BAT expansion primarily through increased lipid accumulation and tissue hypertrophy. In contrast, the *Phb1-Ki*Y114F mutation leads to an increase in relative BAT mass in males with a slight change in adipocyte size or number.

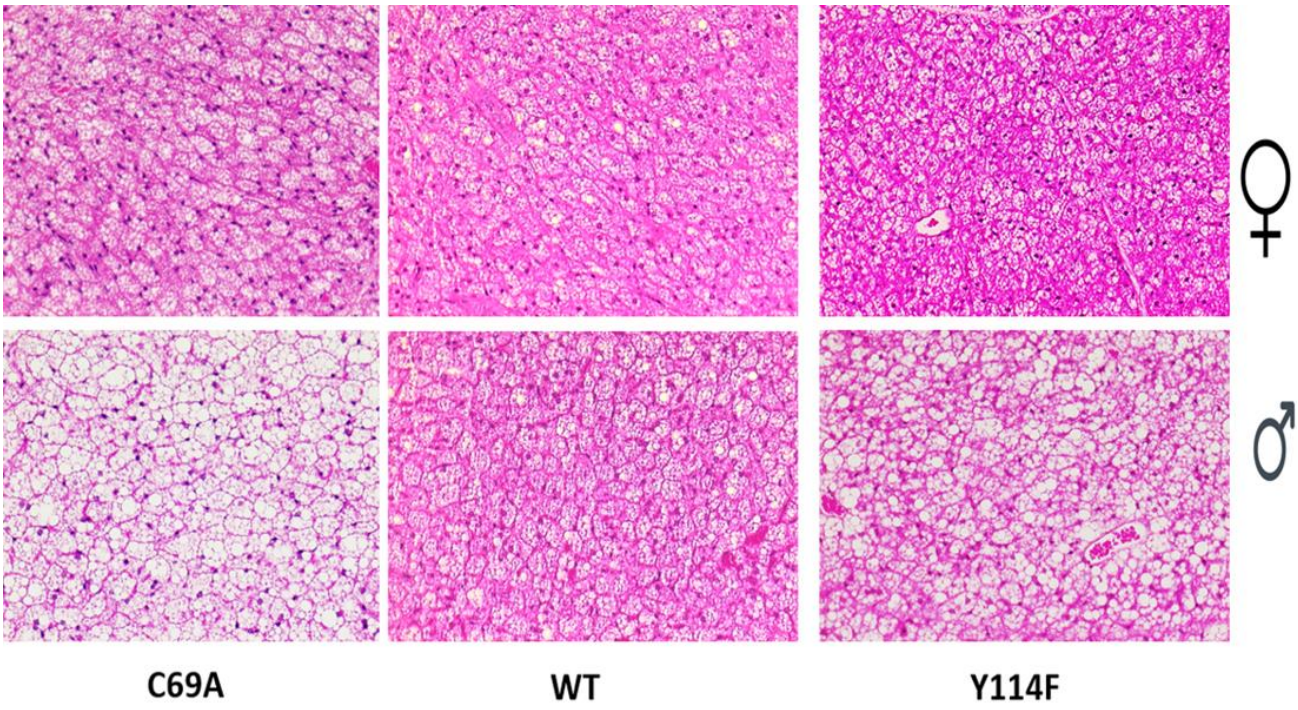

Figure 4.5. Representative histological images of BAT in *Phb1-Ki* mice. Hematoxylin and eosin (H&E) stained BAT sections from female (top row, ♀) and male (bottom row, ♂) wild-type, *Phb1-Ki*C69A, *and Phb1-Ki*Y114F mice at 40× magnification.

4.6 Transmission Electron Microscopy Reveals Mitochondrial Variations in BAT by Genotype and Sex

One of the primary roles of PHB1 is to maintain mitochondrial structure (149). Previous studies have shown that PHB1 influences mitochondrial morphology through its regulation of key fission and fusion proteins (150). Preliminary electron microscopy analysis of BAT mitochondria in *Phb1-Ki* mice revealed alterations in cristae density and mitochondrial shape. In *Phb1-Ki*C69A males, mitochondria frequently displayed elongated shapes with a near-complete loss of cristae compared to wild-type. In contrast, *Phb1-Ki*Y114F females exhibited mitochondria with rounded morphology and densely packed cristae, closely resembling wild-type. These observations are based on examination of single or a limited number of animals per group (n = 1) per genotype and sex, and should be interpreted as preliminary. This data indicates that the importance of Cys69 and Tyr114-linked functions of PHB1 within the BAT has a unique effect on mitochondrial integrity in a sex-dependent manner. TEM analysis showed that modifying specific sites on the PHB1 protein leads to different effects on BAT, depending on both the mutation and the sex of the mouse. In the case of the *Phb1-Ki*C69A mutation, especially in males, we observed disrupted mitochondrial structure in BAT cells. This was associated with increased adipocyte hypertrophy, suggesting enhanced lipid storage (Fig. 4.4A), even though the number of adipocytes didn't change significantly (Fig. 4.3A). In contrast, the *Phb1-Ki*Y114F mutation increased BAT mass mainly in male mice without affecting adipocyte size (Fig. 4.4A) or number (Fig. 4.3A), and in females, it appeared to preserve mitochondrial integrity. These findings can suggest that the *Phb1-Ki*C69A mutation primarily alters mitochondrial function and lipid handling in BAT, while the *Phb1-Ki*Y114F mutation influences BAT mass through a different, likely non-mitochondrial mechanism.

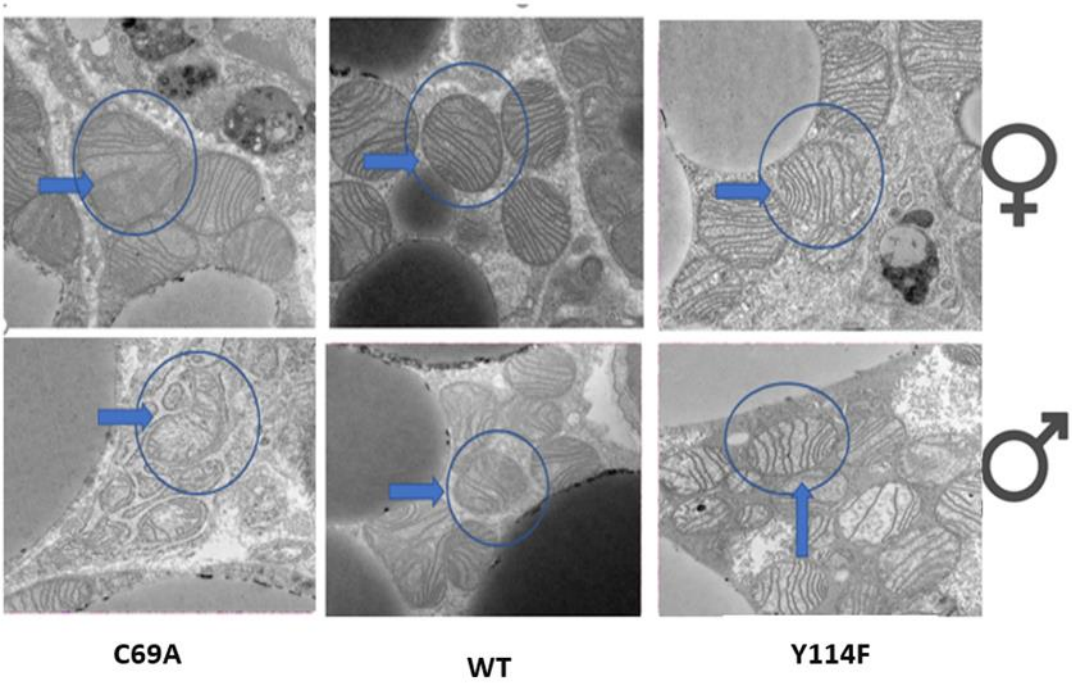

Figure 4.6. Representative electron microscopy images showing mitochondrial ultrastructure in BAT of *Phb1-Ki* mice by sex and genotype. Columns from left to right represent *Phb1-Ki*C69A, wild-type, and *Phb1-Ki*Y114F genotypes. The top row shows images from female mice, and the bottom row from male mice. Blue arrows and circles highlight mitochondria within BAT cells. Magnification = 25000×

4.7 Effects of gonadectomy on body weight in *Phb1-Ki* mice

Phb1-Ki (*Phb1-Ki*C69A *and Phb1-Ki*Y114F) alter BAT morphology and mitochondrial structure in a sex-dependent manner. To examine the potential link between the impact of these mutations on BAT with male and female sex hormones, gonadectomy was performed at the age of 3 months (post-puberty), followed by a 3-month metabolic adaptation period which defined as the time required for mice to physiologically adjust and for metabolic parameters to stabilize in response to the absence of circulating gonadal hormones, before tissue collection. Given the established roles of PHB1 in BAT function (102), adipose tissue homeostasis (103), and glucose metabolism (130), we assessed changes in whole-body weight and BAT mass, glucose tolerance, and insulin sensitivity. This experimental approach is supported by previous findings that sex hormones regulate BAT thermogenesis (60) and mitochondrial integrity, and that PHB1 might mediate these hormonal effects. Analysis of body weight revealed a significant reduction in male wild-type mice following orchidectomy, with orchiectomized animals weighing less than sham-operated controls ($P = 0.01$; Fig. 4.7A). A similar, though non-significant, trend toward lower body weight was observed in *Phb1-Ki*Y114F males post-orchidectomy. In contrast, body weight increased in orchiectomized *Phb1-Ki*C69A male mice; although this change did not reach statistical significance compared to sham-operated *Phb1-Ki*C69A controls (Fig. 4.7A). Notably, orchiectomized *Phb1-Ki*C69A males displayed significantly greater body weight than both orchiectomized wild-type ($P = 0.01$) and orchiectomized *Phb1-Ki*Y114F ($P = 0.001$) male mice. In females, no significant differences in body weight were detected between ovariectomized and sham-operated animals for any genotype (Fig. 4.7B). These results indicate that the effect of gonadectomy on body weight is sex-dependent and further modulated by PHB1 genotype, with

*Phb1-Ki*C69A males uniquely exhibiting increased body weight following testicular hormone removal.

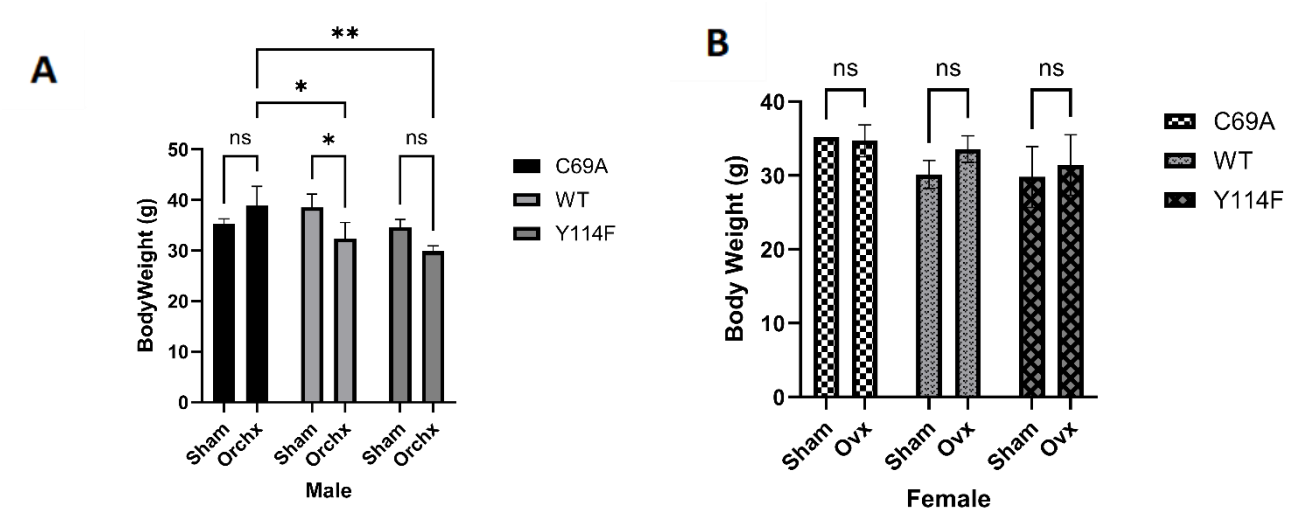

Figure 4.7. Body weight in male and female mice following sham surgery or gonadectomy. (A) Body weight of male mice in each genotype (C69A, WT, Y114F) under sham-operated and orchidectomized (Orchx) conditions. (B) Body weight of female mice in each genotype (C69A, WT, Y114F) under sham-operated and ovariectomized (Ovx) conditions. Bars represent mean ± SD (n = 1–4 mice). Statistical analysis was performed using two-way ANOVA (genotype × surgical status) followed by Tukey's multiple-comparisons test; $P < 0.05$ was considered significant. Significance annotations: ns, not significant; * = $P \leq 0.05$, ** = $P \leq 0.01$.

4.8 Effects of gonadectomy on BAT in *Phb1-Ki* mice

BAT mass is regulated by mitochondrial function and lipid metabolism, processes in which PHB1 plays a central role that is further modulated by sex hormones (9,16,150,151). While PHB1's general importance in mitochondrial integrity and adipose tissue function is well established (82,108), the specific roles of PTMs at PHB1-Cys69 and PHB1-Tyr114 remain to be fully elucidated; current literature does not yet directly address how these individual modifications affect mitochondrial architecture or adipocyte metabolism *in vivo*. These PTMs, however, could plausibly determine PHB1's responsiveness to hormonal signals (104), providing a mechanistic link between post-translational control and metabolic regulation. Measuring BAT mass in *Phb1-Ki* mice with and without gonadectomy can therefore provide critical insights into how PHB1 PTMs and sex hormones collectively modulate BAT homeostasis and metabolic sexual dimorphism. Preliminary data from a single biological sample (n = 1 mice) showed BAT mass as a percentage of body weight (Fig. 4.8B). In male mice, BAT accounted for 0.6% of body weight in *Phb1-Ki*C69A, 0.3% in WT, and 0.4% in *Phb1-Ki*Y114F genotypes under sham-operated conditions. In female mice, sham-operated animals exhibited BAT percentages of 0.5% (*Phb1-Ki*C69A), 0.2% (WT), and 0.6% (*Phb1-Ki*Y114F), whereas ovariectomized animals showed BAT percentages of 0.2% (*Phb1-Ki*C69A), 0.1% (WT), and 0.5% (*Phb1-Ki*Y114F).

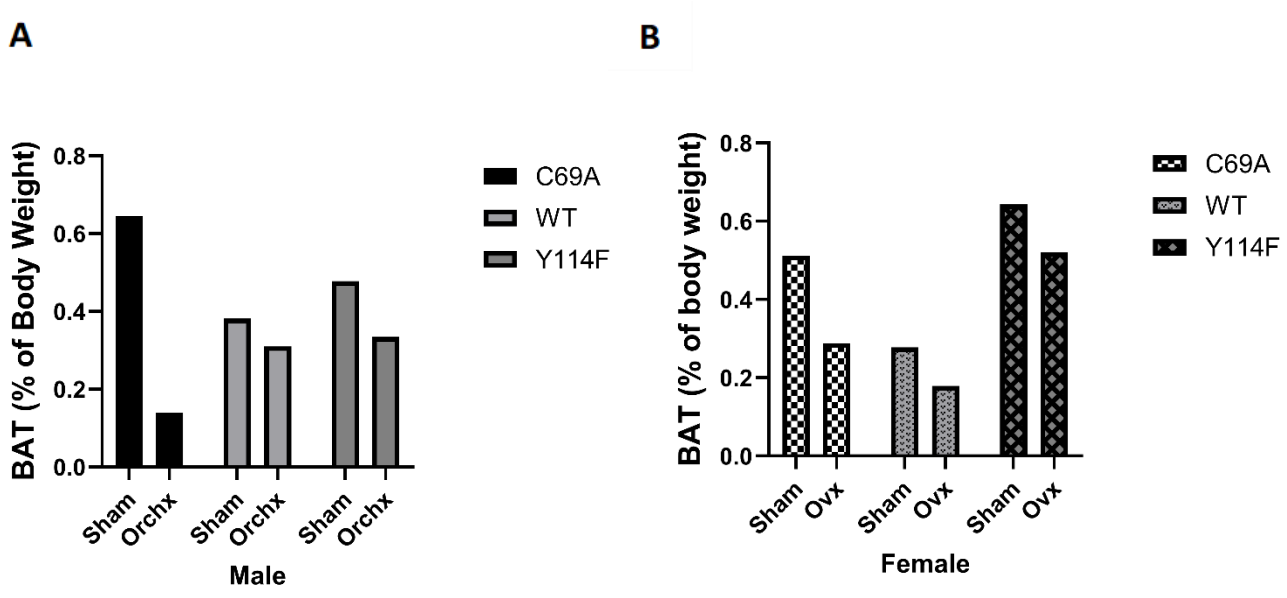

Figure 4.8. BAT as a percentage of body weight in *Phb1-Ki* mice (*Phb1-Ki*C69A, *Phb1-Ki*Y114F) and wild-type controls under sham and gonadectomy conditions. (A) Data for males; (B) data for females. Each bar represents a single biological sample (n = 1 mice); statistical analysis was not performed due to limited sample size.

4.9 Effect of gonadectomy on glucose homeostasis in *Phb1-Ki* mice

Sex steroid hormones are key regulators of metabolic homeostasis, acting through adipose depots to shape energy balance(146). BAT is a major site of glucose disposal and thermogenesis and is strongly sensitive to hormonal status (153). In general, estrogens enhance BAT glucose uptake and mitochondrial performance, whereas androgens are associated with poorer metabolic control (154). In our transgenic work, PHB1-Tg mice become obese regardless of sex, yet impaired glucose regulation emerges predominantly in males, suggesting an interaction between sex steroids and PHB1 in driving sex-dependent metabolic outcomes (104). To probe this relationship further, systemic glucose handling was assessed by conducting GTT and ITT in *Phb1-Ki* mice.

4.9.1 Effect of gonadectomy on glucose homeostasis in *Phb1-Ki* female mice

Glucose tolerance test was performed in female wild-type and *Phb1-Ki*C69A mice to assess how disruption of PTM at PHB1-Cys69 site could affect glucose homeostasis and estrogen responsiveness. We evaluate the effects of genotype (*Phb1-Ki*C69A vs. wild type) and surgical condition (sham-operated vs. ovariectomy) on blood glucose levels over time (Fig. 4.9.1A). Three-way repeated-measures ANOVA of blood glucose during the GTT revealed a significant main effect of time ($F(2.336, 16.36) = 13.57$, $p = 0.0002$), reflecting the expected dynamic changes in glucose levels across time points. No significant main effects of genotype ($F(1, 7) = 1.757$, $p = 0.227$) or surgical status ($F(1, 7) = 0.285$, $p = 0.610$) were detected. No two-way or three-way interactions reached significance (time × genotype: $F(4, 28) = 1.338$, $p = 0.281$; time × gonadal status: $F(4, 28) = 0.634$, $p = 0.643$; genotype × gonadal status: $F(1, 7) = 0.040$, $p = 0.847$; time × genotype × gonadal status: $F(4, 28) = 0.476$, $p = 0.753$). (Fig. 4.9.1A). Specifically, in wild-type females, the AUC increased from approximately 1800 mmol·h/L in sham-operated animals (with intact ovarian hormones) to 2000 mmol·h/L following ovariectomy (absence of circulating ovarian

hormones), representing an ~11% increase. Similarly, *Phb1-Ki*C69A females exhibited an increase in AUC from approximately 1450 mmol·h/L (sham-operated) to 1650 mmol·h/L (ovariectomized), corresponding to a ~14% increase. These results suggest a trend toward impaired glucose tolerance following ovariectomy in both genotypes, likely related to the loss of ovarian sex hormones, although these effects were not statistically significant (Fig. 4.9.1A, B). We also examined glucose hemostasis in female *Phb1-Ki*Y114F mice. The data demonstrated a significant main effect of time on blood glucose levels ($P = 0.0013$) (Fig. 4.9.1C). However, no significant main effects of genotype ($F(1, 8) = 0.102$, $p = 0.758$) or surgical status ($F(1, 8) = 0.106$, $p = 0.754$) were detected. No two-way or three-way interactions reached significance (time × genotype: $F(4, 32) = 0.771$, $p = 0.552$; time × surgical status: $F(4, 32) = 0.300$, $p = 0.876$; genotype × surgical status: $F(1, 8) = 0.117$, $p = 0.741$; time × genotype × surgical status: $F(4, 32) = 0.385$, $p = 0.818$).(Fig. 4.9.1C). This indicates that blood glucose levels changed across time, but the overall pattern and magnitude of these changes were similar between *Phb1-Ki*Y114F females and wild-type controls. AUC analysis provided an integrated assessment of glucose handling throughout the test period. Two-way ANOVA on GTT AUC revealed no significant main effects of genotype ($F(1, 8) = 0.000027$, $p = 0.996$) or surgical status ($F(1, 8) = 0.734$, $p = 0.417$), nor a significant genotype × surgical status interaction ($F(1, 8) = 0.083$, $p = 0.780$). Although statistically significant differences were not detected between groups, trends were observed that may reflect distinct metabolic phenotypes. In wild-type females, AUC increased following ovariectomy from approximately 1850 mmol·h/L (sham-operated) to 2050 mmol·h/L (ovariectomized), representing a ~13% increase. In contrast, *Phb1-Ki*Y114F females exhibited a smaller change in AUC following ovariectomy, rising from approximately 1900 mmol·h/L (sham-operated) to 2000 mmol·h/L (ovariectomized), an increase of ~5%. These differences did not reach statistical

significance, but can suggest that wild-type females may show greater susceptibility to ovariectomy-induced impairments in glucose tolerance compared to *Phb1-Ki*Y114F mutants.

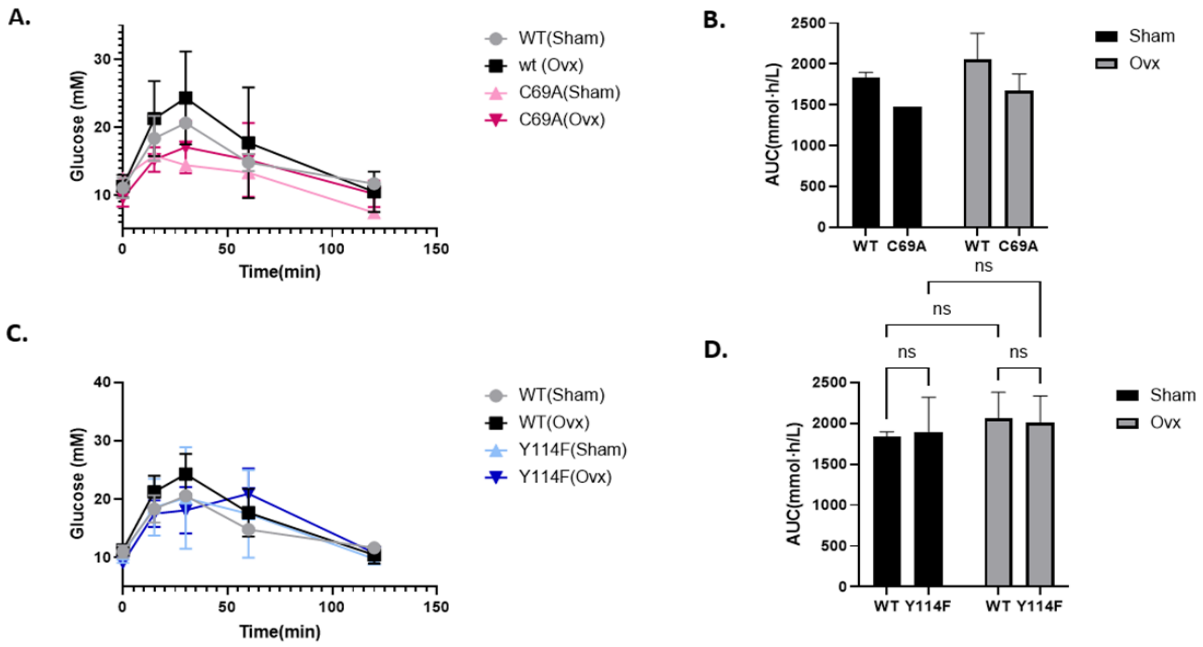

Figure 4.9.1 Glucose Tolerance in Female Wild-Type and *Phb1-Ki* Mice. (**A**) Line graph showing blood glucose levels during the glucose tolerance test in female wild-type and *Phb1-Ki*C69A mice, comparing sham-operated controls and ovariectomized (Ovx) groups. Data are shown as mean ± SD (n = 2–4 mice) for C69A sham SD is not calculated. Statistical analysis was performed using three-way repeated measures ANOVA to compare glucose levels between genotypes, surgery status, and time points during the glucose tolerance test. (**B**) Bar graph presenting AUC analysis from glucose tolerance tests in the same groups as panel A. Data are shown as mean ± SD (n = 1–4 mice). Statistical analysis was assessed using an unpaired Student's t-test. (**C**) Line graph showing blood glucose levels during the glucose tolerance test in female wild-type and *Phb1-Ki*Y114F mice, comparing sham- operated controls and ovariectomized (Ovx) groups. Data are shown as mean ± SD (n = 2–4 mice). Statistical analysis was performed using

three-way repeated measures ANOVA. (**D**) Bar graph summarizing AUC values from glucose tolerance tests in *Phb1-Ki*Y114F and wild-type female mice. Data are shown as mean ± SD (n = 2-4). Statistical analysis was conducted using two-way ANOVA. Significance annotations: ns, not significant; * = $P \leq 0.05$, ** = $P \leq 0.01$.

4.9.2 Effect of gonadectomy on glucose homeostasis in *Phb1-Ki* male mice

Glucose tolerance test was performed in male wild-type and *Phb1-Ki*C69A mice to assess how disruption of PTM at PHB1-Cys69 site affects glucose homeostasis and testosterone responsiveness in males. We assess the effects of genotype (*Phb1-Ki*C69A vs. wild type) and surgical condition (sham-operated vs. orchiectomy) on blood glucose levels over time in male mice (Fig. 4.9.2A). Three-way repeated-measures ANOVA of blood glucose during the GTT revealed a significant main effect of time ($F(1.948, 15.58) = 11.01$, $p = 0.0011$), reflecting the expected dynamic changes in glucose levels across time points. No significant main effects of genotype ($F(1, 8) = 0.375$, $p = 0.557$) or surgical status ($F(1, 8) = 0.422$, $p = 0.534$) were detected. No two-way or three-way interactions reached significance (time × genotype: $F(4, 32) = 0.792$, $p = 0.539$; time × surgical status: $F(4, 32) = 0.281$, $p = 0.888$; genotype × surgical status: $F(1, 8) = 0.006$, $p = 0.940$; time × genotype × surgical status: $F(4, 32) = 0.294$, $p = 0.880$). This indicates that blood glucose levels changed significantly over time, but the pattern of change was similar between *Phb1-Ki*C69A males and wild-type controls. No statistically significant differences in AUC were observed between any groups (Fig. 4.9.2B). However, trends in the data suggest potential metabolic distinctions. Wild-type males demonstrated an increase in AUC following orchidectomy (sham-operated: ~1900 mmol·h/L; orchiectomized: ~2100mmol·h/L), indicating a possible modest impairment in glucose tolerance after testosterone removal. *Phb1-Ki*C69A males exhibited consistently elevated AUC values under both surgical conditions (sham-operated: ~2100 mmol·h/L; orchiectomized: ~2200 mmol·h/L), suggesting a tendency toward glucose intolerance that appeared independent of circulating testosterone. Notably, the magnitude of change in AUC following orchidectomy was smaller in *Phb1-Ki*C69A males (~100 mmol·h/L increase) compared to wild-type males (~200mmol·h/L increase). Taken together, these data suggest that male *Phb1-*

*Ki*C69A mice may display impaired glucose tolerance regardless of hormonal status, contrasting with the improved glucose handling observed in female *Phb1-Ki*C69A mice, and highlight the potential for sex-dependent effects on glucose homeostasis.

We also assessed the effect of orchiectomy on glucose homeostasis in *Phb1-Ki*Y114F. Three-way repeated-measures ANOVA of blood glucose during the GTT revealed a significant main effect of time ($F(2.009, 16.07) = 13.67$, $p = 0.0003$), reflecting the expected dynamic changes in glucose levels across time points. No significant main effects of genotype ($F(1, 8) = 1.144$, $p = 0.316$) or surgical status ($F(1, 8) = 0.226$, $p = 0.648$) were detected. No two-way or three-way interactions reached significance (time × genotype: $F(4, 32) = 0.825$, $p = 0.519$; time × surgical status: $F(4, 32) = 0.272$, $p = 0.894$; genotype × surgical status: $F(1, 8) = 0.011$, $p = 0.917$; time × genotype × surgical status: $F(4, 32) = 0.244$, $p = 0.911$)(Fig. 4.9.2D). However, inspection of the data shows that *Phb1-Ki*Y114F males displayed consistently higher AUC values under both surgical conditions (sham-operated: ~2250 mmol·h/L; orchiectomized: ~2350mmol·h/L) compared to wild-type males (sham-operated: ~1950 mmol·h/L; orchiectomized: ~2050mmol·h/L). Both genotypes exhibited a modest increase in AUC following orchidectomy (~100mmol·h/L). This might suggest that testosterone removal may be associated with slightly worsened glucose tolerance, irrespective of genotype. Although these patterns did not reach statistical significance, they may warrant further investigation in larger cohorts to clarify whether these differences reflect underlying metabolic phenotypes. What stands out is that the *Phb1-KiY114F* mutation seems to specifically affect males, unlike in females, where the impact was minimal, pointing to a clear sex-dimorphic effect of PHB1-Tyr114 phosphorylation disruption.

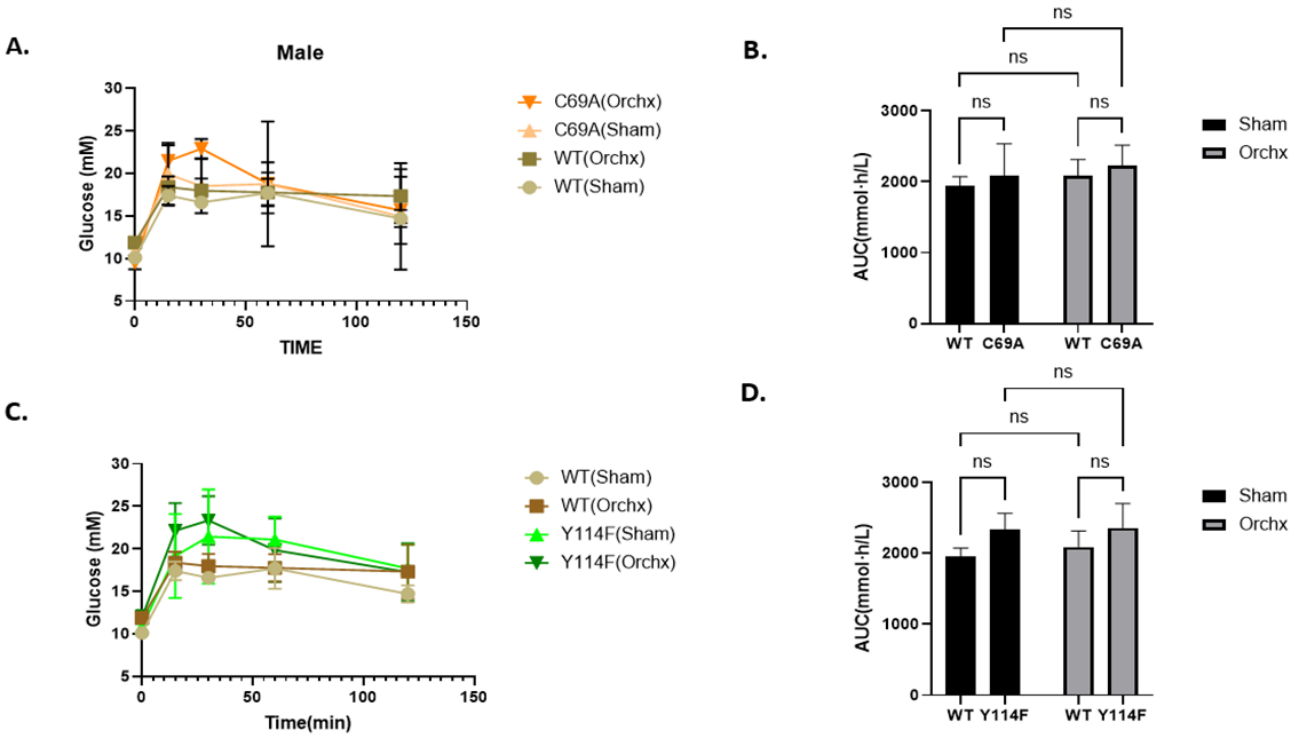

Figure 4.9.2 Glucose Tolerance in Male Wild-Type and *Phb1-Ki* Mice (A) Line graph showing blood glucose levels during the glucose tolerance test in male wild-type and *Phb1-Ki*C69A mice, comparing sham-operated controls and orchiectomized (Orchx) groups. Data are shown as mean ± SD (n = 2–4 mice). Statistical analysis was performed using three-way repeated measures ANOVA to compare glucose levels between genotypes, surgery status, and time points during the glucose tolerance test. **(B)** Bar graph presenting AUC analysis from glucose tolerance tests in the same groups as panel A. Data are shown as mean ± SD (n = 2–4). Statistical analysis was assessed using a two-way ANOVA. (C) Line graph showing blood glucose levels during the glucose tolerance test in male wild-type and Phb1-KiY114F mice, comparing sham-operated controls and orchiectomized (Orchx) groups. Data are shown as mean ± SD (n = 2–4 mice). Statistical analysis was performed using three-way repeated measures ANOVA repeated measures ANOVA. (D) Bar graph summarizing AUC values from glucose tolerance tests in Phb1-KiY114F and wild-type

male mice. Data are shown as mean ± SD (n = 2–4 mice). Statistical analysis was conducted using two-way ANOVA. Significance annotations: ns, not significant; * = $P \leq 0.05$, ** = $P \leq 0.01$.

4.10 Effect of gonadectomy on insulin sensitivity in *Phb1-Ki* mice

To better define the effect of disrupting PHB1-Cys69 and PHB1-Tyr114 sites on sex-related differences in glucose homeostasis, insulin tolerance tests (ITT) were performed. PHB1 is involved in regulating insulin sensitivity through pathways like PIP3/AKT signaling (133), and disrupting its PTMs, like palmitoylation at Cys69 (important for membrane localization) (92) or phosphorylation at Tyr114, could interfere with insulin-stimulated glucose uptake in BAT, muscle, or liver. Since sex-specific metabolic differences are well documented (142), ITT is especially useful for identifying whether these *Phb1* mutations interact with hormone signaling.

4.10.1 Effect of ovariectomy on insulin sensitivity in *Phb1-Ki* female mice

Insulin tolerance test was performed in female wild-type and *Phb1-Ki*C69A mice to directly assess insulin sensitivity and determine whether the improved glucose tolerance observed in GTT was due to enhanced insulin action or alternative mechanisms. We evaluate the effects of genotype (*Phb1*-KiC69A vs. wild type) and surgical condition (sham-operated vs. ovariectomy) on blood glucose levels during the insulin tolerance test in female mice (Fig. 4.10.1A). Three-way repeated-measures ANOVA of blood glucose during the ITT revealed a significant main effect of time ($F(1.654, 9.921) = 9.037$, $p = 0.0074$), reflecting the expected dynamic changes in glucose levels across time points. No significant main effects of genotype ($F(1, 6) = 0.362$, $p = 0.569$) or surgical status ($F(1, 6) = 0.109$, $p = 0.753$) were detected. No two-way or three-way interactions reached significance (time × genotype: $F(4, 24) = 0.203$, $p = 0.934$; time × surgical status: $F(4, 24) = 0.101$, $p = 0.981$; genotype × surgical status: $F(1, 6) = 0.014$, $p = 0.911$; time × genotype × surgical status: $F(4, 24) = 0.074$, $p = 0.990$). (Fig. 4.10.1A). These findings demonstrate that insulin administration reduced glucose levels over time in all groups, and the overall response pattern was

comparable between genotypes and surgical conditions in females. AUC analysis in *Phb1-Ki*C69A females provided an integrated assessment of insulin sensitivity throughout the test period; no statistically significant differences were observed between any of the groups (Fig. 4.10.1B).

The second observation of ITT belongs to *Phb1-Ki*Y114F females. Three-way repeated-measures ANOVA of blood glucose during the ITT revealed a significant main effect of time ($F(1.830, 12.81) = 18.36$, $p = 0.0002$), reflecting the expected dynamic changes in glucose levels across time points. No significant main effects of genotype ($F(1, 7) = 0.216$, $p = 0.656$) or surgical status ($F(1, 7) = 0.051$, $p = 0.828$) were detected. No two-way or three-way interactions reached significance (time × genotype: $F(4, 28) = 0.696$, $p = 0.601$; time × surgical status: $F(4, 28) = 0.510$, $p = 0.729$; genotype × surgical status: $F(1, 7) = 0.546$, $p = 0.484$; time × genotype × surgical status: $F(4, 28) = 0.278$, $p = 0.889$).(Fig. 4.10.1C). This indicates that blood glucose levels changed significantly over time during the insulin tolerance test, but the overall glucose response was similar between *Phb1-Ki*Y114F females and wild-type controls, regardless of surgery status. The bar graph of AUC values (Fig. 4.10.1D) provides an integrated view of these differences. Although these differences were not statistically significant, we observed a trend. In sham-operated mice, both wild-type and *Phb1-Ki*Y114F females had nearly identical AUCs (~850mmol·h/L) (Fig. 4.10.1D), suggesting no baseline difference in insulin sensitivity. However, ovariectomy produced opposite trends in the two genotypes: wild-type females showed improved insulin sensitivity, with AUC decreasing to ~750 mmol·h/L, whereas *Phb1-Ki*Y114F females exhibited a higher AUC (~950mmol·h/L) (Fig. 4.10.1D), indicating reduced insulin sensitivity after estrogen loss.

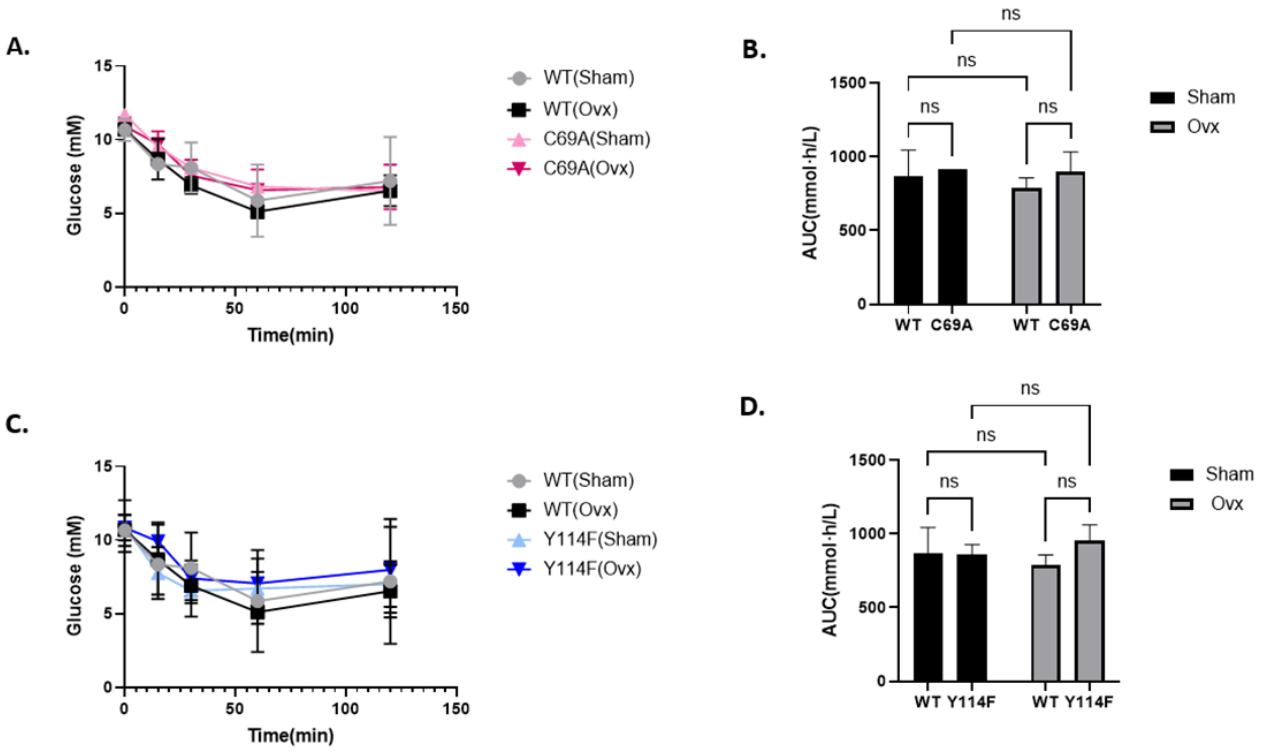

Figure 4.10.1 Insulin tolerance in Female Wild-Type and *Phb1-Ki* Mice (A) Line graph showing blood glucose levels during the insulin tolerance test in female wild-type and *Phb1-KiC69A* mice, comparing sham-operated controls and ovariectomized (Ovx) groups. Data are shown as mean ± SD (n = 2–4 mice). C69A sham is one, and SD has not been calculated. Statistical analysis was performed using three-way repeated measures ANOVA to compare glucose levels between genotypes, surgery status, and time points during the insulin tolerance test. (**B**) Bar graph presenting AUC analysis from insulin tolerance tests in the same groups as panel A. Data are shown as mean ± SD (n = 1–4).

Statistical analysis was assessed using an unpaired Student's t-test. (**C**) Line graph showing blood glucose levels during the insulin tolerance test in female wild-type and *Phb1-Ki*Y114F mice, comparing sham-operated controls and ovariectomized (Ovx) groups. Data are shown as mean ± SD (n = 2–4 mice). Statistical analysis was performed using three-way repeated measures ANOVA.

(**D**) Bar graph summarizing AUC values from insulin tolerance tests in *Phb1-Ki*Y114F and wild-type female mice. Data are shown as mean ± SD (n = 2–4 mice). Statistical analysis was conducted using Two-way ANOVA. Significance annotations: ns, not significant; * = $P \leq 0.05$, **= $P \leq 0.01$.

4.10.2 Effect of orchiectomy on insulin sensitivity in *Phb1-Ki* male mice

Blood glucose levels following the insulin tolerance test demonstrated a significant main effect of time in *Phb1-Ki*C69A male mice (P = 0.0265) (Fig. 4.10.2A), indicating that glucose concentrations changed significantly over the course of the test. Three-way repeated-measures ANOVA of blood glucose during the ITT revealed a significant main effect of time (F (2.074, 16.59) = 4.496, p = 0.027) in *Phb1-Ki*C69A male mice and a significant main effect of surgical status (F (1, 8) = 8.262, p = 0.021), indicating higher overall glucose levels in gonadectomized mice independent of genotype and time. No significant main effect of genotype was detected (F (1, 8) = 0.726, p = 0.419). No two-way or three-way interactions reached significance (time × genotype: F (4, 32) = 0.888, p = 0.482; time × surgical status: F (4, 32) = 0.430, p = 0.786; genotype × surgical status: F (1, 8) = 2.251, p = 0.172; time × genotype × surgical status: F (4, 32) = 0.271, p = 0.895). (Fig. 4.10.2A). These results demonstrate that gonadectomy significantly impaired insulin sensitivity (higher glucose across the ITT curve), while genotype had no detectable main effect and did not modify the surgical status effect. The analysis revealed a significant genotype × surgery interaction (F (1,8) = 8.09, p = 0.0217), indicating that the effect of orchiectomy on insulin sensitivity differed between *Phb1-Ki*C69A and wild-type mice. There was no significant main effect of genotype (F (1,8) = 0.75, p = 0.4130). In contrast, surgical status had a significant main effect on ITT AUC (F (1,8) = 42.63, p = 0.0002). Together, these results suggest that orchiectomy significantly alters insulin responsiveness in male mice and that this effect is modulated by genotype. (Fig. 4.10.2B). These findings indicate that removal of testosterone markedly improves insulin sensitivity in *Phb1-Ki*C69A males. Conversely, insulin sensitivity in wild-type males was relatively unaffected by orchidectomy.

We also examine the effect of orchiectomy on glucose homeostasis in *Phb1-Ki*Y114F. Three-way repeated-measures ANOVA of blood glucose during the ITT revealed no significant main effect of time ($F(1.319, 10.56) = 2.493$, $p = 0.140$). A significant main effect of surgical status was detected ($F(1, 8) = 5.696$, $p = 0.044$), indicating higher overall glucose levels (poorer insulin sensitivity) in gonadectomized mice, independent of genotype and time. No significant main effect of genotype was found ($F(1, 8) = 1.339$, $p = 0.281$), and no two-way or three-way interactions reached significance (time × genotype: $F(4, 32) = 0.815$, $p = 0.525$; time × surgical status: $F(4, 32) = 0.673$, $p = 0.616$; genotype × surgical status: $F(1, 8) = 0.022$, $p = 0.885$; time × genotype × surgical status: $F(4, 32) = 0.921$, $p = 0.464$). (Fig. 4.10.2C). These results demonstrate that gonadectomy significantly impaired insulin sensitivity (higher glucose across the ITT curve), while genotype had no detectable main effect and did not modify the surgical status effect.

The AUC analysis for *Phb1-Ki*Y114F male mice showed no significant genotype × surgery interaction ($F(1,8) = 1.42$, $p = 0.2677$), indicating that the effect of orchiectomy on ITT AUC did not differ between Y114 and wild-type mice. There was also no significant main effect of genotype ($F(1,8) = 0.46$, $p = 0.5180$). However, a significant main effect of surgical status was observed ($F(1,8) = 6.58$, $p = 0.0334$), suggesting that orchiectomy significantly altered insulin responsiveness in male mice, independent of genotype.

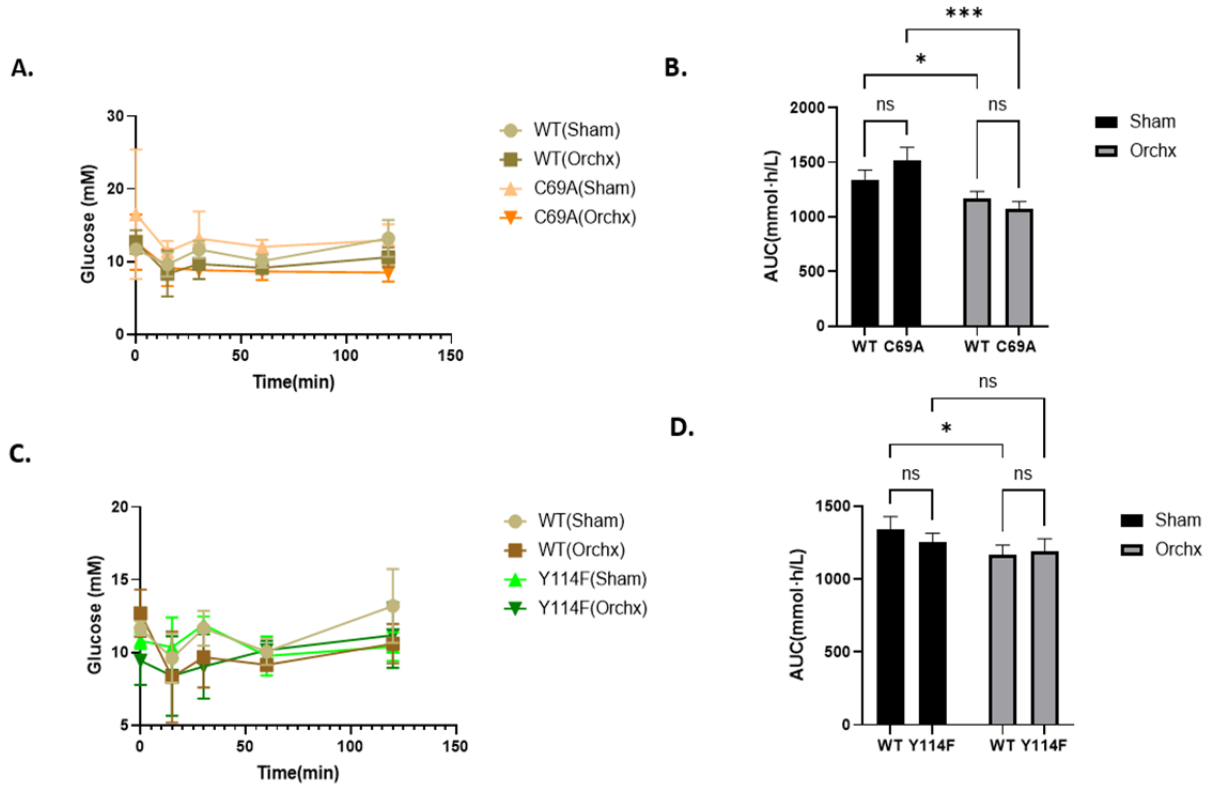

Figure 4.10.2 Insulin Tolerance in Male Wild-Type and *Phb1-Ki* Mice (A) Line graph showing blood glucose levels during the insulin tolerance test in male wild-type and *Phb1-Ki*C69A mice, comparing sham-operated controls and orchiectomized (Orchx) groups. Data are shown as mean± SD (n = 2–4 mice). Statistical analysis was performed using three-way repeated measures ANOVA to compare glucose levels between genotypes, surgery status, and time points during the glucose tolerance test. **(B)** Bar graph presenting AUC analysis from insulin tolerance tests in the same groups as panel A. Data are shown as mean ± SD (n = 2–4). Statistical analysis was assessed using a two -way ANOVA. **(C)** Line graph showing blood glucose levels during the insulin tolerance test in male wild-type and *Phb1-Ki*Y114F mice, comparing sham-operated controls and orchiectomized (Orchx) groups. Data are shown as mean ± SD (n = 2–4 mice). Statistical analysis was performed using three-way repeated measures ANOVA. **(D)** Bar graph summarizing AUC values from insulin tolerance tests in *Phb1-KiY114F* and wild-type male mice. Data are shown as

mean ± SD (n = 2–4 mice). Statistical analysis was conducted using two-way ANOVA. Significance annotations: ns, not significant; * = $P \leq 0.05$, ** = $P \leq 0.01$.

CHAPTER V. DISCUSSION

This study set out to explore how substitutions at two key post-translational modification (PTM) sites of PHB1, PHB1-Cys69 and PHB1-Tyr114, shape BAT biology and whole-body metabolic traits in a sex-specific manner. By integrating whole-body weight measurements, BAT-to-body weight ratios, histomorphometry analysis of adipocyte number, quantifying lipid area, and ultrastructural assessments of mitochondrial morphology, we aimed to develop a mechanistic picture of how these mutations might influence BAT phenotype. A summary of observations is shown in Table 5.1.

Table 5.1 Summary of sex- and mutation-specific BAT/body phenotypes in *Phb1-Ki* mice (*Phb1-Ki*C69A, *Phb1-Ki*Y114*F*) relative to wild type. NS= none significant

	*Phb1-Ki*Y114F male mice	*Phb1-Ki*Y114F female mice	*Phb1-Ki*C69A male mice	*Phb1-Ki*C69A female mice
Weight	Modest ↑ (NS)	Moderate ↑ (NS)	≈ WT (NS)	↑
BAT weight relative to whole-body weight	↑ (vs WT)	≈ WT (no clear change)	↑ (trend)	↑
Bat adipose area	↑ (trend/NS)	↓ (trend/NS)	↑ (noted; significance not established)	↑ (significant)
BAT cell number	↓ (trend/NS)	↑ (trend/NS)	↓ (NS)	↑ (NS)
Mitochondria morphology	Mild alterations; elongated, cristae relatively preserved vs *Phb1-Ki*C69A	Well-structured, round; dense cristae	Elongated, severe cristae loss	Mild elongation, partial cristae preservation (less severe than males)

A consistent theme emerged from the baseline whole-body weight data: female mice carrying either the *Phb1-Ki*Y114F or *Phb1-Ki*C69A mutations on a C57BL/6 background exhibited greater body weights than their wild-type counterparts, while males showed weights comparable to controls. Specifically, *Phb1-Ki*C69A males did not show any significant weight difference from wild-type, whereas *Phb1-Ki*Y114F males displayed a modest increase in weight, although this was not statistically significant when compared to wild-type. All experimental groups including age,

diet, and housing were matched to control for environmental variables. These observations reveal a pronounced sex effect on weight gain driven by PHB1 mutations.

Contextualizing these results with the existing literature presents several complexities. Wang et al. (126) investigated adipocyte-specific PHB1 knockout mice (on a C57BL/6 background), focusing exclusively on male animals, and demonstrated that targeted loss of PHB1 in adipose tissue conferred resistance to high-fat diet-induced weight gain compared to wild-type controls (126). In contrast, the current study introduced structural mutations in PHB1 (*Phb1-Ki*C69A and *Phb1-Ki*Y114F) with knock-in models expressing mutant PHB1 throughout the whole body, not limited to adipose tissue, and analyses included both sexes. This broader expression pattern was associated with increased body weight, most notably in females, while males showed minimal or non-significant changes. These distinctions in genetic strategy, tissue-specific knockout versus whole-body knock-in combined with differences in sex inclusion and mutation type, make direct comparisons challenging. Ande et al. (131) explored PHB1 overexpression in adipose tissue and observed weight gain in both sexes, with sex-dependent differences. While that model shares the context of PHB1's impact on body weight, direct comparison is complicated because the mutants are expressed only in adipose tissue, whereas the models described here are expressed globally, potentially influencing other tissues and systemic metabolism (131).

Further, previous work from our laboratory group on *Phb1-Ki*C69A mice showed a different pattern: males gained weight significantly, while female weight increases were non-significant compared to wild type (143). In contrast, in the present cohort, no significant weight difference was observed between *Phb1-Ki*C69A males and females, with females actually trending heavier a reversal of the usual sex-related weight difference in C57BL/6 mice. This observation may be influenced by cohort effects, such as a smaller sample size in males and the presence of an

unusually lean individual. Examination of weight trends in an independent set of mice purchased for gonadectomy did not reveal the same female-biased pattern in pre-surgery data.

Taken together, these findings suggest that the mode of PHB1 alteration, whether knockout, overexpression, or point mutation, can markedly affect the direction and magnitude of weight change, and that sex remains a pivotal modifier of phenotype. Differences in tissue specificity of mutant expression, sample size, or cohort variability may also contribute to divergent outcomes.

The preliminary findings in *Phb1-Ki*C69A mice indicate sex-specific alterations in BAT architecture and cellularity. Male mutants showed a tendency toward increased BAT weight, accompanied by a non-significant decrease in cell number and a notable increase in adipocyte area compared with wild-type controls. In females, increased BAT weight was observed along with non-significant elevations in cell number and a significant expansion of adipocyte area. Interpreting increased BAT weight requires examining both tissue mass and cell number(134). If BAT weight rises without a change in cell count, this suggests adipocyte hypertrophy; when both weight and cell number increase, it indicates combined hyperplasia and hypertrophy, an atypical expansion pattern for BAT (155,156). Elevated BAT weight is frequently associated with lipid accumulation (134) and may reflect a phenotype shift toward lipid storage reminiscent of white adipose tissue, potentially due to diminished thermogenic capacity (157).

Studies have shown that BAT hypertrophy can arise from changes in mitochondrial oxidative capacity influenced by mitochondrial shape and cristae density (158,159). PHB1, by anchoring to the inner mitochondrial membrane and forming a super complex with PHB2, is essential in this process (160). When a mutation at PHB1-Cys69 (palmitoylation) impairs membrane anchoring, mitochondrial structure is disrupted. This specifically affects OPA1-dependent cristae organization, reducing mitochondrial number and inner membrane integrity (124) and thereby

limiting proper localization of UCP1, a critical component of BAT thermogenesis (161). As a result, BAT shifts from energy expenditure toward increased lipid storage (161). Further electron microscopy findings support this mechanism: analyses revealed distinct genotype- and sex-specific mitochondrial changes in BAT. In *Phb1-Ki*C69A males, mitochondria were notably elongated with severe cristae loss, indicative of compromised membrane organization and oxidative capacity, which can result in fat accumulation and hypertrophy, consistent with our observations in male *Phb1-Ki*C69A mice. In females with the same mutation, mitochondria were slightly elongated but showed less severe structural impairment. Taken together, these mitochondrial structural abnormalities, reduced thermogenic function, and increased lipid storage characterize the impaired BAT phenotype(161).

It is important to note a unique aspect of our model. Compared with prior BAT-focused PHB1 genetically modified models, our *Phb1 knock-in* mice (PTM-site substitutions) provide a systems-level *in vivo* readout of PHB1 function that preserves endogenous expression in all cell types while modulating its activity. In contrast, Gao. et al. (127) used an endothelial cell-specific *Phb1* knockout (EC-KO) and showed that loss of endothelial PHB1 limits long-chain fatty acid (LCFA) flux into adipose tissue, most notably BAT, thereby impairing triglyceride clearance and shifting whole-body fuel use toward glucose under high-fat diet conditions (127). Our direct assessments of BAT mitochondrial ultrastructure indicate that, beyond vascular substrate delivery, cell-intrinsic mitochondrial alterations arise when PHB1 is perturbed, consistent with a second, adipocyte-autonomous mechanism. Together, these findings point to dual control of BAT by PHB1: an extrinsic endothelial gate for lipid transport and an intrinsic mitochondrial scaffold, with the balance modulated by sex and diet.

To explain the pronounced sex differences, we observed males showing more compromised BAT than females, and given that these differences occurred independently of diet, housing, or other environmental factors, a role for PHB1–sex hormone interactions is likely. This interpretation is supported by previous observations; for example, in Mito-Ob mice, adipocyte-specific PHB1 overexpression produced sex-dependent BAT remodeling, with the female BAT phenotype less compromised than in males (104). The literature further suggests that estrogen enhances PHB1 expression and mitochondrial integrity, providing protection, whereas testosterone reduces PHB1 and exacerbates mitochondrial disruption (111,120).

Sex-related differences in BAT remodeling are evident in *Phb1-Ki*C69A model. Female mice exhibit increased cell number (hyperplasia) alongside hypertrophy, whereas males display a reduction in cell number with pronounced hypertrophy. This pattern contrasts with a previous study using adipocyte-specific *Phb1* knockout, where no differences in cell number were observed; it is worth noting that, in that model, knockout was induced after initial adipogenesis, likely preventing any impact on cell recruitment and limiting the phenotype primarily to adipocyte hypertrophy (102). In the current model, the *Phb1* mutation is present from the beginning, affecting BAT development throughout all stages. As a result, females experience a combined effect of hyperplasia and hypertrophy, whereas males show mainly hypertrophy with reduced cell number. These results suggest that the timing and nature of PHB1 disruption play a critical role in determining BAT cellularity and remodeling and highlight a pronounced sex-dependent divergence potentially driven by differential hormonal modulation of PHB1's roles in proliferation and adipocyte growth.

Before presenting our observations in the *Phb1-Ki*Y114F model, it is important to note that palmitoylation at PHB1-Cys69 is required for its translocation to the plasma membrane, which

subsequently enables specific post-translational modifications such as tyrosine phosphorylation and protein interactions associated with membrane signaling functions (92). As such, the phenotype of *Phb1-Ki*Y114F mutants reflects the specific consequences of PHB1-Tyr114 phosphorylation, whereas the phenotype of *Phb1-Ki*C69A mutants arises from disruption of both PHB1-Cys69 palmitoylation and its downstream phosphorylation at *Phb1-Ki*Y114F (120).

In male *Phb1-Ki*Y114F mutants, BAT mass relative to body weight was significantly higher compared to wild-type controls, whereas in females, BAT mass remained comparable to wild-type. This increase in BAT in males was accompanied by a reduction in adipocyte number and hypertrophy of the remaining cells, consistent with impaired lipolysis and early features of a whitening-like phenotype. In contrast, females displayed an increased number of smaller adipocytes without hypertrophy, indicating preserved hyperplasia and overall healthier BAT expansion. Compared to wild-type females, *Phb1-Ki*Y114F females also showed reduced fat accumulation, supporting the idea of a more resilient BAT phenotype.

Electron microscopy confirmed these sex-dependent differences. BAT mitochondria from male *Phb1-Ki*Y114F mice exhibited mild morphological alterations but retained relatively dense cristae compared to *Phb1-Ki*C69A mutants, suggesting partial preservation of oxidative capacity. In females, mitochondria appeared well-structured with densely packed cristae, consistent with intact thermogenic potential.

PHB1-Tyr114 phosphorylation of PHB1 has been implicated in regulating MAPK–ERK and PI3K–Akt signaling, a conclusion supported by both established literature and observations from the m-Mito-Ob model. These studies indicate that PHB1 phosphorylation at PHB1-Tyr114 acts as a switch, modulating the balance between ERK- and Akt-driven pathways (117,133,162,163). that are central to BAT biology and mitochondrial regulation (164–166) . ERK integrates sympathetic

input to drive early adipogenesis, lipolysis, and thermogenic activation (166), while PI3K–Akt promotes hyperplasia, glucose uptake, lipid metabolism, and UCP1 expression (164). Disruption of ERK signaling is expected to impair differentiation, reduce lipolysis, and diminish thermogenic activation (166), which aligns with the phenotype of male *Phb1-Ki*Y114F mutants showing reduced adipocyte number, hypertrophy, and lipid accumulation. By contrast, the phenotype of *Phb1-Ki*Y114F females suggests compensation, enabling maintenance of adipocyte hyperplasia and mitochondrial quality despite the absence of PHB1-Tyr114 phosphorylation.

The sexual dimorphism in this model is particularly striking. While males exhibit whitening-like remodeling of BAT, females retain healthy adipocyte cellularity, mitochondrial structure. Estrogen-mediated protection likely plays a central role, as estrogen supports mitochondrial integrity, enhances Akt signaling, and limits lipid accumulation (111,120,167), buffering females against the metabolic consequences of *Phb1-Ki*Y114F substitution.

Taken together, these findings suggest that PHB1-Tyr114 phosphorylation may play an important role in modulating ERK- and Akt-dependent signaling in BAT, particularly in males. The relatively preserved mitochondrial morphology and BAT function observed in females could reflect a compensatory influence of estrogen. Thus, the observed phenotypes likely reflect sex-dependent differences in adipocyte differentiation, lipid handling, and mitochondrial integrity. The gonadectomy experiments provided an opportunity to probe whether adult gonadal hormones are required to maintain these sex-specific phenotypes. Removal of ovarian or testicular hormones in adulthood did not significantly change whole-body weight in any genotype, including wild-type. This is in line with prior work showing that weight changes after gonadectomy are highly context-dependent, often emerging under high-fat diets, thermoneutral housing, or prolonged post-surgical intervals, but minimal under standard chow and room-temperature conditions (168,169).

BAT is a central sink for glucose disposal and a major driver of adaptive thermogenesis(170), and both processes are strongly modulated by sex hormones. Prior work shows that estrogen enhances BAT glucose uptake and mitochondrial efficiency, whereas testosterone tends to exacerbate metabolic dysfunction(171).

In females, both *Phb1-Ki*C69A and wild-type (WT) mice in the sham state cleared glucose better than their ovariectomized (OVX) counterparts (trend), consistent with estrogen supporting glucose disposal (172). Overall, the C69A mutation affects glucose tolerance in a sex-dependent manner. Female *Phb1-Ki*C69A mice consistently exhibited lower GTT AUC values than wild-type controls under both sham and ovariectomy conditions, indicating a trend toward improved glucose handling. In contrast, male *Phb1-Ki*C69A mice showed higher GTT AUC values than wild-type mice under both sham and orchiectomy conditions, consistent with impaired glucose tolerance. Importantly, gonadectomy produced similar directional effects within each sex regardless of genotype, indicating that responsiveness to sex hormone removal is preserved. Female ITT AUCs were comparable across groups; WT sham vs OVX was not significant, and *Phb1-Ki*C69A sham and OVX were similar. Visually, *Phb1-Ki*C69A AUCs were modestly higher than WT in both hormone states, suggesting a trend toward lower insulin sensitivity in *Phb1-Ki*C69A females. This means that their improved glucose tolerance seen in the GTT cannot be explained by insulin sensitivity, but must come from other mechanisms of glucose control.

This dissociation in females implies that better GTT performance is unlikely to be explained by classical insulin sensitization. Instead, insulin-independent mechanisms may contribute e.g., BAT-driven glucose uptake via GLUT1 (153), altered hepatic glucose output (173), or sympathetic/thermogenic programs that increase glucose disposal without requiring stronger insulin signaling (153). These possibilities align with literature showing estrogen-supported BAT

metabolism and suggest that PHB1 loss may shift the balance toward insulin-independent glucose clearance in females (102). This idea is supported by the findings in PHB Ad-KO mice, where lipid intolerance due to defective fatty acid uptake led to increased reliance on glucose, such that Ad-KO animals actually cleared glucose better than WT under high-fat diet conditions (102). In both cases, disruption of PHB function seems to limit efficient lipid utilization, pushing metabolism toward greater glucose use. Thus, our observations in *Phb1-Ki*C69A females may represent a similar adaptive mechanism, consistent with prior reports of PHB's role in balancing lipid versus glucose metabolism.

These findings are consistent with a testosterone-dependent component of insulin resistance in *Phb1-Ki*C69A males: removing testosterone improves insulin sensitivity in mutants, whereas WT are largely unchanged. This pattern suggests that testosterone exacerbates the metabolic defect associated with the *Phb1-Ki*C69A mutation. Disrupting palmitoylation likely weakens PHB1's ability to organize the membrane sites where insulin receptors connect to the PI3K pathway (124). Testosterone may worsen this defect by altering lipid metabolism and promoting pro-inflammatory signals, which together drive insulin resistance (174). Removing testosterone restores normal insulin sensitivity, even though the PHB1 mutation remains, highlighting an interaction between PHB1 palmitoylation and androgen signaling in the regulation of insulin action.

In female GTT AUC, ovariectomy did not produce significant changes in either genotype; however, both WT and *Phb1-Ki*Y114F showed a numerical rise after OVX (ns). Thus, any attenuation of the OVX effect in *Phb1-Ki*Y114F, if present, was modest and not significant. Baseline glucose handling was not strongly disrupted. In female ITT, ovariectomy had opposite, non-significant trends by genotype: WT showed a small decrease in AUC (trend toward improved insulin sensitivity), whereas *Phb1-Ki*Y114F showed a small increase in AUC (trend toward

reduced sensitivity). Neither comparison reached statistical significance. After ovariectomy, however, the two groups began to show different patterns, with *Phb1-Ki*Y114F females trending toward reduced insulin sensitivity compared to wild-type.

In males, under sham conditions *Phb1-Ki*Y114F mice showed numerically higher GTT AUC than wild-type (trend). After orchidectomy, the *Phb1-Ki*Y114F AUC did not change (ns), whereas wild-type showed a slight, non-significant increase. Overall, these patterns suggest a testosterone-independent tendency toward poorer glucose clearance in *Phb1-Ki*Y114F males, but all comparisons were non-significant. These parallel, non-significant AUC decreases after orchidectomy suggest a minor improvement in insulin sensitivity in both genotypes, with no clear *Phb1-Ki*Y114F specific effect within the limits of our sample size. This suggests that, unlike the *Phb1-Ki*C69A mutation (which interacts strongly with testosterone), the PHB1-Tyr114 change affects insulin signaling in a more limited way it slightly weakens the strength of the pathway but does not disrupt its basic structure. Collectively, these results suggest that the *Phb1-Ki*Y114F mutation slightly weakens the strength of insulin signaling and metabolic adaptation to hormonal changes but does not fundamentally disrupt pathway integrity or precipitate overt insulin resistance. In contrast to more disruptive mutations like *Phb1-Ki*C69A, which strongly interact with sex hormones and drive pronounced metabolic defects, *Phb1-Ki*Y114F acts as a modest modulator, only subtly affecting glucose and insulin handling within the limits of the current sample size.

Comparison of *Phb1knock-in* with the Mito-Ob and m-Mito-Ob transgenics reveals a shared male-biased vulnerability but different hormone dependencies. In Mito-Ob males, orchidectomy modestly improves GTT yet does not improve ITT, indicating partial androgen dependence for glucose tolerance with insulin resistance that is largely androgen-independent; females are largely

preserved, and ovariectomy produces little or no change in GTT and ITT (110). In *Phb1-Ki*C69A, males show poor glucose clearance and insulin resistance with a clear testosterone-dependent component orchidectomy significantly improves ITT, whereas *Phb1-Ki*C69A females repeatedly trend toward better GTT than WT under both sham and OVX without a parallel ITT advantage, consistent with greater insulin-independent disposal (e.g., BAT-driven uptake/substrate switching). In *Phb1-Ki*Y114F , effects are milder: males show a trend toward higher GTT AUC that is largely testosterone-independent, and females exhibit small, non-significant OVX-related shifts, with ITT broadly comparable to WT, consistent with PHB1-Tyr114 acting as a signal-tuning site rather than a determinant of signaling architecture (120). Reports on m-Mito-Ob similarly point to sex-dependent remodeling with relative female protection, but without the strong androgen-reversible defect seen in *Phb1-Ki*C69A. Together, these comparisons suggest that PHB1-Cys69 post-translational modification loss drives pronounced, sex- and hormone-modulated phenotypes, whereas PHB1-Tyr114 post translational modification loss mainly fine-tunes metabolic adaptation, and that the Mito-Ob background shows a mixed pattern: partial androgen dependence for GTT in males, preserved female control after OVX, and persistent male insulin resistance on ITT.

Together, our results support a model in which PHB1 post-translational state gates how sex hormones might shape BAT and systemic glucose control: loss of Cys69 PTM perturbs membrane organization of insulin signaling and exposes a testosterone-sensitive liability in males (rescued by orchidectomy), while in females, glucose handling can be maintained via insulin-independent routes.

Study Limitations

This study faced several methodological and technical limitations that warrant acknowledgment to provide the proper context for interpreting the results. First, Due to technical constraints, comprehensive quantification of protein expression in BAT lysates could not be reliably achieved. Although our original experimental plan included assessment of key proteins involved in BAT function and mitochondrial biology, such as prohibitin 1, prohibitin 2, UCP1, and additional markers, to enable detailed characterization of BAT in mutant versus wild-type mice, many planned Western blot analyses yielded insufficient data quality. This limitation restricted our ability to draw robust conclusions regarding molecular mechanisms underlying the observed phenotypes. Furthermore, while subcellular fractionation was performed to separate mitochondrial and membrane compartments, inadequate fraction purity and cross-contamination prevented reliable interpretation of compartment-specific protein localization. These challenges are consistent with previously reported technical limitations associated with protein extraction and fractionation from adipose tissue, particularly under conditions requiring high sensitivity and stringent validation. Sample size constituted another important constraint. Fewer animals per genotype and sex than initially planned reduced the statistical power of the study, raising the risk of type II errors and limiting the capacity to detect subtle genotype- or sex-dependent effects. This issue is particularly relevant in studies of metabolic phenotypes, where biological variability demands robust experimental sampling to achieve meaningful inference.

Additionally, the method used to measure BAT weight may have introduced inaccuracies. Rather than weighing BAT immediately upon dissection, tissue samples were frozen and later thawed, cleaned, and weighed. Since BAT in this region is embedded within WAT, careful dissection was needed to isolate pure BAT. However, this trimming and weighing process was time-consuming,

which is a concern because key transcription factors in BAT, such as PPARγ, C/EBPα, and C/EBPβ, are known to degrade rapidly after tissue collection. Due to the instability of these proteins, this method is not ideal when the goal is to assess their expression levels. Based on current literature, non-invasive imaging approaches are considered more suitable alternatives. Techniques such as MRI (e.g., proton density fat fraction or chemical shift imaging) can estimate BAT volume without compromising tissue integrity. Additionally, 18F-FDG PET (fluorodeoxyglucose positron emission tomography) is widely used to measure BAT metabolic activity, as it detects glucose uptake in response to thermogenic stimulation (e.g., cold exposure). These imaging methods not only avoid protein degradation but also provide both structural and functional insights into BAT physiology. Therefore, this protocol can alter physical properties, impact weight measurement validity, and potentially compromise protein integrity for downstream analyses, a known concern, as highlighted in best-practice tissue handling literature. Other fat depots (such as WAT and SAT) were not weighed, preventing a complete assessment of depot-specific fat distribution and limiting integrative analysis across adipose tissue compartments.

Taken together, these methodological limitations may have affected the precision of tissue weight data, the accuracy of protein quantification, and the interpretation of subcellular molecular findings. Future work should address these issues by increasing sample size, improving fractionation purity with validated compartmental markers, performing immediate post-dissection tissue measurements, and employing optimized protocols for protein extraction from BAT and other depots. Despite these constraints, the major patterns and conclusions presented here are supported by the available data, though caution is warranted in interpreting finer molecular details or drawing broad generalizations.

Future Directions

Building on the findings and acknowledged methodological constraints in this study, several key avenues for future research are recommended to deepen understanding of PHB1 post-translational modifications, BAT biology, and metabolic regulation:

1. Given the absence of statistically significant differences in GTT outcomes in the present study, which may be attributable to limited sample size, future studies should repeat these experiments using adequately powered cohorts to ensure sufficient statistical sensitivity. Increasing sample size will allow more definitive evaluation of the effects of genotype and gonadectomy on glucose tolerance.
2. To pin down the tissue sources of the GTT and ITT effects, perform hyper insulinemic–euglycemic clamps with radiolabeled 2-deoxyglucose to quantify glucose uptake in BAT, skeletal muscle, and WAT and to assess suppression of hepatic glucose production, and pair this with ^18F-FDG PET/CT at room temperature vs mild cold to visualize depot-specific BAT uptake and compare *Phb1-Ki*C69A vs *Phb1-Ki*Y114F across sex and ± gonadectomy.
3. Add context-challenge arms, thermoneutral housing and high-fat diet, to unmask latent phenotypes, and include aging cohorts to test the durability of female protection.
4. To establish hormone–mechanism causality, perform replacement studies (OVX ± graded estradiol; ORX ± testosterone or an androgen-receptor antagonist) with GTT and ITT, hyper insulinemic-euglycemic clamps, and acute signaling readouts, and pair them with receptor genetics, BAT specific ERα or AR deletion on *Phb1-Ki*C69A or *Phb1-Ki*Y114F backgrounds, to test necessity and sufficiency.

Chapter IV: Conclusion

This study explored the importance of conserved PTMs sites at Cys69 and Tyr114 residues in PHB1 may influence BAT morphology, mitochondrial structure, and metabolic parameters in male and female mice. Overall, while several genotype- and sex-related trends were observed, most of the measured differences were not statistically significant, and therefore should be interpreted cautiously as preliminary observations rather than definitive effects. Body weight analysis indicated that female *Phb1-Ki*C69A mice tended to weigh more than wild-type females, whereas *Phb1-Ki*Y114F females showed a smaller, non-significant increase. In males, no clear genotype-related differences were detected. These results suggest possible sex-linked variation in the influence of PHB1 PTMs on body weight, but the lack of statistical significance limits firm conclusions. Quantitative histological assessment revealed that male *Phb1-Ki*C69A mice showed a larger average brown adipocyte area compared with wild-type males, whereas female *Phb1-Ki*C69A and *Phb1-Ki*Y114F mice displayed modest increases that did not reach significance. Adipocyte number per field was generally similar among genotypes, although female knock-in mice showed a trend toward higher cell counts compared with males. These observations suggest that the *Phb1-Ki*C69A mutation may be associated with adipocyte hypertrophy, while the *Phb1-Ki*Y114F variant might influence cell number; however, these trends remain tentative. Electron microscopy provided qualitative evidence of altered mitochondrial appearance in BAT, particularly in *Phb1-Ki*C69A males, where cristae appeared reduced and mitochondrial shape more elongated compared with wild-type. In contrast, *Phb1-Ki*Y114F females exhibited mitochondria that appeared similar to controls. As these findings were based on limited biological replicates (n = 1 mice), they should be viewed as descriptive observations that require validation in larger cohorts. Following gonadectomy, no statistically significant changes were detected in

body weight, BAT mass, or glucose and insulin tolerance across genotypes and sexes. Some non-significant trends were noted: orchiectomy in *Phb1-Ki*C69A males was associated with slightly higher body weight and improved insulin sensitivity, whereas ovariectomy tended to worsen glucose tolerance in both wild-type and knock-in females. These patterns suggest potential hormone-related modulation of PHB1-linked pathways but remain speculative given the small sample sizes. Nonetheless, several sex-dependent tendencies were observed that may reflect subtle effects of these PTMs on adipose tissue characteristics and metabolic regulation. These exploratory findings form a useful basis for future studies with increased sample sizes and mechanistic assays to better define the contribution of PHB1 modifications to mitochondrial function and metabolic homeostasis.

References

1. Caballero B. The global epidemic of obesity: an overview. Epidemiol Rev. 2007;29:1–5.

2. Gesta S, Tseng YH, Kahn CR. Developmental origin of fat: tracking obesity to its source. Cell. 2007 Oct 19;131(2):242–56.

3. Kershaw EE, Flier JS. Adipose tissue as an endocrine organ. J Clin Endocrinol Metab. 2004 June;89(6):2548–56.

4. Richard AJ, White U, Elks CM, Stephens JM. Adipose Tissue: Physiology to Metabolic Dysfunction. Feingold KR, Ahmed SF, Anawalt B, Blackman MR, Boyce A, Chrousos G, et al., editors. Endotext. 2000;

5. Cannon B, Nedergaard J. Brown adipose tissue: function and physiological significance. Physiol Rev. 2004 Jan;84(1):277–359.

6. Saely CH, Geiger K, Drexel H. Brown versus White Adipose Tissue: A Mini-Review. Gerontology. 2010 Dec 7;58(1):15–23.

7. Cypess AM, Lehman S, Williams G, Tal I, Rodman D, Goldfine AB, et al. Identification and Importance of Brown Adipose Tissue in Adult Humans. N Engl J Med. 2009 Apr 9;360(15):1509–17.

8. Park A, Kim WK, Bae KH. Distinction of white, beige and brown adipocytes derived from mesenchymal stem cells. World J Stem Cells. 2014 Jan 26;6(1):33–42.

9. Sidossis L, Kajimura S. Brown and beige fat in humans: thermogenic adipocytes that control energy and glucose homeostasis. J Clin Invest. 2015 Feb 2;125(2):478–86.

10. Ikeda K, Maretich P, Kajimura S. The Common and Distinct Features of Brown and Beige Adipocytes. Trends Endocrinol Metab. 2018 Mar 1;29(3):191–200.

11. Sanchez-Gurmaches J, Hung CM, Guertin DA. Emerging Complexities in Adipocyte Origins and Identity. Trends Cell Biol. 2016 May;26(5):313–26.

12. Kajimura S, Spiegelman BM, Seale P. Brown and Beige Fat: Physiological Roles beyond Heat Generation. Cell Metab. 2015 Oct 6;22(4):546–59.

13. Shao M, Wang QA, Song A, Vishvanath L, Busbuso NC, Scherer PE, et al. Cellular Origins of Beige Fat Cells Revisited. Diabetes. 2019 Oct;68(10):1874–85.

14. Fedorenko A, Lishko PV, Kirichok Y. Mechanism of fatty-acid-dependent UCP1 uncoupling in brown fat mitochondria. Cell. 2012 Oct 12;151(2):400–13.

15. Magro BS, Dias DPM. Brown and beige adipose tissue: New therapeutic targets for metabolic disorders. Health Sci Rev. 2024 Mar 1;10:100148.

16. Rajakumari S, Wu J, Ishibashi J, Lim HW, Giang AH, Won KJ, et al. EBF2 determines and maintains brown adipocyte identity. Cell Metab. 2013 Apr 2;17(4):562–74.

17. Tseng YH, Kokkotou E, Schulz TJ, Huang TL, Winnay JN, Taniguchi CM, et al. New role of bone morphogenetic protein 7 in brown adipogenesis and energy expenditure. Nature. 2008 Aug 21;454(7207):1000–4.

18. Fu C, Chin-Young B, Park G, Guzmán-Seda M, Laudier D, Han WM. WNT7A suppresses adipogenesis of skeletal muscle mesenchymal stem cells and fatty infiltration through the alternative Wnt-Rho-YAP/TAZ signaling axis. Stem Cell Rep. 2023 Mar 30;18(4):999–1014.

19. Tontonoz P, Spiegelman BM. Fat and beyond: the diverse biology of PPARgamma. Annu Rev Biochem. 2008;77:289–312.

20. Lefterova MI, Zhang Y, Steger DJ, Schupp M, Schug J, Cristancho A, et al. PPARγ and C/EBP factors orchestrate adipocyte biology via adjacent binding on a genome-wide scale. Genes Dev. 2008 Nov 1;22(21):2941–52.

21. Harms MJ, Ishibashi J, Wang W, Lim HW, Goyama S, Sato T, et al. Prdm16 is required for the maintenance of brown adipocyte identity and function in adult mice. Cell Metab. 2014 Apr 1;19(4):593–604.

22. Inagaki T, Sakai J, Kajimura S. Transcriptional and epigenetic control of brown and beige adipose cell fate and function. Nat Rev Mol Cell Biol. 2016 Aug;17(8):480–95.

23. Tabuchi C, Sul HS. Signaling Pathways Regulating Thermogenesis. Front Endocrinol. 2021 Mar 26;12:595020.

24. Spalding KL, Arner E, Westermark PO, Bernard S, Buchholz BA, Bergmann O, et al. Dynamics of fat cell turnover in humans. Nature. 2008 June 5;453(7196):783–7.

25. Berry R, Jeffery E, Rodeheffer MS. Weighing in on Adipocyte Precursors. Cell Metab. 2014 Jan 7;19(1):8–20.

26. Wang W, Ishibashi J, Trefely S, Shao M, Cowan AJ, Sakers A, et al. A PRDM16-driven metabolic signal from adipocytes regulates precursor cell fate. Cell Metab. 2019 July 2;30(1):174-189.e5.

27. Mottillo EP, Balasubramanian P, Lee YH, Weng C, Kershaw EE, Granneman JG. Coupling of lipolysis and de novo lipogenesis in brown, beige, and white adipose tissues during chronic β3-adrenergic receptor activation. J Lipid Res. 2014 Nov;55(11):2276–86.

28. Markussen LK, Rondini EA, Johansen OS, Madsen JGS, Sustarsic EG, Marcher AB, et al. Lipolysis regulates major transcriptional programs in brown adipocytes. Nat Commun. 2022 July 8;13(1):3956.

29. Gallardo-Montejano VI, Yang C, Hahner L, McAfee JL, Johnson JA, Holland WL, et al. Perilipin 5 links mitochondrial uncoupled respiration in brown fat to healthy white fat remodeling and systemic glucose tolerance. Nat Commun. 2021 June 3;12(1):3320.

30. Morak M, Schmidinger H, Riesenhuber G, Rechberger GN, Kollroser M, Haemmerle G, et al. Adipose Triglyceride Lipase (ATGL) and Hormone-Sensitive Lipase (HSL) Deficiencies Affect Expression of Lipolytic Activities in Mouse Adipose Tissues. Mol Cell Proteomics MCP. 2012 Dec;11(12):1777–89.

31. Li Y, Li Z, Ngandiri DA, Llerins Perez M, Wolf A, Wang Y. The Molecular Brakes of Adipose Tissue Lipolysis. Front Physiol. 2022;13:826314.

32. Mottillo EP, Bloch AE, Leff T, Granneman JG. Lipolytic products activate peroxisome proliferator-activated receptor (PPAR) α and δ in brown adipocytes to match fatty acid oxidation with supply. J Biol Chem. 2012 July 20;287(30):25038–48.

33. Yessoufou A, Wahli W. Multifaceted roles of peroxisome proliferator-activated receptors (PPARs) at the cellular and whole organism levels. Swiss Med Wkly. 2010 Sept 15;

34. Haemmerle G, Moustafa T, Woelkart G, Büttner S, Schmidt A, van de Weijer T, et al. ATGL-mediated fat catabolism regulates cardiac mitochondrial function via PPAR-α and PGC-1. Nat Med. 2011 Sept;17(9):1076–85.

35. Ahmadian M, Abbott MJ, Tang T, Hudak CSS, Kim Y, Bruss M, et al. Desnutrin/ATGL Is Regulated by AMPK and Is Required for a Brown Adipose Phenotype. Cell Metab. 2011 June 8;13(6):739–48.

36. Bartelt A, Bruns OT, Reimer R, Hohenberg H, Ittrich H, Peldschus K, et al. Brown adipose tissue activity controls triglyceride clearance. Nat Med. 2011 Feb;17(2):200–5.

37. Wade G, McGahee A, Ntambi JM, Simcox J. Lipid Transport in Brown Adipocyte Thermogenesis. Front Physiol. 2021;12:787535.

38. Bartelt A, Weigelt C, Cherradi ML, Niemeier A, Tödter K, Heeren J, et al. Effects of adipocyte lipoprotein lipase on *de novo* lipogenesis and white adipose tissue browning. Biochim Biophys Acta BBA - Mol Cell Biol Lipids. 2013 May 1;1831(5):934–42.

39. Song Z, Xiaoli AM, Yang F. Regulation and Metabolic Significance of De Novo Lipogenesis in Adipose Tissues. Nutrients. 2018 Sept 29;10(10):1383.

40. Townsend KL, Tseng YH. Brown Fat Fuel Utilization and Thermogenesis. Trends Endocrinol Metab TEM. 2014 Apr;25(4):168–77.

41. Ameer F, Scandiuzzi L, Hasnain S, Kalbacher H, Zaidi N. *De novo* lipogenesis in health and disease. Metabolism. 2014 July 1;63(7):895–902.

42. Heine M, Fischer AW, Schlein C, Jung C, Straub LG, Gottschling K, et al. Lipolysis Triggers a Systemic Insulin Response Essential for Efficient Energy Replenishment of Activated Brown Adipose Tissue in Mice. Cell Metab. 2018 Oct 2;28(4):644-655.e4.

43. Chondronikola M, Volpi E, Børsheim E, Porter C, Saraf MK, Annamalai P, et al. Brown Adipose Tissue Activation Is Linked to Distinct Systemic Effects on Lipid Metabolism in Humans. Cell Metab. 2016 June 14;23(6):1200–6.

44. Chang JS. Recent insights into the molecular mechanisms of simultaneous fatty acid oxidation and synthesis in brown adipocytes. Front Endocrinol. 2023 Feb 21;14.

45. Cheng CF, Ku HC, Lin H. PGC-1α as a Pivotal Factor in Lipid and Metabolic Regulation. Int J Mol Sci. 2018 Nov 2;19(11):3447.

46. Jung SM, Doxsey WG, Le J, Haley JA, Mazuecos L, Luciano AK, et al. In vivo isotope tracing reveals the versatility of glucose as a brown adipose tissue substrate. Cell Rep. 2021 July 27;36(4):109459.

47. Labbé SM, Caron A, Bakan I, Laplante M, Carpentier AC, Lecomte R, et al. In vivo measurement of energy substrate contribution to cold-induced brown adipose tissue thermogenesis. FASEB J Off Publ Fed Am Soc Exp Biol. 2015 May;29(5):2046–58.

48. Ma SW, Foster DO. Uptake of glucose and release of fatty acids and glycerol by rat brown adipose tissue in vivo. Can J Physiol Pharmacol. 1986 May;64(5):609–14.

49. Censin JC, Peters SAE, Bovijn J, Ferreira T, Pulit SL, Mägi R, et al. Causal relationships between obesity and the leading causes of death in women and men. PLoS Genet. 2019 Oct;15(10):e1008405.

50. Kaikaew K, Grefhorst A, Visser JA. Sex Differences in Brown Adipose Tissue Function: Sex Hormones, Glucocorticoids, and Their Crosstalk. Front Endocrinol. 2021 Apr 13;12:652444.

51. Law J, Bloor I, Budge H, Symonds ME. The influence of sex steroids on adipose tissue growth and function. Horm Mol Biol Clin Investig. 2014 July;19(1):13–24.

52. Kim SN, Jung YS, Kwon HJ, Seong JK, Granneman JG, Lee YH. Sex differences in sympathetic innervation and browning of white adipose tissue of mice. Biol Sex Differ. 2016;7:67.

53. Rodríguez AM, Quevedo-Coli S, Roca P, Palou A. Sex-dependent dietary obesity, induction of UCPs, and leptin expression in rat adipose tissues. Obes Res. 2001 Sept;9(9):579–88.

54. Choi DK, Oh TS, Choi JW, Mukherjee R, Wang X, Liu H, et al. Gender difference in proteome of brown adipose tissues between male and female rats exposed to a high fat diet. Cell Physiol Biochem Int J Exp Cell Physiol Biochem Pharmacol. 2011;28(5):933–48.

55. Ouellet V, Routhier-Labadie A, Bellemare W, Lakhal-Chaieb L, Turcotte E, Carpentier AC, et al. Outdoor temperature, age, sex, body mass index, and diabetic status determine the prevalence, mass, and glucose-uptake activity of 18F-FDG-detected BAT in humans. J Clin Endocrinol Metab. 2011 Jan;96(1):192–9.

56. Brendle C, Werner MK, Schmadl M, la Fougère C, Nikolaou K, Stefan N, et al. Correlation of Brown Adipose Tissue with Other Body Fat Compartments and Patient Characteristics: A Retrospective Analysis in a Large Patient Cohort Using PET/CT. Acad Radiol. 2018 Jan;25(1):102–10.

57. Justo R, Frontera M, Pujol E, Rodríguez-Cuenca S, Lladó I, García-Palmer FJ, et al. Gender-related differences in morphology and thermogenic capacity of brown adipose tissue mitochondrial subpopulations. Life Sci. 2005 Jan 21;76(10):1147–58.

58. Valle A, Santandreu FM, García-Palmer FJ, Roca P, Oliver J. The serum levels of 17beta-estradiol, progesterone and triiodothyronine correlate with brown adipose tissue thermogenic parameters during aging. Cell Physiol Biochem Int J Exp Cell Physiol Biochem Pharmacol. 2008;22(1–4):337–46.

59. Persichetti A, Sciuto R, Rea S, Basciani S, Lubrano C, Mariani S, et al. Prevalence, mass, and glucose-uptake activity of ^{18}F-FDG-detected brown adipose tissue in humans living in a temperate zone of Italy. PloS One. 2013;8(5):e63391.

60. Quarta C, Mazza R, Pasquali R, Pagotto U. Role of sex hormones in modulation of brown adipose tissue activity. J Mol Endocrinol. 2012 Aug;49(1):R1-7.

61. Malpique R, Gallego-Escuredo JM, Sebastiani G, Villarroya J, López-Bermejo A, de Zegher F, et al. Brown adipose tissue in prepubertal children: associations with sex, birthweight, and metabolic profile. Int J Obes 2005. 2019 Feb;43(2):384–91.

62. Kuryłowicz A. Estrogens in Adipose Tissue Physiology and Obesity-Related Dysfunction. Biomedicines. 2023 Feb 24;11(3):690.

63. Björnström L, Sjöberg M. Mechanisms of Estrogen Receptor Signaling: Convergence of Genomic and Nongenomic Actions on Target Genes. Mol Endocrinol. 2005 Apr 1;19(4):833–42.

64. Cheung SWM, Yiu JHC, Chin KTC, Cai J, Xu A, Wong CM, et al. Content of stress granules reveals a sex difference at the early phase of cold exposure in mice. Am J Physiol-Endocrinol Metab. 2024 Jan;326(1):E29–37.

65. Okamatsu-Ogura Y, Kuroda M, Tsutsumi R, Tsubota A, Saito M, Kimura K, et al. UCP1-dependent and UCP1-independent metabolic changes induced by acute cold exposure in brown adipose tissue of mice. Metabolism. 2020 Dec;113:154396.

66. Martínez de Morentin PB, González-García I, Martins L, Lage R, Fernández-Mallo D, Martínez-Sánchez N, et al. Estradiol Regulates Brown Adipose Tissue Thermogenesis via Hypothalamic AMPK. Cell Metab. 2014 July 1;20(1):41–53.

67. Grefhorst A, van den Beukel JC, van Houten ELA, Steenbergen J, Visser JA, Themmen AP. Estrogens increase expression of bone morphogenetic protein 8b in brown adipose tissue of mice. Biol Sex Differ. 2015;6:7.

68. Lapid K, Lim A, Berglund ED, Lu Y. Estrogen receptor inhibition enhances cold-induced adipocyte beiging and glucose tolerance. Diabetes Metab Syndr Obes Targets Ther. 2019 Aug 14;12:1419–36.

69. Schmidt SL, Bessesen DH, Stotz S, Peelor FF, Miller BF, Horton TJ. Adrenergic control of lipolysis in women compared with men. J Appl Physiol Bethesda Md 1985. 2014 Nov 1;117(9):1008–19.

70. Rodríguez AM, Monjo M, Roca P, Palou A. Opposite actions of testosterone and progesterone on UCP1 mRNA expression in cultured brown adipocytes. Cell Mol Life Sci CMLS. 2002 Oct 1;59(10):1714–23.

71. Hashimoto O, Noda T, Morita A, Morita M, Ohtsuki H, Sugiyama M, et al. Castration induced browning in subcutaneous white adipose tissue in male mice. Biochem Biophys Res Commun. 2016 Sept 30;478(4):1746–50.

72. Gasparini SJ, Swarbrick MM, Kim S, Thai LJ, Henneicke H, Cavanagh LL, et al. Androgens sensitise mice to glucocorticoid-induced insulin resistance and fat accumulation. Diabetologia. 2019 Aug;62(8):1463–77.

73. Panning B. X-chromosome inactivation: the molecular basis of silencing. J Biol. 2008 Oct 27;7(8):30.

74. Mishra S, Singh KK. Sex-specific differences in mitochondrial function and its role in health disparities. In: Principles of Gender-Specific Medicine. Elsevier; 2023. p. 129–44.

75. Fang H, Disteche CM, Berletch JB. X Inactivation and Escape: Epigenetic and Structural Features. Front Cell Dev Biol. 2019 Oct 1;7:219.

76. Altus MS, Wood CM, Stewart DA, Roskams AJI, Friedman V, Henderson T, et al. Regions of evolutionary conservation between the rat and human prohibitin-encoding genes. Gene. 1995 June 9;158(2):291–4.

77. Cruz-Bustos T, Ibarrola-Vannucci AK, Díaz-Lozano I, Ramírez JL, Osuna A. Characterization and functionality of two members of the SPFH protein superfamily, prohibitin 1 and 2 in Leishmania major. Parasit Vectors. 2018 Dec 4;11(1):622.

78. Mishra S, Murphy LC, Murphy LJ. The Prohibitins: emerging roles in diverse functions. J Cell Mol Med. 2006;10(2):353–63.

79. McClung JK, Danner DB, Stewart DA, Smith JR, Schneider EL, Lumpkin CK, et al. Isolation of a cDNA that hybrid selects antiproliferative mRNA from rat liver. Biochem Biophys Res Commun. 1989 Nov 15;164(3):1316–22.

80. Jupe ER, Liu XT, Kiehlbauch JL, McClung JK, Dell'Orco RT. Prohibitin in breast cancer cell lines: loss of antiproliferative activity is linked to 3' untranslated region mutations. Cell Growth Differ Mol Biol J Am Assoc Cancer Res. 1996 July;7(7):871–8.

81. Charles A Janeway J, Travers P, Walport M, Shlomchik MJ. Antigen Recognition by B-cell and T-cell Receptors. In: Immunobiology: The Immune System in Health and Disease 5th edition. Garland Science; 2001.

82. Merkwirth C, Langer T. Prohibitin function within mitochondria: Essential roles for cell proliferation and cristae morphogenesis. Biochim Biophys Acta BBA - Mol Cell Res. 2009 Jan 1;1793(1):27–32.

83. He B, Feng Q, Mukherjee A, Lonard DM, DeMayo FJ, Katzenellenbogen BS, et al. A repressive role for prohibitin in estrogen signaling. Mol Endocrinol Baltim Md. 2008 Feb;22(2):344–60.

84. Ross JA, Robles-Escajeda E, Oaxaca DM, Padilla DL, Kirken RA. The prohibitin protein complex promotes mitochondrial stabilization and cell survival in hematologic malignancies. Oncotarget. 2017 July 1;8(39):65445–56.

85. UniProt Consortium. UniProt: the Universal Protein Knowledgebase in 2025. Nucleic Acids Res. 2025 Jan 6;53(D1):D609–17.

86. Wang S, Fusaro G, Padmanabhan J, Chellappan SP. Prohibitin co-localizes with Rb in the nucleus and recruits N-CoR and HDAC1 for transcriptional repression. Oncogene. 2002 Dec;21(55):8388–96.

87. Garin J, Diez R, Kieffer S, Dermine JF, Duclos S, Gagnon E, et al. The phagosome proteome: insight into phagosome functions. J Cell Biol. 2001 Jan 8;152(1):165–80.

88. Giannotta M, Fragassi G, Tamburro A, Vanessa C, Luini A, Sallese M. Prohibitin: A Novel Molecular Player in KDEL Receptor Signalling. BioMed Res Int. 2015;2015:319454.

89. Nijtmans LG, de Jong L, Artal Sanz M, Coates PJ, Berden JA, Back JW, et al. Prohibitins act as a membrane-bound chaperone for the stabilization of mitochondrial proteins. EMBO J. 2000 June 1;19(11):2444–51.

90. Merkwirth C, Dargazanli S, Tatsuta T, Geimer S, Löwer B, Wunderlich FT, et al. Prohibitins control cell proliferation and apoptosis by regulating OPA1-dependent cristae morphogenesis in mitochondria. Genes Dev. 2008 Feb 15;22(4):476–88.

91. Kasashima K, Sumitani M, Satoh M, Endo H. Human prohibitin 1 maintains the organization and stability of the mitochondrial nucleoids. Exp Cell Res. 2008 Mar 10;314(5):988–96.

92. Ande SR, Mishra S. Palmitoylation of prohibitin at cysteine 69 facilitates its membrane translocation and interaction with Eps 15 homology domain protein 2 (EHD2). Biochem Cell Biol Biochim Biol Cell. 2010 June;88(3):553–8.

93. Yurugi H, Tanida S, Ishida A, Akita K, Toda M, Inoue M, et al. Expression of prohibitins on the surface of activated T cells. Biochem Biophys Res Commun. 2012 Apr 6;420(2):275–80.

94. Lucas CR, Cordero-Nieves HM, Erbe RS, McAlees JW, Bhatia S, Hodes RJ, et al. Prohibitins and the cytoplasmic domain of CD86 cooperate to mediate CD86 signaling in B lymphocytes. J Immunol Baltim Md 1950. 2013 Jan 15;190(2):723–36.

95. Terashima M, Kim KM, Adachi T, Nielsen PJ, Reth M, Köhler G, et al. The IgM antigen receptor of B lymphocytes is associated with prohibitin and a prohibitin-related protein. EMBO J. 1994 Aug 15;13(16):3782–92.

96. Sharma A, Vasanthapuram R, M Venkataswamy M, Desai A. Prohibitin 1/2 mediates Dengue-3 entry into human neuroblastoma (SH-SY5Y) and microglia (CHME-3) cells. J Biomed Sci. 2020 Apr 19;27(1):55.

97. Wintachai P, Wikan N, Kuadkitkan A, Jaimipuk T, Ubol S, Pulmanausahakul R, et al. Identification of prohibitin as a Chikungunya virus receptor protein. J Med Virol. 2012 Nov;84(11):1757–70.

98. Signorile A, Sgaramella G, Bellomo F, De Rasmo D. Prohibitins: A Critical Role in Mitochondrial Functions and Implication in Diseases. Cells. 2019 Jan 18;8(1):71.

99. Artal-Sanz M, Tavernarakis N. Prohibitin couples diapause signalling to mitochondrial metabolism during ageing in C. elegans. Nature. 2009 Oct 8;461(7265):793–7.

100. Lourenço AB, Artal-Sanz M. The Mitochondrial Prohibitin (PHB) Complex in C. elegans Metabolism and Ageing Regulation. Metabolites. 2021 Sept 17;11(9):636.

101. Lourenço AB, Rodríguez-Palero MJ, Doherty MK, Cabrerizo Granados D, Hernando-Rodríguez B, Salas JJ, et al. The Mitochondrial PHB Complex Determines Lipid Composition and Interacts With the Endoplasmic Reticulum to Regulate Ageing. Front Physiol. 2021 July 1;12:696275.

102. Gao Z, Daquinag AC, Fussell C, Djehal A, Désaubry L, Kolonin MG. Prohibitin Inactivation in Adipocytes Results in Reduced Lipid Metabolism and Adaptive Thermogenesis Impairment. Diabetes. 2021 Oct;70(10):2204–12.

103. Ande SR, Xu Z, Gu Y, Mishra S. Prohibitin has an important role in adipocyte differentiation. Int J Obes 2005. 2012 Sept;36(9):1236–44.

104. Ande SR, Nguyen KH, Padilla-Meier GP, Wahida W, Nyomba BLG, Mishra S. Prohibitin overexpression in adipocytes induces mitochondrial biogenesis, leads to obesity development, and affects glucose homeostasis in a sex-specific manner. Diabetes. 2014 Nov;63(11):3734–41.

105. Salameh A, Daquinag AC, Staquicini DI, An Z, Hajjar KA, Pasqualini R, et al. Prohibitin/annexin 2 interaction regulates fatty acid transport in adipose tissue. JCI Insight. 1(10):e86351.

106. Daquinag AC, Gao Z, Fussell C, Immaraj L, Pasqualini R, Arap W, et al. Fatty acid mobilization from adipose tissue is mediated by CD36 posttranslational modifications and intracellular trafficking. JCI Insight. 2021 Sept 8;6(17):e147057.

107. Rupert JE, Kolonin MG. Fatty acid translocase: a culprit of lipid metabolism dysfunction in disease. Immunometabolism Cobham Surrey Engl. 2022 Aug 15;4(3):e00001.

108. Liu D, Lin Y, Kang T, Huang B, Xu W, Garcia-Barrio M, et al. Mitochondrial Dysfunction and Adipogenic Reduction by Prohibitin Silencing in 3T3-L1 Cells. PLoS ONE. 2012 Mar 30;7(3):e34315.

109. Chang E, Varghese M, Singer K. Gender and Sex Differences in Adipose Tissue. Curr Diab Rep. 2018 July 30;18(9):69.

110. Xu YXZ, Ande SR, Mishra S. Gonadectomy in Mito-Ob mice revealed a sex-dimorphic relationship between prohibitin and sex steroids in adipose tissue biology and glucose homeostasis. Biol Sex Differ. 2018 Aug 29;9:37.

111. Mishra S, Nyomba BG. Prohibitin: A hypothetical target for sex-based new therapeutics for metabolic and immune diseases. Exp Biol Med Maywood NJ. 2019 Feb;244(2):157–70.

112. Walsh CT, Garneau-Tsodikova S, Gatto GJ. Protein posttranslational modifications: the chemistry of proteome diversifications. Angew Chem Int Ed Engl. 2005 Dec 1;44(45):7342–72.

113. Hunter T. The age of crosstalk: phosphorylation, ubiquitination, and beyond. Mol Cell. 2007 Dec 14;28(5):730–8.

114. Khoury GA, Baliban RC, Floudas CA. Proteome-wide post-translational modification statistics: frequency analysis and curation of the swiss-prot database. Sci Rep. 2011 Sept 13;1:90, srep00090.

115. Zhong Q, Xiao X, Qiu Y, Xu Z, Chen C, Chong B, et al. Protein posttranslational modifications in health and diseases: Functions, regulatory mechanisms, and therapeutic implications. MedComm. 2023 May 2;4(3):e261.

116. Ande SR, Xu YXZ, Mishra S. Prohibitin: a potential therapeutic target in tyrosine kinase signaling. Signal Transduct Target Ther. 2017 Dec 15;2:17059.

117. Ande SR, Gu Y, Nyomba BLG, Mishra S. Insulin induced phosphorylation of prohibitin at tyrosine 114 recruits Shp1. Biochim Biophys Acta. 2009 Aug;1793(8):1372–8.

118. Mishra S, Ande SR, Nyomba BLG. The role of prohibitin in cell signaling. FEBS J. 2010 Oct;277(19):3937–46.

119. Ande SR, Moulik S, Mishra S. Interaction between O-GlcNAc modification and tyrosine phosphorylation of prohibitin: implication for a novel binary switch. PloS One. 2009;4(2):e4586.

120. Mishra S, Nyomba BG. Prohibitin – At the crossroads of obesity-linked diabetes and cancer. Exp Biol Med. 2017 June;242(11):1170–7.

121. Dennis KMJH, Heather LC. Post-translational palmitoylation of metabolic proteins. Front Physiol. 2023 Feb 24;14:1122895.

122. Fernando V, Zheng X, Walia Y, Sharma V, Letson J, Furuta S. S-Nitrosylation: An Emerging Paradigm of Redox Signaling. Antioxidants. 2019 Sept 17;8(9):404.

123. Jian C, Xu F, Hou T, Sun T, Li J, Cheng H, et al. Deficiency of PHB complex impairs respiratory supercomplex formation and activates mitochondrial flashes. J Cell Sci. 2017 Aug 1;130(15):2620–30.

124. Ban T, Kuroda K, Nishigori M, Yamashita K, Ohta K, Koshiba T. Prohibitin 1 tethers lipid membranes and regulates OPA1-mediated membrane fusion. J Biol Chem. 2024 Dec 13;301(1):108076.

125. Townsend K, Tseng YH. Brown adipose tissue. Adipocyte. 2012 Jan 1;1(1):13–24.

126. Wang X, Kim S, Guan Y, Parker R, Rodrigues RM, Feng D, et al. Deletion of adipocyte prohibitin 1 exacerbates high-fat diet-induced steatosis but not liver inflammation and fibrosis. Hepatol Commun. 2022 Oct 5;6(12):3335–48.

127. Gao Z, Daquinag AC, Yu Y, Kolonin MG. Endothelial Prohibitin Mediates Bidirectional Long-Chain Fatty Acid Transport in White and Brown Adipose Tissues. Diabetes. 2022 July 1;71(7):1400–9.

128. Bize P, Lowe I, Lehto Hürlimann M, Heckel G. Effects of the Mitochondrial and Nuclear Genomes on Nonshivering Thermogenesis in a Wild Derived Rodent. Integr Comp Biol. 2018 Sept 1;58(3):532–43.

129. Prohibitin is expressed in pancreatic β-cells and protects against oxidative and proapoptotic effects of ethanol - Lee - 2010 - The FEBS Journal - Wiley Online Library. [cited 2025 July 24]; Available from: https://febs.onlinelibrary.wiley.com/doi/10.1111/j.1742-4658.2009.07505.x

130. Mao J, Zhang J, Cai L, Cui Y, Liu J, Mao Y. Elevated prohibitin 1 expression mitigates glucose metabolism defects in granulosa cells of infertile patients with endometriosis. Mol Hum Reprod. 2022 May 27;28(6):gaac018.

131. Ande SR, Nguyen KH, Grégoire Nyomba BL, Mishra S. Prohibitin-induced, obesity-associated insulin resistance and accompanying low-grade inflammation causes NASH and HCC. Sci Rep. 2016 Mar 23;6(1):23608.

132. Vessal M, Mishra S, Moulik S, Murphy LJ. Prohibitin attenuates insulin-stimulated glucose and fatty acid oxidation in adipose tissue by inhibition of pyruvate carboxylase. FEBS J. 2006;273(3):568–76.

133. Ande SR, Mishra S. Prohibitin interacts with phosphatidylinositol 3,4,5-triphosphate (PIP3) and modulates insulin signaling. Biochem Biophys Res Commun. 2009 Dec 18;390(3):1023–8.

134. Jung SM, Sanchez-Gurmaches J, Guertin DA. Brown Adipose Tissue Development and Metabolism. Handb Exp Pharmacol. 2019;251:3–36.

135. Wu J, Cohen P, Spiegelman BM. Adaptive thermogenesis in adipocytes: is beige the new brown? Genes Dev. 2013 Feb 1;27(3):234–50.

136. Mauvais-Jarvis F. Sex differences in metabolic homeostasis, diabetes, and obesity. Biol Sex Differ. 2015;6:14.

137. Rodriguez-Cuenca S, Pujol E, Justo R, Frontera M, Oliver J, Gianotti M, et al. Sex-dependent thermogenesis, differences in mitochondrial morphology and function, and adrenergic response in brown adipose tissue. J Biol Chem. 2002 Nov 8;277(45):42958–63.

138. Gómez-García I, Trepiana J, Fernández-Quintela A, Giralt M, Portillo MP. Sexual Dimorphism in Brown Adipose Tissue Activation and White Adipose Tissue Browning. Int J Mol Sci. 2022 July 26;23(15):8250.

139. Zhou Z, Moore TM, Drew BG, Ribas V, Wanagat J, Civelek M, et al. Estrogen receptor α controls metabolism in white and brown adipocytes by regulating Polg1 and mitochondrial remodeling. Sci Transl Med. 2020 Aug 5;12(555):eaax8096.

140. Blondin DP, Haman F, Swibas TM, Hogan-Lamarre S, Dumont L, Guertin J, et al. Brown adipose tissue metabolism in women is dependent on ovarian status. Am J Physiol Endocrinol Metab. 2024 May 1;326(5):E588–601.

141. Lantero Rodriguez M, Schilperoort M, Johansson I, Svedlund Eriksson E, Palsdottir V, Kroon J, et al. Testosterone reduces metabolic brown fat activity in male mice. J Endocrinol. 2021 Sept 3;251(1):83–96.

142. Keuper M, Jastroch M. The good and the BAT of metabolic sex differences in thermogenic human adipose tissue. Mol Cell Endocrinol. 2021 Aug 1;533:111337.

143. Bernier K. Investigating the white adipose tissue phenotype in the male and female Phb1-C69A knock-in mice. 2024 Mar 27 [cited 2025 June 26]; Available from: http://hdl.handle.net/1993/38105

144. Frontiers | RNA-Seq Reveals Different Gene Expression in Liver-Specific Prohibitin 1 Knock-Out Mice [Internet]. [cited 2025 Dec 19]. Available from: https://www.frontiersin.org/journals/physiology/articles/10.3389/fphys.2021.717911/full

145. Nguyen KH, Ande SR, Mishra S. Prohibitin: an unexpected role in sex dimorphic functions. Biol Sex Differ. 2016 June 24;7:30.

146. Rosen ED, Spiegelman BM. Adipocytes as regulators of energy balance and glucose homeostasis. Nature. 2006 Dec 14;444(7121):847–53.

147. Charan J, Kantharia ND. How to calculate sample size in animal studies? J Pharmacol Pharmacother. 2013 Oct;4(4):303–6.

148. Kamal AHM, Kim WK, Cho K, Park A, Min JK, Han BS, et al. Investigation of adipocyte proteome during the differentiation of brown preadipocytes. J Proteomics. 2013 Dec 6;94:327–36.

149. Yoshinaka T, Kosako H, Yoshizumi T, Furukawa R, Hirano Y, Kuge O, et al. Structural Basis of Mitochondrial Scaffolds by Prohibitin Complexes: Insight into a Role of the Coiled-Coil Region. iScience. 2019 Sept 3;19:1065–78.

150. Wang K, Liu CY, Zhang XJ, Feng C, Zhou LY, Zhao Y, et al. miR-361-regulated prohibitin inhibits mitochondrial fission and apoptosis and protects heart from ischemia injury. Cell Death Differ. 2015 June;22(6):1058–68.

151. Mauvais-Jarvis F, Clegg DJ, Hevener AL. The Role of Estrogens in Control of Energy Balance and Glucose Homeostasis. Endocr Rev. 2013 June;34(3):309–38.

152. Lerner A, Kewada D, Ahmed A, Hardy K, Christian M, Franks S. Androgen Reduces Mitochondrial Respiration in Mouse Brown Adipocytes: A Model for Disordered Energy Balance in Polycystic Ovary Syndrome. Int J Mol Sci. 2020 Dec 29;22(1):243.

153. Stanford KI, Middelbeek RJW, Townsend KL, An D, Nygaard EB, Hitchcox KM, et al. Brown adipose tissue regulates glucose homeostasis and insulin sensitivity. J Clin Invest. 2013 Jan;123(1):215–23.

154. Steiner BM, Berry DC. The Regulation of Adipose Tissue Health by Estrogens. Front Endocrinol. 2022 May 26;13:889923.

155. Jo J, Gavrilova O, Pack S, Jou W, Mullen S, Sumner AE, et al. Hypertrophy and/or Hyperplasia: Dynamics of Adipose Tissue Growth. PLOS Comput Biol. 2009 Mar 27;5(3):e1000324.

156. Pellegrinelli V, Carobbio S, Vidal-Puig A. Adipose tissue plasticity: how fat depots respond differently to pathophysiological cues. Diabetologia. 2016 June 1;59(6):1075–88.

157. Rangel-Azevedo C, Santana-Oliveira DA, Miranda CS, Martins FF, Mandarim-de-Lacerda CA, Souza-Mello V. Progressive brown adipocyte dysfunction: Whitening and impaired nonshivering thermogenesis as long-term obesity complications. J Nutr Biochem. 2022 July;105:109002.

158. Crabtree A, Neikirk K, Marshall AG, Vang L, Whiteside AJ, Williams Q, et al. Defining Mitochondrial Cristae Morphology Changes Induced by Aging in Brown Adipose Tissue. Adv Biol. 2024 Jan;8(1):e2300186.

159. Kotzbeck P, Giordano A, Mondini E, Murano I, Severi I, Venema W, et al. Brown adipose tissue whitening leads to brown adipocyte death and adipose tissue inflammation. J Lipid Res. 2018 May;59(5):784–94.

160. Lange F, Ratz M, Dohrke JN, Le Vasseur M, Wenzel D, Ilgen P, et al. In situ architecture of the human prohibitin complex. Nat Cell Biol. 2025 Apr;27(4):633–40.

161. Johnson JM, Peterlin AD, Balderas E, Sustarsic EG, Maschek JA, Lang MJ, et al. Mitochondrial phosphatidylethanolamine modulates UCP1 to promote brown adipose thermogenesis. Sci Adv. 2023 Feb 24;9(8):eade7864.

162. Rajalingam K, Wunder C, Brinkmann V, Churin Y, Hekman M, Sievers C, et al. Prohibitin is required for Ras-induced Raf-MEK-ERK activation and epithelial cell migration. Nat Cell Biol. 2005 Aug;7(8):837–43.

163. Han EKH, Mcgonigal T, Butler C, Giranda VL, Luo Y. Characterization of Akt overexpression in MiaPaCa-2 cells: prohibitin is an Akt substrate both in vitro and in cells. Anticancer Res. 2008;28(2A):957–63.

164. Hinoi E, Iezaki T, Fujita H, Watanabe T, Odaka Y, Ozaki K, et al. PI3K/Akt is involved in brown adipogenesis mediated by growth differentiation factor-5 in association with activation of the Smad pathway. Biochem Biophys Res Commun. 2014 July 18;450(1):255–60.

165. Li J, Sun M, Tang M, Song X, Zheng K, Meng T, et al. Mechanism of PI3K/Akt-mediated mitochondrial pathway in obesity-induced apoptosis (Review). Biomed Rep. 2025 Mar 1;22(3):1–8.

166. Kassouf T, Sumara G. Impact of Conventional and Atypical MAPKs on the Development of Metabolic Diseases. Biomolecules. 2020 Aug 29;10(9):1256.

167. Velarde MC. Pleiotropic actions of estrogen: a mitochondrial matter. Physiol Genomics. 2013 Feb 4;45(3):106–9.

168. Kaikaew K, Steenbergen J, Themmen APN, Visser JA, Grefhorst A. Sex difference in thermal preference of adult mice does not depend on presence of the gonads. Biol Sex Differ. 2017 July 11;8:24.

169. Klappenbach CM, Wang Q, Jensen AL, Glodosky NC, Delevich K. Sex and timing of gonadectomy relative to puberty interact to influence weight, body composition, and feeding behaviors in mice. Horm Behav. 2023 May 1;151:105350.

170. Chondronikola M, Volpi E, Børsheim E, Porter C, Annamalai P, Enerbäck S, et al. Brown Adipose Tissue Improves Whole-Body Glucose Homeostasis and Insulin Sensitivity in Humans. Diabetes. 2014 Nov 13;63(12):4089–99.

171. Herz CT, Kulterer OC, Prager M, Marculescu R, Langer FB, Prager G, et al. Sex differences in brown adipose tissue activity and cold-induced thermogenesis. Mol Cell Endocrinol. 2021 Aug 20;534:111365.

172. Klinge CM. Estrogenic Control of Mitochondrial Function and Biogenesis. J Cell Biochem. 2008 Dec 15;105(6):1342–51.

173. Petersen MC, Shulman GI. Mechanisms of Insulin Action and Insulin Resistance. Physiol Rev. 2018 Oct 1;98(4):2133–223.

174. Kelly DM, Jones TH. Testosterone: a metabolic hormone in health and disease. J Endocrinol. 2013 June;217(3):R25-45.